The Impact of S1P Receptors on the High-Density Lipoprotein-mediated Cholesterol Efflux in Chinese Hamster Ovary Cells

Inaugural-Dissertation

zur

Erlangung des Doktorgrades

Dr. rer. nat.

der Fakultät für

Biologie

an der

Universität Duisburg-Essen

vorgelegt von

Kristina Manthe

aus Emden

Februar 2019

Die der vorliegenden Arbeit zugrundeliegenden Experimente wurden am Institut für Pathophysiologie des Universitätsklinikums Essen durchgeführt.

1. Gutachter: Prof. Dr. Bodo Levkau

2. Gutachter: Prof. Dr. Elke Cario

Vorsitzender des Prüfungsausschusses: PD Dr. Bernd Giebel

Tag der mündlichen Prüfung: 30. August 2019

DOI: 10.17185/duepublico/70529
URN: urn:nbn:de:hbz:464-20190917-093437-0

Table of contents

Abbreviations

ABC	ATP-binding cassette
Abca1	ATP-binding cassette transporter protein A-1 (murine gene)
Abcg1	ATP-binding cassette transporter protein G-1 (murine gene)
ACAT	Acyl-CoA:cholesterol acyltransferase
amp	Ampicillin
APS	Ammonium persulfate
ATP	Adenosine triphosphate
Apo	Apolipoprotein
BLT-1	Block lipid transport-1
bp	Base pairs
BSA	Bovine serum albumin
C1P	Ceramide-1-phosphate
$CaCl_2$	Calcium chloride
cAMP	Cyclic adenosine monophosphate
cDNA	Complementary DNA
CHO	Chinese hamster ovary
CO_2	Carbon dioxide
CoA	Coenzyme A
DMEM	Dulbecco's Modified Eagle's Medium
DMSO	Dimethyl sulfoxide
DNA	Deoxyribonucleic acid
dNTP	Deoxynucleotide triphosphate
E. coli	*Escherichia coli*
EDG	Endothelial differentiation gene
EDTA	Ethylene diamine tetraacetic acid
eGFP	Enhanced green fluorescent protein
eNOS	Endothelial nitric oxide synthase
ER	Endoplasmic reticulum
ERK	Extracellular signal-related kinase
FACS	Fluorescence-activated cell sorting

FBS	Fetal bovine serum
Fig.	Figure
FSC	Forward scatter
Gapdh	Glyceraldehyde 3-phosphate dehydrogenase (murine gene)
GDP	Guanosine diphosphate
GFP	Green fluorescent protein
GPCR	G protein-coupled receptor
GTP	Guanosine triphosphate
H_2O_2	Hydrogen peroxide
HBS	HEPES-buffered saline
HCl	Hydrogen chloride
HDL	High-density lipoprotein
HEPES	4-(2-hydroxyethyl)-1-piperazineethanesulfonic acid
HIV-1	Human immunodeficiency virus type 1
HMG-CoAR	3-hydroxy-3-methylglutaryl CoA reductase
HRP	Horseradish peroxidase
hS1P1	Human sphingosine-1-phosphate receptor 1
IDL	Intermediate-density lipoproteins
IRES	Internal ribosome entry site
kb	Kilo base
KBr	Potassium bromide
LB	Luria-Bertani
LCAT	Lecithin:cholesterol acyltransferase
LDL	Low-density lipoprotein
LPP	Lipid phosphate phosphatase
LTR	Long terminal repeat
LV	Lentiviral vector
LXR	Liver X receptor
MAP	Mitogen-activated protein
MAPK	Mitogen-activated protein kinase
MCS	Multiple cloning site

MEM	Minimum Essential Medium
MFI	Mean fluorescence intensity
$MgCl_2$	Magnesium chloride
µg	Microgram
µM	Micromolar
mM	Millimolar
Na_2HPO_4	Disodium hydrogen phosphate
NaCl	Sodium chloride
$NaHCO_3$	Sodium hydrogen carbonate
NaOH	Sodium hydroxide
NEDD4	Neural precursor cell-expressed developmentally downregulated 4
NHERF	Na^+/H^+ exchanger regulatory factor
nm	Nanometer
NO	Nitric oxide
NP-40	Nonyl phenoxypolyethoxylethanol
PBS	Phosphate buffered saline
PCR	Polymerase chain reaction
PDZ	Postsynaptic density 95, discs-large, zonula occludens-1
PI3K	Phosphatidylinositol 3-kinase
PLTP	Phospholipid transfer protein
PMSF	Phenylmethane sulfonyl fluoride
PVDF	Polyvinylidene difluoride
RCT	Reverse cholesterol transport
Rev	Reticuloendotheliosis virus
rHDL	Reconstituted HDL
RNA	Ribonucleic acid
rpm	Rounds per minute
RPMI	Roswell Park Memorial Institute
RSV	Rous sarcoma virus
RT-PCR	Quantitative reverse transcription polymerase chain reaction
RXR	Retinoid X receptor

S1P	Sphingosine-1-phosphate
S1P1-5	Sphingosine-1-phosphate receptor 1-5 (human protein)
S1PR	Sphingosine-1-phosphate receptor (human gene)
S1pr	Sphingosine-1-phosphate receptor (murine gene)
Scarb1	Scavenger receptor type B class 1 (murine gene)
SDS	Sodium dodecyl sulfate
SFFV	Spleen focus-forming virus
SIN	Self inactivating
SK	Sphingosine kinase
Spns2	Spinster homolog 2
SPP	S1P phosphatase
SPT	Serine palmitoyl transferase
SR-BI/SRB1	Scavenger receptor type B class 1
SSC	Side scatter
Tab.	Table
TAE	Tris-acetat-EDTA
TRIP6	Thyroid receptor interacting protein 6
VLDL	Very low-density lipoproteins
VSV-G	Vesicular stomatitis virus G glycoprotein
v/v	Volume per volume
WPRE	Woodchuck hepatitis virus post-transcriptional regulatory element
w/v	Weight per volume
WWP2	WW domain-containing E3 ubiquitin protein ligase 2 (atrophin-1-interacting protein 2)
x *g*	Gravity; centrifugal force (g = 9,81 m s^{-2})

List of figures

List of tables

1 Introduction

High-density lipoprotein (HDL) particles are the major chaperones of sphingosine-1-phosphate (S1P) in the body (Christoffersen et al., 2011) and several biological functions are mediated by HDL-S1P signaling (Argraves and Argraves, 2007; Levkau, 2015; Sattler and Levkau, 2009). S1P receptors as well as the scavenger receptor class B type 1 (SR-BI), the HDL receptor, may be involved in these pathways. However, the role of HDL-S1P and S1P receptors in the SR-BI-mediated removal of cholesterol from cells and signaling pathways is still unknown.

1.1 Cholesterol and lipoprotein metabolism

Cholesterol plays an important role in the fluidity of cellular membranes and is present in all tissues and blood, either as free cholesterol or stored in a fatty-acetylated form (Ikonen, 2006). The amphipathic sterol cholesterol is a precursor of steroid hormones and bile acids (Russell and Setchell, 1992), and modulates the stability and fluidity of membranes in all animal cells (Crockett, 1998). It is synthesized *de novo* or can be supplied through the diet via the receptor-mediated endocytosis of low-density lipoproteins (LDL). In order to protect the cells from excess cholesterol and prevent cardiovascular diseases, a balance between cholesterol biosynthesis, intake and removal must be maintained. Thus, the body relies on a tightly regulated mechanism that enables conversion of cholesterol to steroid hormones or bile acids or enables excretion into the bile (Ikonen, 2006; Simons and Ikonen, 2000).

All cells in the body are capable of synthesizing cholesterol, however, the liver is the major site for cholesterol synthesis and the only organ which can degrade and eliminate large quantities of cholesterol (Cohen, 2008). Cholesterol is synthesized from acetate, which is converted via the complex mevalonate pathway by sequential enzymatic reactions, starting with the condensation of acetyl coenzyme A (acetyl-CoA) to isopentenyl pyrophosphate. The rate-limiting enzyme in this pathway is the 3-hydroxy-3-methylglutaryl CoA reductase (HMG-CoAR). HMG-CoAR allows the irreversible generation of mevalonate from HMG-CoA within the endoplasmic reticulum (ER), the site of cholesterol synthesis (Ikonen, 2006).

Both synthesized and dietary cholesterol are insoluble in water and are therefore transported in the vascular system as cholesteryl esters in form of lipoprotein particles, mostly LDL and HDL (Ikonen, 2006).

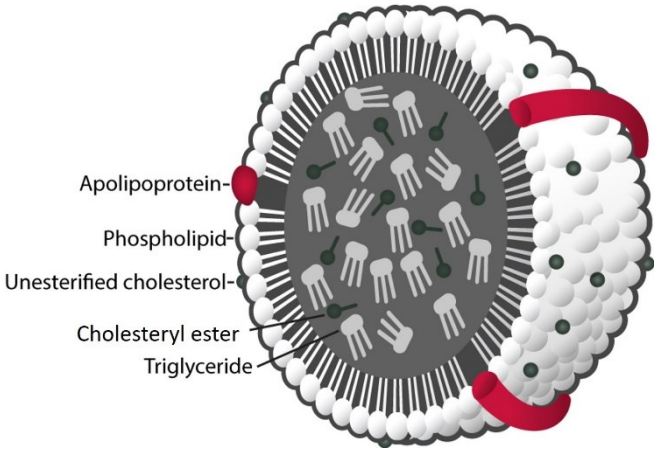

Figure 1: Representative schematic of a lipoprotein structure
Lipoproteins are spherical structures consisting of a hydrophobic core of cholesteryl esters and triglycerides. The core is surrounded by phospholipids and apolipoproteins. (Modified from Mabtech, 2019. *Apolipoproteins.* Retrieved February 3, 2019, from https://www.mabtech.com)

Lipoproteins are synthesized by the liver and intestine and they consist of a hydrophobic core composed of cholesteryl esters and triglycerides surrounded by apolipoproteins and polar phospholipids. Lipoproteins are classified according to their density into chylomicrons, chylomicron remnants, very low-density lipoproteins (VLDL), intermediate-density lipoproteins (IDL), LDL, and HDL. Chylomicron remnants, VLDL, IDL, and LDL are pro-atherogenic lipoproteins, whereas HDL has anti-atherogenic properties (Feingold and Grunfeld, 2000). An increasing concentration of LDL-cholesterol in the blood leads to the expression of LDL receptors on hepatocytes and LDL-cholesterol can enter the cells via endocytosis upon binding to the receptors. The internalized receptors are recycled to the cell surface and LDL-derived cholesteryl esters are delivered to lysosomes where they are hydrolyzed to cholesterol by acid lipase. This free cholesterol is then transported to the cellular plasma membrane, ER or other cellular compartments. Brown and Goldstein discovered that rising levels of cholesterol in the ER result in a suppression of genes encoding the HMG-CoAR and the LDL receptor, as well as downregulation of *de novo* cholesterol synthesis (Goldstein and Brown, 1984). Furthermore, the ER-resident acyl-CoA:cholesterol acyltransferase (ACAT) is activated to detoxify free cholesterol to cholesteryl esters which is stored in cytoplasmic lipid droplets (Brown and Goldstein, 1986; Ikonen, 2006). Another mechanism to regulate cholesterol homeostasis is the

cholesterol efflux mechanism, called the reverse cholesterol transport (RCT). The RCT involves the removal of cholesterol from peripheral cells and delivery to the liver for the excretion and was first described by Glomset in 1968 (Glomset, 1968). Peripheral cells and tissues primarily receive cholesterol from VLDL and LDL rather than synthesizing it. They can only eliminate excess cholesterol by efflux to extracellular acceptors, as they do not express pathways to catabolize cholesterol. HDL particles and lipid-free apolipoprotein A-I (apoA-I), the major protein of HDL, serve as cholesterol acceptors in the cholesterol efflux. HDL particles interact via apoA-I with binding sites on the cell surfaces. Thereby resulting in an intracellular signal that leads to translocation of intracellular free cholesterol to the plasma membrane (Spady, 1999). Free cholesterol is converted to cholesteryl ester within HDL and returned to the liver, where it is excreted into the bile and eliminated via the feces or degraded to bile acids (Fielding and Fielding, 1995).

The previously mentioned transport mechanisms play an important role to balance the cholesterol metabolism in the body. Therefore, when the concentration of LDL-cholesterol in the body increases due to reduced expression of LDL receptors and reduced levels of HDL, the cholesterol homeostasis is disturbed and may result in the initiation of atherosclerotic vascular diseases (Babiak and Rudel, 1987; Huszar et al., 2000).

1.2 Atherosclerosis

Atherosclerosis is an inflammatory disease and one of the major problems causing cardiovascular diseases leading to many deaths worldwide (Fairweather, 2014; Lusis, 2000). Atherosclerosis is characterized by the accumulation of fibrous elements and lipids inside the artery walls, migration of inflammatory and vascular smooth muscle cells, and development of macrophage foam cells (Hartman and Frishman, 2014; Libby, 2002; Lusis, 2000). This plaque formation causes thickening of the arterial intima and formation of a thrombus, resulting in cardiac ischemia which then can lead to stroke or myocardial infarction (Lusis, 2000; Ross, 1999). Smoking, male gender, hypertension, predisposition for obesity and diabetes mellitus are potent risk factors which increase the risk to develop atherosclerosis (Ellulu et al., 2016; Rafieian-Kopaei et al., 2014). Reduced expression levels of LDL receptors and high plasma levels of LDL-cholesterol play an important role in initiating atherosclerosis. Elevated LDL-

cholesterol levels change the endothelial permeability of arteries, which results in the penetration of LDL-cholesterol into the intima. Once trapped in the artery, LDL-cholesterol undergoes oxidative modifications (oxLDL) and activates the endothelium to mediate inflammatory processes which contribute to the recruitment of circulating monocytes, macrophages and T-lymphocytes (Frostegård, 2013; Lusis, 2000; Ross, 1999).

1.3 Structure and metabolism of HDL

As mentioned, lipoproteins are involved in the control of cholesterol metabolism and are important players in the pathogenesis of atherosclerosis. While high levels of LDL particles in the blood correlate with a high risk in developing cardiovascular diseases, high levels of HDL have an atheroprotective function (Hegele, 2009). HDL particles are a heterogeneous group of lipoproteins composed of cholesteryl esters and triglycerides in the core, surrounded by apolipoproteins embedded in a monolayer of phospholipids, unesterified cholesterol (Kontush et al., 2015; Lund-Katz et al., 2003) and sphingolipids, such sphingomyelin and biologically active sphingosine-1-phosphate (S1P; Kontush et al., 2015; Sattler et al., 2010). Two major HDL subclasses, HDL2 and HDL3, were identified according to their densities, whereby HDL3 are small, dense particles and HDL2 larger, less dense particles. However, HDL species in human plasma differ in lipid and protein composition, particle size, shape and density. The two HDL subclasses can further be fractionated into various HDL subspecies on the basis of their physicochemical properties by different techniques, but all have a high density between 1.063 g/ml and 1.21 g/ml in common (Kontush et al., 2015; Lund-Katz et al., 2003). According to their migration behavior in agarose gel electrophoresis, the majority of HDL particles in human plasma are large mature, spherical shaped alpha-HDL particles. A minor group of HDL particles are pre-beta HDL which are poorly lipidated, discoidal particles consisting of mostly apoA-I, the predominant 28 kDa apolipoprotein in HDL, embedded in phospholipids and some free cholesterol (Kontush et al., 2015; Kontush and Chapman, 2006). Other protein components of HDL include apoA-II, the second major apolipoprotein in HDL, and some minor apolipoproteins (C, D, E, F, H, J, L, and M; Kontush et al. 2015). The lecithin:cholesterol acyltransferase (LCAT) and the phospholipid transfer protein (PLTP) are also carried by HDL and involved in the HDL metabolism. LCAT catalyzes the conversion of free cholesterol on

the HDL surface to cholesteryl ester, thereby resulting in the migration of cholesteryl esters to the core of HDL. PLTP transfers phospholipids to HDL particles, thereby regulating the HDL size (Kontush et al., 2015).

Nascent lipid-poor pre-beta HDL and lipid-free apoA-I are generated by the liver and intestine or by interconversion of HDL2 and HDL3, which in turn serve as precursors for the generation of mature HDL2 and HDL3. The precursors become lipid-rich alpha-shaped HDL3 particles by incorporating phospholipids and free cholesterol from peripheral cells during the RCT, or from other lipoproteins. The HDL particles continue to grow to large HDL2 particles by fusion with other HDL3 particles and continuous esterification of cholesterol (von Eckardstein et al., 2001).

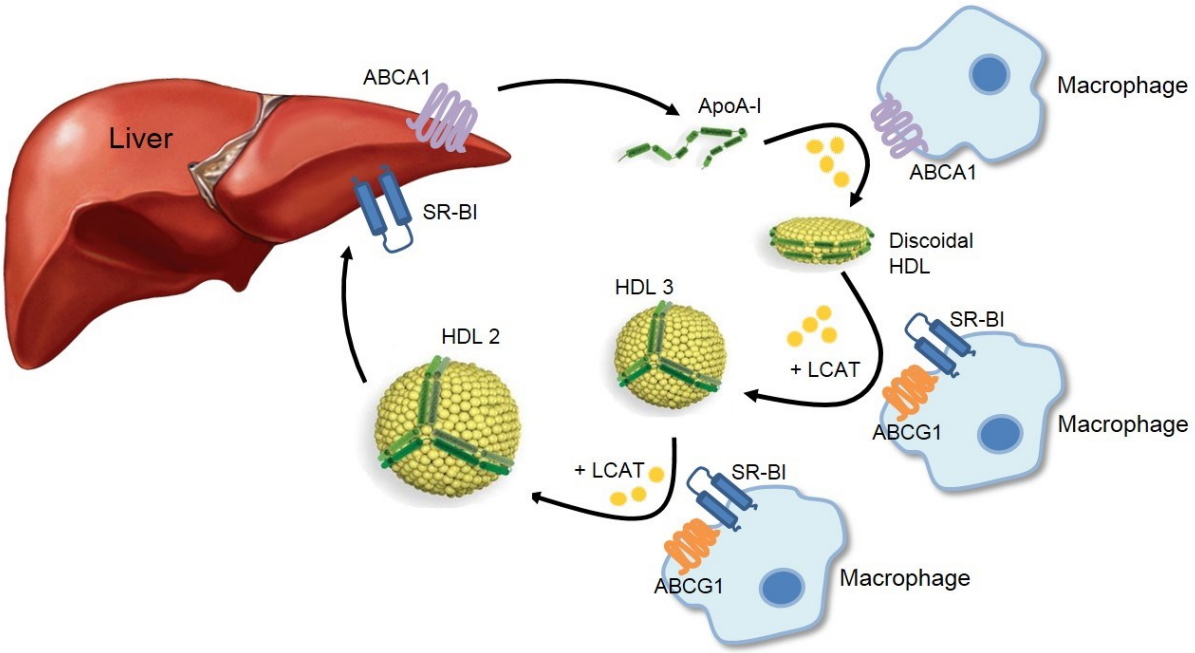

Figure 2: HDL maturation in the reverse cholesterol transport pathway.
Lipid-free apoA-I is secreted by the liver and released to the plasma for circulation to macrophages. ApoA-I takes up phospholipids and free cholesterol from macrophages via the transporter protein ABCA1, thereby forming lipid-poor discoidal HDL particles. Acquiring additional lipids by other transporters, ABCG1 or SR-BI, transforms HDL in spherical HDL3 particles. LCAT converts free cholesterol to cholesteryl esters, which migrate to the core of HDL. Transportation of further free cholesterol transforms HDL3 to large HDL2 particles. HDL-cholesterol can be delivered by HDL directly to the liver via SR-BI. ApoA-I, apolipoprotein A; ABCA1, ATP-binding cassette A 1; ABCG1, ATP-binding cassette G 1; HDL, high-density lipoprotein; LCAT, lecithin:cholesterol acyltransferase; SR-BI, scavenger receptor class B type 1. (Modified from Remaley, A.T. et al., *Cardiovasc Res.* 2014 Aug:103(3):423-8)

1.4 Beneficial HDL functions in atherosclerosis

HDL has been described to protect against atherosclerosis, as it possesses anti-inflammatory functions, preserves LDL particles from oxidation, and plays an important role in the RCT by removing excess cholesterol from peripheral cells (Ansell et al., 2004; Ohashi et al., 2005; Sattler and Levkau, 2009). Oxidative modified LDL retains in the artery wall and leads to the stimulation of inflammatory pathways. Macrophages are recruited to the inflamed sites and take up the modified LDL, which leads to the formation of macrophage foam cells, and therefore the formation of an atherosclerotic plaque and further inflammatory responses. By binding of oxidized lipids via apoA-I and the ability of the HDL-associated enzyme paraoxonase to break down these oxidized lipids, HDL can inhibit oxidation of LDL. Therefore HDL decreases the risk for cytotoxic foam cell formation, hence protecting from atherosclerosis and inflammatory responses (Ansell et al., 2004; Aviram et al., 1998). As mentioned, the reverse transport of peripheral cholesterol to the liver, thus preventing macrophage foam cell formation, is considered as an important anti-atherogenic function of HDL. The HDL receptor scavenger receptor type B class 1 (SR-BI) is known to play a critical role in this pathway (Phillips, 2014).

1.5 The scavenger receptor type B class 1

The HDL receptor SR-BI (gene name *Scarb1*) is a glycoprotein of the class B scavenger receptor family with an approximate molecular mass of 82 kDa. SR-BI proteins have a heavily *N*-glycosylated extracellular domain, two transmembrane domains, and cytoplasmic N- and C-terminal domains. The receptor is highly expressed in several tissues and types of cells, such as hepatocytes, macrophages, endothelial cells but also in steroidogenic tissues, including ovarian steroidogenic cells. Besides acting as a high affinity receptor for HDL, SR-BI can also bind LDL, VLDL, and phospholipids (Krieger, 2001). In mediating cellular uptake of several lipids including cholesteryl esters, phospholipids, and trigylcerides from HDL, SR-BI participates in the RCT pathway and in HDL metabolism (Phillips, 2014; Yancey et al., 2003). However, SR-BI also mediates bidirectional movement of free cholesterol between cells and HDL, depending on the direction of the cholesterol gradient (Yancey et al., 2003). The phospholipid content of HDL is crucial for free cholesterol flux from cells to HDL, as SR-BI does not mediate the transport of free cholesterol to lipid-free apoA-I (Phillips,

2014; Yancey et al., 2003). Previous studies have shown that SR-BI is localized in lipid rafts and/or caveolae (enriched in caveolin proteins) of the plasma membrane, which are cholesterol and sphingolipid enriched membrane microdomains (Babitt et al., 1997; Graf et al., 1999). Caveolae are found at the cell surface throughout the body (Gratton et al., 2004) and participate in the SR-BI-mediated uptake of cholesteryl ester (Graf et al., 1999). Overexpression of hepatic SR-BI has been shown to increase the transport of HDL-cholesterol to the liver and excretion into bile (Kozarsky et al., 1997), thereby reducing the development of atherosclerosis, which was shown in LDL-receptor deficient mouse models (Arai et al., 1999; Kozarsky et al., 2000). On the contrary, the development of atherosclerosis was increased through the deletion of SR-BI in LDL receptor or apoE knockout mice (Covey et al., 2003; Trigatti et al., 1999).

1.6 Mechanism of cholesterol efflux in the RCT

The RCT is a mechanism by which excess cholesterol from peripheral tissues is taken up by macrophages and transferred to HDL and further transported to the liver for excretion. Therefore, the RCT is considered a preventive mechanism in the occurrence of atherosclerosis (Rosenson et al., 2012). Movement of cholesterol from cells to HDL is mediated along with the removal of phospholipids by passive and active efflux processes. Aqueous diffusion and SR-BI mediated diffusion are passive processes, whereas active processes involve the transmembrane transporters adenosine triphosphate (ATP)-binding cassette A 1 (ABCA1) and G 1 (ABCG1; Phillips 2014; Oram 2003). The aqueous diffusion is a bidirectional process, driven by a cholesterol concentration gradient. Incubation of cholesterol-loaded HDL and cells results in an exchange of cholesterol between HDL and the cell plasma membrane. The rate of this simple diffusion is dependent on the size of HDL. Smaller HDL particles are more capable of absorbing cholesterol from cell membranes (Yancey et al., 2003).

1.6.1 SR-BI-mediated cholesterol flux

In the cholesterol efflux pathway, mature HDL binds via apoA-I to the extracellular domain of SR-BI with high affinity (Shen et al., 2014; Valacchi et al., 2011). Binding of HDL results in release of cholesteryl esters from the HDL core without internalizing the lipoprotein (Rodrigueza et al., 1999). As mentioned, this is a passive transport

mechanism, this implies that cholesteryl esters move along a concentration gradient (Phillips, 2014). Several studies reported a decrease of HDL-cholesterol in the circulation by hepatic overexpression of SR-BI in mouse models, thus indicating an important function in reducing development of atherosclerosis (Ji et al., 1999; Kozarsky et al., 1997, 2000, Ueda et al., 1999, 2000; Wang et al., 1998).

1.6.2 ABC transporter-mediated cholesterol efflux

The ABCA1 and ABCG1 transmembrane transporters require ATP as an energy source and mediate the active removal of free cholesterol from peripheral cells. The acceptors for the ABCG1-mediated cholesterol efflux are mature HDL particles whereas lipid-free apoA-I is the major binding protein for ABCA1. Especially macrophages highly express ABCA1 and ABCG1 on their surfaces. Macrophages can take up massive amounts of unesterified cholesterol and turn it into less toxic cholesteryl ester by the action of the ACAT (Cavelier et al., 2006).

ABCA1 mediates transportation of cholesterol from cholesterol-enriched plasma membranes to apoA-I, thereby forming HDL (Yancey et al., 2003). Studies in 1999 (Hayden et al., 1999; Lawn et al., 1999; Rust et al., 1999; Schmitz et al., 1999) identified mutations of the ABCA1 expressing gene in patients with Tangier disease, resulting in defective ABCA1 transporters. These studies revealed that patients with Tangier disease have poorly lipidated apoA-I and do not possess the capability to form mature HDL particles, resulting in severely reduced levels of HDL in plasma (Yancey et al., 2003). How exactly apoA-I interacts with ABCA1 has not been discovered yet. However, a few studies indicate that apoA-I binding to ABCA1 is important for cholesterol removal from lipid domains, but must be dependent on further yet unknown processes (Oram, 2003). The transcription of the ABCA1 gene can be induced by several molecules, such as cyclic adenosine monophosphate (cAMP), cytokines, such as interferon-γ, or by activated nuclear receptors, liver X receptor (LXR) alpha or beta and retinoid X receptor (RXR; Oram, 2003; Santamarina-Fojo et al., 2001). Activation of LXR and RXR is triggered by binding to excess oxidized cholesterol and retinoid acid, respectively (Oram, 2003).

1.7 Sphingolipid metabolism

First described by John L. W. Thudichum in 1884 while studying the chemical composition of the brain (Thudichum, 1884), sphingolipids are known today to play a role in membrane biology and are also involved in many physiological and pathophysiological processes (Gault et al., 2010). Hundreds of different sphingolipids are ubiquitously synthesized in animals, plants and fungi, and play a role in cell membrane composition of eukaryotes (Gault et al., 2010; Hannun and Bell, 1989). However, sphingolipids not only have structural functions, they are signaling molecules regulating specific cellular targets, such as protein kinases, lipases, enzymes, and receptors (Hannun and Obeid, 2017). Many sphingolipids play an important role in cardiovascular diseases, oncology, diabetes, adipositas, immunological and neurological diseases (Hannun and Obeid, 2017). An altered sphingolipid metabolism is observed in many pathological conditions. Patients with coronary artery disease, for example, showed decreased levels of the sphingolipid metabolite S1P in plasma and HDL (Sattler et al., 2010). Important sphingolipid metabolites include ceramides, sphingosine, S1P, and ceramide-1-phosphate (C1P). By regulating signaling pathways, these metabolites are involved in cellular processes including cell growth, differentiation, cell migration, inflammation, and apoptosis (Hannun and Obeid, 2008). All sphingolipids have the sphingoid long chain base backbone in common, mostly sphingosine, a polar head group, and a fatty acid linked by an amide to the sphingoid base. Furthermore, all sphingolipids derive from the lipid ceramide. Once ceramide is generated, it serves as a precursor for more complex sphingolipid metabolites. Ceramides can be generated in three ways. The *de novo* biosynthesis is initiated in the cytosolic compartment of the ER and involves the action of the serine palmitoyl transferase (SPT), which generates 3-keto-dihydrosphingosine from the condensation of serine and palmitoyl coenzyme A (CoA). Sequential reactions lead to the formation of ceramide, which can differ in length of the fatty acid chain, saturation and hydroxylation. Ceramide can also be formed by acetylation of sphingosine through ceramide synthases in the salvage pathway, or by hydrolysis of sphingomyelin through sphingomyelinases. Ceramides differ in length and serve as precursors for sphingomyelin which is generated in the Golgi and act as an important member of the plasma membrane. Ceramides can also be phosphorylated to C1P or catabolized by the action of one of five distinct ceramidases (acid ceramidase, neutral ceramidase, alkaline ceramidase 1, alkaline ceramidase 2, and alkaline ceramidase 3) to form

sphingosine. Sphingosine in turn can be phosphorylated to S1P which is catalyzed by ATP-dependent sphingosine kinases, SK1 or SK2 (Coant et al., 2017; Hannun and Obeid, 2008). The two sphingosine kinases are localized in different cellular compartments. SK1 is localized in the cytosol and translocates to the plasma membrane upon activation, whereas SK2 is mainly found in the nucleus, but also in the plasma membrane, cytosol, and associated with mitochondria or with the ER under stress conditions (Evangelisti et al., 2016; Saba and Hla, 2004). Synthesis and degradation of S1P are tightly regulated to maintain cellular S1P levels. Intracellular S1P is degraded by either two distinct ER-resident S1P phosphatases, SPP1 and SPP2, or by ER-located S1P lyase. The two SPPs belong to the family of lipid phosphate phosphatases (LPPs). The action of SPP1 and SPP2 involves the reversible dephosphorylation of S1P to sphingosine, whereas degradation of S1P at the C2-C3 bond to phosphoethanolamine and hexadecenal by S1P lyase represents an irreversible degradation mechanism. Extracellular S1P is rapidly dephosphorylated to sphingosine by unspecific membrane-bound LPPs. Besides degrading extracellular S1P, LPPs also catalyze dephosphorylation of ceramide-1-phosphate, phosphatidic acid, and lysophosphatidic acid, thereby regulating the intracellular lysophospholipid content (Takabe et al., 2008).

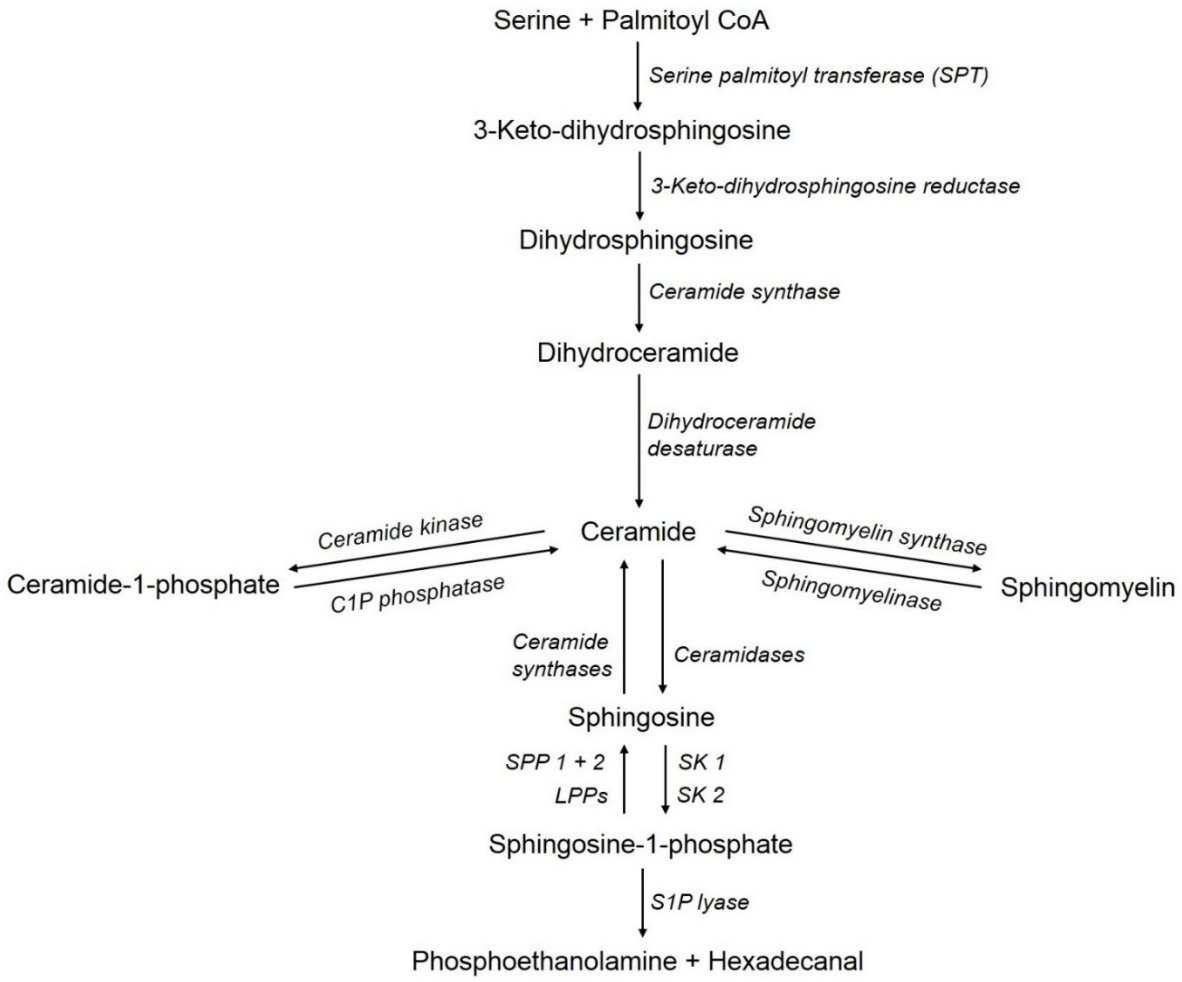

Figure 3: Pathway of sphingolipid *de novo* biosynthesis.
Schematic pathway of sphingolipid biosynthesis from serine and palmitoyl CoA to phosphoethanolamine and hexadecanal. (Modified from Hannun, Y.A. and Obeid, L.M., *Nat Rev Mol Cell Biol.* 2018 Mar;19(3):175-91)

1.8 Sphingosine-1-phosphate

Initially recognized only as an intermediate molecule in the process of sphingosine degradation, S1P is known today to act as an important lipid signaling molecule regulating multiple cellular processes in eukaryotes, such as cell growth and suppression of ceramide-mediated apoptosis (Spiegel and Milstien, 2003). Due to the tight regulation of S1P generation and degradation, cellular levels of S1P are generally in the low nanomolar range (Tani et al., 2005), while high levels of S1P (0.1 µM-1 µM) are found in human blood and lymphatic fluid (Hammad et al., 2012; Karuna et al., 2011; Sattler et al., 2010; Yatomi et al., 1997). The main sources of plasma S1P are

blood cells (i.e. erythrocytes, platelets, and leukocytes) (Książek et al., 2015; Tani et al., 2005) and endothelial cells represent the major source of S1P in lymph (Pappu et al., 2007; Pham et al., 2010; Venkataraman et al., 2008). Some studies also reported mast cells and macrophages as sources for S1P (Jolly et al., 2004, 2005; Xiong et al., 2013).

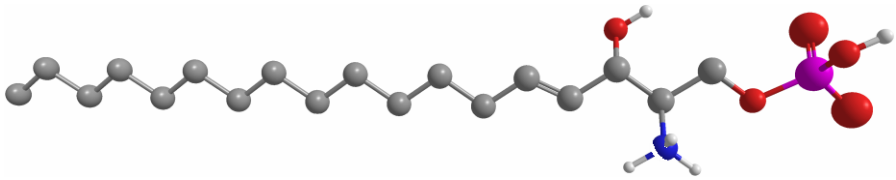

Figure 4: Three-dimensional molecular structure of sphingosine-1-phosphate.
Grey, carbon; white, hydrogen; red, oxygen; blue, nitrogen; purple, phosphate.
(Kindly provided by Julian Jentsch)

Once produced in cells, S1P can function as a second messenger mobilizing calcium to elicit intracellular responses for cell proliferation (Ader et al., 2009; Ishii et al., 2004; Olivera and Spiegel, 1993) and survival (Cuvillier et al., 1996). S1P can also be secreted out of the cells to bind to specific G protein-coupled receptors (termed S1P1-S1P5) in the plasma membrane (Zhou and Blom, 2015). S1P is able to move freely between membranes. However, transporter proteins are necessary in order to secrete S1P out of the cell. Some authors hypothesize that the ABC transporter family is involved in the release of S1P from several tissues in rodents (Kobayashi et al., 2009; Mitra et al., 2006; Sato et al., 2007; Takabe et al., 2010). The Spinster homolog 2 (Spns2) transporter has also been reported to be involved in the S1P release from cells. Spns2 as a S1P transporter was first identified in zebrafish (Kawahara et al., 2009; Osborne et al., 2008) and regulates S1P-dependend trafficking of T and B cells in mice (Fukuhara et al., 2012).

1.8.1 S1P signaling via S1P receptors

Extracellular S1P exerts many effects by binding to and activating five specific S1P receptors (S1PRs), S1P1-S1P5 (formerly endothelial differentiation gene, EDG1-5). These receptors belong to the G protein-coupled receptor (GPCR) family and are ubiquitously expressed in different cell types (Brinkmann, 2007; Strub et al., 2010). All GPCRs have seven helical segments in common that span the membrane, an extracellular *N*-terminal domain, and an intracellular *C*-terminal domain. A GPCR interacts with a heterotrimeric G protein possessing an α-, β-, and γ-subunit. Ligand binding to a GPCR results in conformational change in the receptor. Upon ligand binding, the guanosine diphosphate (GDP) bound to the α-subunit (Gα) is exchanged by guanosine triphosphate (GTP) which results in subsequent Gα activation as well as dissociation from the receptor and $\beta\gamma$-subunits. The activated Gα can then interact with other membrane proteins to transduce an intracellular or intercellular signal (Pierce et al., 2002; Tuteja, 2009). More than 20 α-subunits have been identified so far which can all be separated into four Gα protein classes ($G_{i/o}$, G_s, G_q, $G_{12/13}$; Conklin and Bourne, 1993; Neer, 1995).

The expression of the five S1PRs is dependent on the tissue and cell type. S1P1-S1P3 are widely expressed in a variety of different cell types and are necessary for the maturation of the vasculature during embryogenesis (Anliker and Chun, 2004; Brinkmann, 2007; Kono et al., 2004), whereas S1P4 was only discovered in hematopoietic and lymphoid tissues as well as in the lung (Gräler et al., 1998). S1P5 was identified to be expressed in the brain, spleen, and skin (Anliker and Chun, 2004). Binding of S1P to one of the S1PRs has been studied *in vitro* in many cell types (Sanchez and Hla, 2004) and occurs in the low nanomolar range (2-30 nM; Murata et al., 2000). Coupling of S1P to the receptors results in the activation of phospholipase C, Rac and Rho GTPases, activation of mitogen-activated protein (MAP) kinases and phosphatidylinositol 3-kinase (PI3K)/Akt signaling pathways, or inhibition of adenylyl cyclase (Ishii et al., 2004; Sanchez and Hla, 2004). S1P binding results in activation or inhibition of various signaling pathways to regulate cellular responses such as cell differentiation, cell migration, and cell survival via different G proteins.

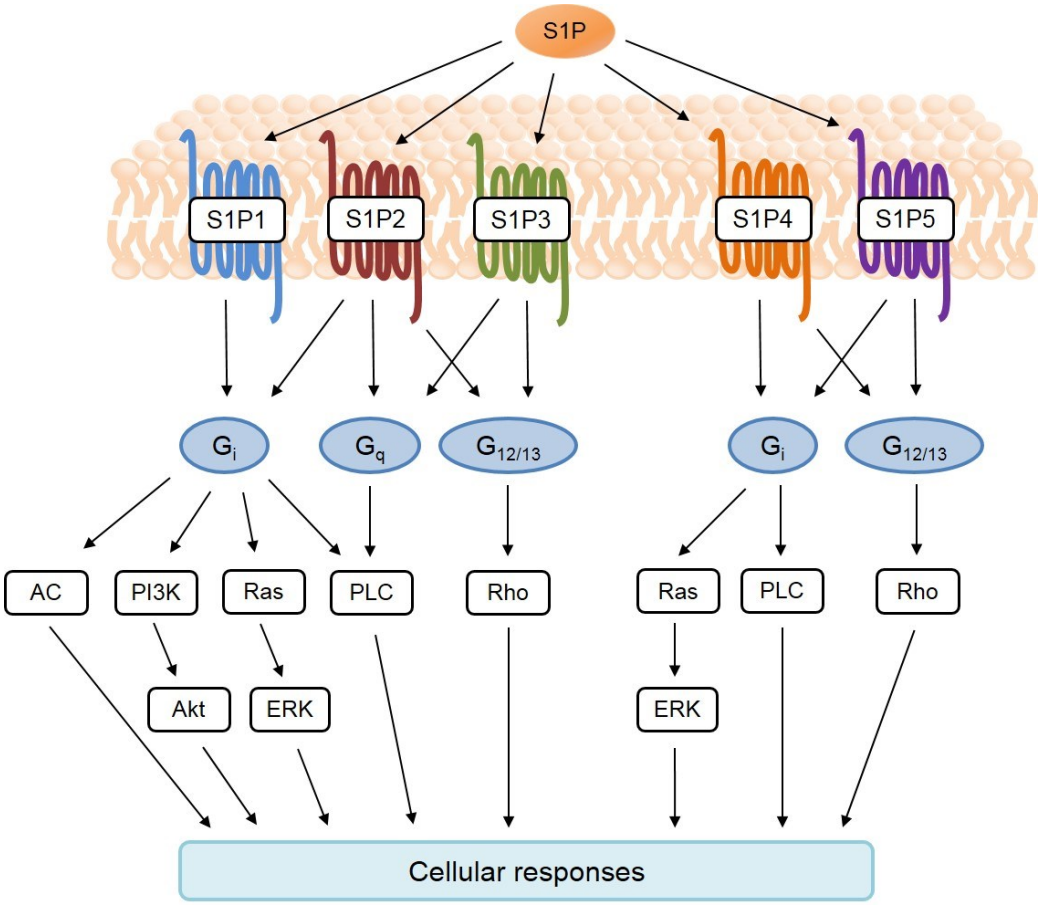

Figure 5: S1P signaling via five G protein-coupled S1P receptors.
Binding of S1P to various S1P receptors leads to activation or inhibition of downstream signaling pathways through coupling to G proteins, and activation of cellular responses. AC, adenylyl cyclase-cyclic AMP; PI3K, phosphatidylinositol 3-kinase; ERK, extracellular signal-regulated kinase; PLC, phospholipase C. (Modified from Spiegel, S. and Milstien, S., *Nat Rev Mol Cell Biol.* 2003 May;4(5):397-407)

In this study, the S1PRs of interest are the human receptors S1P1, S1P2, and S1P3. The first identified S1PR was S1P1, which was isolated *in vitro* from differentiating human umbilical vein endothelial cells (Hla and Maciag, 1990). This receptor is highly expressed on immune cells, in endothelial cells of the cardiovascular system, in the brain, lung, spleen and kidney (Strub et al., 2010), and has been shown to regulate vascular development, angiogenesis and trafficking of immune cells via the G_i protein (Means et al., 2008). In contrast, S1P2 and S1P3 elicit downstream signaling pathways via G_i, G_q and $G_{12/13}$ (Spiegel and Milstien, 2003). Studies have shown that activation of S1P2 results in pro-atherosclerotic effects (Skoura et al., 2011), whereas binding of S1P to S1P1 and S1P3 exerts mainly anti-atherosclerotic functions. In detail, the

stimulation of S1P1 and S1P3 by HDL-associated S1P promotes endothelial cell migration and survival (Kimura et al., 2003), and the activation of S1P3 by HDL-S1P results in NO-dependent vasorelaxation (Nofer et al., 2004).

1.8.2 S1P contribution to HDL-mediated biological functions

Due to its amphipathic structure, extracellular S1P needs to bind to carriers to be present in biological fluids. In the blood circulation, bioactive S1P is mostly associated with apoM (65-80 %) of HDL (Christoffersen et al., 2011; Kontush et al., 2007; Sattler et al., 2010) followed by albumin (~30 %) and other lipoproteins (Aoki et al., 2005). However, only 5 % of the apoM-carring HDL particles actually bind S1P (Christoffersen et al., 2006, 2011). Binding of S1P occurs with high affinity which makes HDL the major carrier for S1P (Kontush et al., 2007). As a consequence, high plasma levels of HDL-S1P positively correlate with high plasma levels of HDL-cholesterol comprising apoA-I and apo A-II (Sattler and Levkau, 2009; Zhang et al., 2005). This finding supports the role of S1P in contributing to atheroprotective properties of HDL (Levkau, 2015; Sato and Okajima, 2010; Sattler and Levkau, 2009). Various functions of HDL *in vitro* and *in vivo* can be attributed to HDL-associated S1P by binding to S1P receptors (Kimura et al., 2003; Miura et al., 2003; Nofer et al., 2001, 2004; Sattler and Levkau, 2009; Theilmeier et al., 2006). For instance, HDL-associated S1P is a potent mediator in stimulating long-term responses in cells, such as improving endothelial barrier integrity as well as the nitric oxide (NO)-dependent vasodilation, endothelial angiogenesis, and various anti-oxidative, anti-inflammatory, and anti-apoptotic functions are induced by HDL-S1P (Sattler and Levkau, 2009).

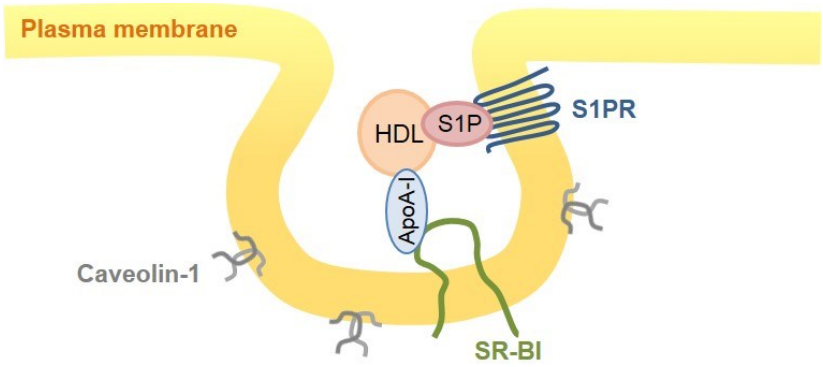

Figure 6: Illustration of a possible interaction between S1PRs and SR-BI via HDL in caveolae.

Studies identified S1PRs to be located in caveolae, where also SR-BI has been found (Graf et al., 1999; Gratton et al., 2004; Igarashi and Michel, 2000; Means et al., 2008), suggesting an interaction between S1PRs and SR-BI (Fig. 6). However, if and how HDL-signaling via S1PRs interact with SR-BI-mediated functions within these membrane microdomains, needs to be determined.

2 Aim of the study

HDL is a complex molecule carrying several proteins and hundreds of lipids including S1P, the bioactive sphingolipid, which is responsible in part for many biological HDL functions. By stimulating various signaling pathways and the delivery of excess unesterified cholesterol from peripheral cells to the liver in the reverse cholesterol transport pathway, HDL plays a central role in atheroprotection and cardiovascular medicine. As recently recognized, HDL delivers endogenous or exogenously supplied S1P to the cell surface, where S1P couples to S1P receptors exerting their own downstream signaling pathways and inducing multiple responses involved in immunomodulation, inflammation and cardiovascular functions. However, if and how S1P receptors are involved in HDL functions that are mediated by SR-BI is not known. As an important step toward understanding a possible relationship between S1P receptors and the SR-BI-mediated removal of cholesterol from cells to acceptors, cell lines overexpressing the SR-BI receptor and/or S1P receptors will be used to study the interaction between both in the removal of cholesterol. In this regard, the first aim of this study is to evaluate the influence of S1P receptors 1-3 on the export of cholesterol from CHO cells to two cholesterol acceptors, lipid-free apoA-I and mature HDL. In addition, in order to evaluate whether prior stimulation of the S1P receptors might alter the cholesterol efflux, S1P receptors will be stimulated before studying cholesterol efflux.

The second part of this study will focus on the cholesterol efflux to HDL in CHO cells co-expressing SR-BI with the S1P receptors such as S1P1. To this end, a lentiviral vector system of the third generation will be generated, expressing the murine SR-BI receptor tagged to a myc-peptide along with the fluorescent protein eGFP. Furthermore, the vector construct will be incorporated into CHO-K1 cell lines as well as CHO cells expressing human S1P1 (CHO-hS1P1). Further studies include the implementation of the transduced cell lines in the study of cholesterol efflux to HDL with and without S1P stimulation using ^{3}H-cholesterol, and the assessment of any interactions between SR-BI and S1P1 in the cholesterol efflux.

The third part of this study will test whether there is an interaction between SR-BI and S1P1 in cellular signaling pathways, such as MAP kinases. To attain this, the transduced CHO cells will be stimulated with S1P or HDL to assess the impact of SR-BI on the S1P1-mediated MAPK pathway as a functional readout for S1P signaling in this system.

3 Materials

3.1 Chemicals, reagents and solutions

Description	Supplier
[1,2-^{3}H(N)]-Cholesterol	Perkin Elmer, Waltham, MA, USA
2-Mercaptoethanol	Sigma-Aldrich, St. Louis, MO, USA
2-Propanol	Carl Roth, Karlsruhe, Germany
Acrylamide 4K solution, 30 % Mix 37.5:1	AppliChem, Darmstadt, Germany
Agar, dehydrated, Bacto™	Becton Dickinson, Franklin Lakes, NJ, USA
Agarose	Biozym Scientific, Hessisch Oldendorf, Germany
Ammonium persulfate (APS), ≥98 %	Sigma-Aldrich, St. Louis, MO, USA
Ampicillin sodium salt powder	Sigma-Aldrich, St. Louis, MO, USA
Antibiotic-Antimycotic solution, (100x) (Gibco™)	Thermo Fisher Scientific, Waltham, MA, USA
Apolipoprotein A-I, human	Acris Antibodies, Herford, Germany
Aprotinin	Sigma-Aldrich, St. Louis, MO, USA
Aqua ad iniectabilia (pure water)	B. Braun Melsungen, Melsungen, Germany
Bromophenol blue	Sigma-Aldrich, St. Louis, MO, USA
Chloroquine diphosphate salt	Sigma-Aldrich, St. Louis, MO, USA
Coomassie brilliant blue R 250	Merck, Darmstadt, Germany
Dimethyl sulfoxide (DMSO)	Sigma-Aldrich, St. Louis, MO, USA
Disodium hydrogen phosphate (Na_2HPO_4)	Sigma-Aldrich, St. Louis, MO, USA
DMEM, high glucose (4.5 g/l)	Thermo Fisher Scientific, Waltham, MA, USA
DNA ladder, 1 kb, GeneRuler™	Thermo Fisher Scientific, Waltham, MA, USA

DNA loading dye, 6x	Thermo Fisher Scientific, Waltham, MA, USA
Ethylene diamine tetraacetic acid (EDTA)	Sigma-Aldrich, St. Louis, MO, USA
Ethidium bromide, 0.07 %	Inno-Train Diagnostik, Kronberg im Taunus, Germany
FastDigest Green Buffer, 10x	Thermo Fisher Scientific, Waltham, MA, USA
Fetal bovine serum (FBS)	Thermo Fisher Scientific, Waltham, MA, USA
Geneticin™ Selective Antibiotic (G418 Sulfate), 50 mg/ml	Thermo Fisher Scientific, Waltham, MA, USA
Gentamicin, 10 mg/ml (Gibco™)	Thermo Fisher Scientific, Waltham, MA, USA
Glycine	AppliChem, Darmstadt, Germany
Ham's F-12 Nutrient Mixture, GlutaMAX™-I Supplement	Thermo Fisher Scientific, Waltham, MA, USA
HCl, 6 M	AppliChem, Darmstadt, Germany
HEPES buffer solution, 1 M	Thermo Fisher Scientific, Waltham, MA, USA
Human Plasma	University Hospital Essen, Germany
Hydrogen peroxide (H_2O_2), 30 %	AppliChem, Darmstadt, Germany
Isopropyl alcohol	Carl Roth, Karlsruhe, Germany
iQ™ SYBR® Green Supermix	Bio-Rad, Hercules, CA, USA
Leupeptin	Sigma-Aldrich, St. Louis, MO, USA
L-Glutamine, 200 mM	Thermo Fisher Scientific, Waltham, MA, USA
Luminol sodium salt	Sigma-Aldrich, St. Louis, MO, USA
MEM alpha, no nucleosides, powder	Thermo Fisher Scientific, Waltham, MA, USA
MEM non-essential amino acids solution (100 x)	Thermo Fisher Scientific, Waltham, MA; USA

Methanol	Merck Millipore, Darmstadt, Germany
NaCl	Sigma-Aldrich, St. Louis, MO, USA
NaOH, 8 M	AppliChem, Darmstadt, Germany
n-Hexan, 95 %	AppliChem, Darmstadt, Germany
Nonfat dried milk powder	AppliChem, Darmstadt, Germany
Nonidet® P 40 Substitute (NP-40)	Honeywell International (Fluka), Morris Plains, NJ, USA
p-Coumeric acid	Sigma-Aldrich, St. Louis, MO, USA
Phenylmethylsulfonyl fluoride (PMSF)	Sigma-Aldrich, St. Louis, MO, USA
Phosphate buffered saline (PBS) powder	AppliChem, Darmstadt, Germany
Penicillin/Streptomycin, 100x	Thermo Fisher Scientific, Waltham, MA, USA
Potassium bromide	Sigma-Aldrich, St. Louis, MO, USA
Prestained protein ladder Cozy™	highQu, Kraichtal, Germany
Protamine sulfate	Sigma-Aldrich, St. Louis, MO, USA
Sandoz 58-035 (Acyl-CoA:cholesterol acyltransferase inhibitor)	Sigma-Aldrich, St. Louis, MO, USA
Sodium deoxycholate	Sigma-Aldrich, St. Louis, MO, USA
Sodium dodecyl sulfate (SDS) ultrapure	AppliChem, Darmstadt, Germany
Sodium hydrogen carbonate ($NaHCO_3$)	AppliChem, Darmstadt, Germany
Sodium orthovanadate	Sigma-Aldrich, St. Louis, MO, USA
Sodium pyruvate (100 mM)	Thermo Fisher Scientific, Waltham, MA, USA
Sphingosine-1-phosphate, D-erythro; (dissolved in methanol)	Enzo Life Sciences, Zandhoven, Belgium
TEMED, 99 %, p.a.	Carl Roth, Karlsruhe, Germany
Tris base for buffer solutions	AppliChem, Darmstadt, Germany
Trypan blue solution, 0.4 %	Sigma-Aldrich, St. Louis, MO, USA

Trypsin-EDTA, 0.25 %	Thermo Fisher Scientific, Waltham, MA, USA
Tryptone, Bacto™	Becton Dickinson, Franklin Lakes, NJ, USA
Tween® 20	Honeywell International (Riedel-de Haën), Morris Plains, NJ, USA
Yeast Extract, Bacto™	Becton Dickinson, Franklin Lakes, NJ, USA

3.2 Consumable material

Description	Supplier
96 fast PCR plate fullskirt	Sarstedt, Nümbrecht, Germany
Centrifuge tubes (15 ml, 50 ml)	Sarstedt, Nümbrecht, Germany
Chromatography filter paper (3 mm)	Whatman, Maidstone, UK
Pipet tips (10, 20, 200, 1000, 1250 µl)	Sarstedt, Nümbrecht, Germany
PVDF Immobilon®-P transfer membrane (0.45 µm)	Merck Millipore, Burlington, MA, USA
Micro tubes SafeSeal (0.2, 1.5, 2.0 ml)	Sarstedt, Nümbrecht, Germany
Parafilm® M	Bemis, Neenah, WI, USA
Sterile syringe filters, 0.2 µm	Sartorius, Göttingen, Germany
Tissue culture dishes (10 cm)	Sarstedt, Nümbrecht, Germany
Tissue culture flasks T-75 (75 cm^2)	Sarstedt, Nümbrecht, Germany
Tissue culture plates (6-well, 24-well, 96-well)	Sarstedt, Nümbrecht, Germany
Transpartent adhesive qPCR foil	Sarstedt, Nümbrecht, Germany
ZelluTrans dialysis membranes T2, ø 6.4 mm	Carl Roth, Karlsruhe, Germany

3.3 Kits

Description	Supplier
innuPREP RNA Mini Kit	Analytik Jena, Jena, Germany
MinElute Reaction Cleanup Kit	Qiagen, Hilden, Germany
Plasmid Maxi Kit	Qiagen, Hilden, Germany
QIAquick Gel Extraction Kit	Qiagen, Hilden, Germany
Rapid DNA Ligation Kit	Thermo Fisher Scientific, Waltham, MA, USA
RevertAid First Strand cDNA Synthesis Kit	Thermo Fisher Scientific, Waltham, MA, USA

3.4 Devices and reusable material

Description	Supplier
Autoclav Varioklav®	Thermo Fisher Scientific, Waltham, MA, USA
BioPhotometer®	Eppendorf, Hamburg, Germany
Centrifuge 5415 D	Eppendorf, Hamburg, Germany
Centrifuge 5810 R	Eppendorf, Hamburg, Germany
Centrifuge Allegra® X-15R	Beckman Coulter, Brea, CA, USA
CO_2-Incubator CB 150	Binder, Tuttlingen, Germany
Dialysis tubing clips	Megro GmbH & Co. KG, Wesel, Germany
Flow cytometer FACSAria™ III	Becton Dickinson, Franklin Lakes, NJ, USA
Flow cytometer Gallios™ 10/3	Beckman Coulter, Brea, CA, USA
Glass serological pipets, Pyrex®, (5 ml, 10 ml)	Corning, Corning, NY, USA
Ice machine	Scotsman AF-100

Inverted microscope Eclipse TE300	Nikon, Amsterdam, Netherlands
Liquid scintillation analyzer Tri-Carb® 2910TR	Perkin Elmer, Waltham, MA, USA
Magnetic stirrer RCT basic IKAMAG®	IKA, Staufen im Breisgau, Germany
Mini PROTEAN® 3 System	Bio-Rad, Hercules, CA, USA
Mini Trans-Blot® System	Bio-Rad, Hercules, CA, USA
Molecular imager ChemiDoc™ XRS+	Bio-Rad, Hercules, CA, USA
Neubauer hemocytometer	Paul Marienfeld, Lauda-Königshofen, Germany
Peltier Thermal Cycler PTC-200	Bio-Rad (MJ Research), Hercules, CA, USA
pH meter inoLab pH Level 2	WTW by Xylem Analytics, Weilheim, Dinslaken, Germany
Pipets Discovery Comfort single channel (DV10, DV20, DV200, DV1000)	HTL, Warsaw, Poland
Pipet controller pipetus®	Hirschmann Laborgeräte, Eberstadt, Germany
Precision weighing balance LE225D-OCE	Sartorius, Göttingen, Germany
Refrigerated centrifuge 1K15	Sigma-Aldrich, St. Louis, MO, USA
Safety cabinet LaminAir® HB 2472	Heraeus, Hanau, Germany
Screw capped centrifuge tubes (16 x 76 mm)	Beckman Coulter, Brea, CA, USA
Synergy HT microplate reader	BioTek Instruments, Winooski, VT, USA
Thermal cycler C1000™	Bio-Rad, Hercules, CA, USA
Thermal cycler iCycler®	Bio-Rad, Hercules, CA, USA
Thermomixer comfort	Eppendorf, Hamburg, Germany
Ultracentrifuge Optima™ LE-80K	Beckman Coulter, Brea, CA, USA
Ultrasonic homogenizer Labsonic®-M	B. Braun Biotech International, Melsungen, Germany

Vortex	Heidolph, Schwabach, Germany
Water bath	Köttermann Labortechnik

3.5 Software

Description	Supplier
Kaluza Analysis	Beckman Coulter, Brea, CA, USA
KC4™ v3.4	BioTek Instruments, Winooski, VT, USA
Prism 5	GraphPad Software, La Jolla, CA, USA
QuantaSmart™ v4.00	Perkin Elmer, Waltham, MA, USA
Vector NTI®	Thermo Fisher Scientific, Waltham, MA, USA

3.6 Vectors for virus production

1) pBMN.SR-BI.c-myc.IRES.eGFP (generated by the research group of Prof. Dr. Bodo Levkau, Institute for Pathophysiology, University Hospital Essen, Germany)

2) pRRLSIN.cPPT.SFFV.MCS.IRES.eGFP.WPre (LV.IRES.eGFP)

3) pHRSIN.SFFV.eGFP.WPre (LV.eGFP)

4) pGag-pol

5) pRSV-Rev

6) pVSV-G

The plasmids 2) – 6) were kindly provided by Prof. Dr. Hannes Klump (Institute for Transfusion Medicine, University Hospital Essen, Germany).

3.7 Enzymes

Description	Supplier
*Mlu*I FD	Thermo Fisher Scientific, Waltham, MA, USA
Phusion Hot Start II DNA Polymerase, 2 U/µl	Thermo Fisher Scientific, Waltham, MA, USA
*Pst*I FD	Thermo Fisher Scientific, Waltham, MA, USA
*Sca*I FD	Thermo Fisher Scientific, Waltham, MA, USA
T4 DNA ligase, 5 U/µl	Thermo Fisher Scientific, Waltham, MA, USA
Taq polymerase, 5 U/µl	Qiagen, Hilden, Germany
*Xba*I FD	Thermo Fisher Scientific, Waltham, MA, USA

3.8 Oligonucleotides for molecular cloning

All oligonucleotides were ordered in concentrations at 100 µM from Eurofins MWG Operon, Ebersberg, Germany. Oligonucleotides were diluted to 10 µM with 10 mM Tris-HCL (pH 8.0) before usage.

Primer A	5’- aatcTCTAGACCACCATGGGCGGCAGCTCCAGGGCGCGCTG-3’
Primer B	5’- aatcACGCGTTAGAGATCCTCTTCGGAGATGAG-3’

3.9 Strains of bacteria

Description	Supplier
Escherichia coli XL-10 Gold Ultracompetent	Agilent Technologies, Santa Clara, CA, USA

3.10 Oligonucleotide primers for SYBR Green reverse transcription polymerase chain reaction (RT-PCR)

All oligonucleotide primers were ordered in concentrations at 50 µM from BioTez, Berlin, Germany.

eGFP forward	5'-ACGTAAACGGCCACAAGTTC-3'
eGFP reverse	5'-AAGTCGTGCTGCTTCATGTG-3'
Human *S1PR1* forward	5'-CCCTCTCAGACCTGTTGGCAGGAG-3'
Human *S1PR1* reverse	5'-CTGGGCGGGAGTGAGCTTGTA-3'
Human *S1PR2* forward	5'-TTGGCCATCGTGGCCCTGTACG-3'
Human *S1PR2* reverse	5'-CTAGCGTCTGCGGGGCGGCCAT-3'
Human *S1PR3* forward	5'-CGCATCTACTTCCTGGTGAAG-3'
Human *S1PR3* reverse	5'-ACCACAATCACCACGGTCCG-3'
Murine *Abca1* forward	5'-GGAAGAAGCCTTGGGTTGA-3'
Murine *Abca1* reverse	5'-GTGGGGTGAGACATGTGGA-3'
Murine *Abcg1* forward	5'-GATCTAGGCAGAAGGCACTTG-3'
Murine *Abcg1* reverse	5'-TTTCCCAGAGATCCCTTTCA-3'
Murine *Gapdh* forward	5'-AGGTCGGTGTGAACGGATTTG-3'
Murine *Gapdh* reverse	5'-TGTAGACCATGTAGTTGAGGTCA-3'
Murine *Scarb1* forward	5'-TTTGGAGTGGTAGTAAAAAGGGC-3'
Murine *Scarb1* reverse	5'-TGACATCAGGGACTCAGAGTAG-3'

3.11 Cell lines

CHO-K1: A subclone of the parental CHO cell line derived from an ovary of an adult Chinese hamster initiated by T. T. Puck in 1957 (ATCC, 2017).

This was a kind gift of PD Dr. Markus Tölle, Charité, Universitätsmedizin Berlin, Germany.

CHO-hS1P1: CHO-K1 cells transfected with the human $S1P_1$ receptor. Received from Novartis, Basel, Switzerland.

CHO-hS1P2: CHO-K1 cells transfected with the human $S1P_2$ receptor. Received from Novartis, Basel, Switzerland.

CHO-hS1P3: CHO-K1 cells transfected with the human $S1P_3$ receptor. Received from Novartis, Basel, Switzerland.

HEK293T: A subclone of the human embryonic kidney (HEK293) cell line. Expresses the SV40 large T-antigen (ATCC, 2018).

Kindly provided by Prof. Dr. Hannes Klump, Institute of Transfusion Medicine, University Hospital Essen.

HT-1080: Human fibrosarcoma cell line generated from a 35-year old Caucasian male (ATCC, 2014).

Kindly provided by Prof. Dr. Hannes Klump, Institute of Transfusion Medicine, University Hospital Essen.

3.12 Cell culture media

Efflux medium for all CHO cells

90 % MEM alpha

25 mM HEPES

20 mM L-Glutamine

1 % Antibiotic-Antimycotic (1x)

Medium for CHO-K1, CHO-MOCK and CHO-SRB1 cells

90 % Ham’s F-12 Nutrient Mixture

10 % FBS

1 % Antibiotic-Antimycotic (1x)

Medium for CHO-hS1P1, CHO-hS1P1-MOCK and CHO-hS1P1-SRB1 cells

90 % MEM alpha

25 mM HEPES

0.5 mg/ml Geneticin (G418)

10 % FBS

1 % L-Glutamine

1 % Antibiotic-Antimycotic (1x)

Medium for HEK293T cells

90 % DMEM with L-glutamine, high glucose (4.5 g/l)

10 % heat inactivated FBS

1 % Sodium pyruvate

1 % Penicillin (100 U/ml)/Streptomycin (100 µg/ml)

Transduction medium for CHO-K1 cells

90 % F-12 Nutrient Mixture + GlutaMax^{TM}-I

10 % heat inactivated FBS

1 % Antibiotic-Antimycotic (1x)

2 % HEPES

0.1 % Protamine sulfate (4 mg/ml stock solution in H_2O)

Transduction medium for CHO-hS1P1 cells

90 % MEM alpha

10 % heat inactivated FBS

20 mM L-Glutamine

1 % Antibiotic-Antimycotic (1x)

0.5 mg/ml Geneticin (G418)

2 % HEPES

0.1 % Protamine sulfate (4 mg/ml stock solution in H_2O)

Transfection medium for HEK293T cells

90 % DMEM with L-glutamine, high glucose (4.5 g/l)

10 % heat inactivated FBS

1 % Sodium pyruvate

1 % Penicillin (100 U/ml)/Streptomycin (100 µg/ml)

25 µM Chloroquine

Medium for HT1080 cells

90 % DMEM with L-glutamine, high glucose (4.5 g/l)

10 % heat inactivated FBS

1 % Sodium pyruvate

1 % MEM non-essential amino acids

1 % Penicillin (100 U/ml)/Streptomycin (100 µg/ml)

3.13 Antibodies

Description	Supplier
EDG1 (H60) anti-rabbit polyclonal antibody	Santa Cruz Biotechnology, Dallas, TX, USA
GAPDH anti-mouse monoclonal antibody	HyTest, Turku, Finnland
HRP horse anti-mouse IgG antibody (peroxidase)	Vector Laboratories, Burlingame, CA, USA
HRP goat anti-rabbit IgG antibody (peroxidase)	Vector Laboratories, Burlingame, CA, USA
Myc-Tag (9B11) anti-mouse monoclonal antibody	Cell Signaling Technology, Danvers, MA, USA
Phospho-p44/42 MAPK (pERK1/2) (Thr202/Tyr204) polyclonal antibody	Cell Signaling Technology, Danvers, MA, USA

3.14 Media, buffers and solutions

Bacterial Growth Media

LB medium	LB agar
10 g Tryptone	15 g Bacto agar
5 g Yeast extract	Ad 1 liter LB medium
5 g NaCl	
Adjust volume to 1 liter with aqua bidest.	

Ampicillin (100 mg/ml) was added to bacterial growth media after autoclave sterilization.

Agarose gel electrophoresis

50x TAE buffer

242 g Tris base

100 ml Na_2EDTA, 0.5 M

57.1 ml Acetic acid

Ad 1 liter aqua bidest.

pH 8.0

1x TAE buffer

20 % 50x TAE buffer

80 % Aqua bidest.

0.8 % (w/v) Agarose gel

0.8 g Agarose

100 ml TAE buffer, 1x

6 drops of ethidium bromide

1 % (w/v) Agarose gel

1 g Agarose

100 ml TAE buffer, 1x

6 drops of ethidium bromide

Loading dye mix

5 µl DNA loading dye, 6x

20 µl aqua ad iniectabilia

Cell culture and virus production

2x HEPES-buffered saline (HBS) solution

1.4 M NaCl

0.25 M HEPES buffer grade

10 mM Na_2HPO_4

Aqua bidest.

Adjust pH between 7.1 to 7.2

Filter sterilization

1x PBS

4.77 g PBS powder

500 ml aqua bidest.

Sterilized by autoclaving

Sodium dodecyl sulfate polyacrylamide gel electrophoresis (SDS-PAGE)

Lysis buffer

1x PBS

1 % NP-40

0.5 g Sodium deoxycholate

0.1 % SDS

4x Sample buffer

1.0 ml 0.5 M Tris-HCl, pH 6.8

0.8 ml Glycerol

1.6 ml 10 % SDS

0.4 ml 1 % Bromophenol blue

0.4 ml 2-Mercaptoethanol

3.8 ml Aqua bidest.

1 drop of 5 M NaOH

1 % Bromophenol blue

1 g Bromophenol blue

80 ml Aqua bidest.

NaOH until solution turns blue

Adjust volume to 100 ml with aqua bidest.

4 % Stacking gel

990 µl 30 % Acrylamide mix

1.89 ml 0.5 M Tris-HCl, pH 6.8

75 µl 10 % SDS

4.5 ml Aqua bidest.

37.5 µl 10 % APS

7.5 µl TEMED

12 % Resolving gel

4 ml 30 % Acrylamide mix

2.5 ml 1.5 M Tris-HCl, pH 8.8

100µl 10 % SDS

3.3 ml Aqua bidest.

100 µl 10 % APS

4 µl TEMED

1.5 M Tris-HCl, pH 8.8

27.23 g Tris base

80 ml dH_2O

Adjust pH to 8.8 with HCl

Adjust volume to 150 ml with aqua bidest.

0.5 M Tris-HCl, pH 6.8

6.06 g Tris base

~60 ml dH_2O

Adjust pH to 6.8 with HCl

Adjust volume to 100 ml with aqua bidest.

10 % (w/v) APS

0.05 g APS

500 µl Aqua bidest.

10 % (w/v) SDS

1.0 g SDS

10 ml Aqua bidest.

10x Running buffer

30.30 g Tris base

144.10 g Glycine

10 g SDS

Adjust volume to 1 liter with aqua bidest.

1x Running buffer

50 ml 10x Running buffer

450 ml Aqua bidest.

Immunoblotting and immunodetection

Transfer buffer

3.03 g Tris base

14.40 g Glycine

200 ml Methanol

800 ml ice-cold aqua bidest.

1x PBS

9.55 g PBS powder

1 liter aqua bidest.

Washing buffer

50 ml 5 % nonfat dried milk in 1x PBS

450 ml 1x PBS

250 µl Tween® 20

0.1 M Tris-HCl, pH 8.6

12.1 g Tris base

800 ml Aqua bidest.

Adjust pH to 8.6 with HCl

Adjust volume to 1 liter with aqua bidest.

Luminol solution

12.5 mg Luminol

50 ml 0.1 M Tris-HCl, pH 8.6

Coumaric acid solution

6.5 mg p-Coumaric acid

5 ml DMSO

ECL mixture

1 ml Luminol solution

100 µl Coumaric solution

0.3 µl 30 % H_2O_2

4 Methods

4.1 Cloning lentiviral transfer vectors

The murine SR-BI gene (*Scarb1*) fused with a c-myc was cloned into the backbone of a self-inactivating (SIN) lentiviral transfer plasmid of third generation containing a reporter gene encoding for the enhanced green fluorescent protein (eGFP). Lentiviral vectors were produced in HEK293T cells (see 3.2).

4.1.1 Primer design for molecular cloning

All PCR primers used for molecular cloning were designed with the Vector NTI® software (Thermo Fisher Scientific, Waltham, MA, USA) and ordered from Eurofins MWG Operon, Ebersberg, Germany. Primers used are listed in section 3.8.

4.1.2 Amplification of the gene fragment by polymerase chain reaction (PCR)

The coding sequence of SR-BI.c-myc was amplified by standard PCR reactions using a Phusion Hot Start II DNA Polymerase protocol (Thermo Fisher Scientific, Waltham, MA, USA). The plasmid pBMN.SR-BI.c-myc.IRES.eGFP was used as a template. A temperature gradient PCR program was performed to find the optimal annealing temperature for the template primers. The pipetting and cycling instructions are listed in Tables 1 and 2.

Amplified PCR products were analyzed on a 1 % (w/v) agarose gel using 5 µl PCR product and 25 µl loading dye mix. The agarose gel was submerged in a horizontal electrophoresis tank containing 1x TAE buffer. In order to determine the fragment sizes, a 1 kb DNA ladder (GeneRuler™, Thermo Fisher Scientific, Waltham, MA, USA) was additionally loaded onto the gel. DNA fragments were separated at 100 V for 60 min. All clean PCR products (SR-BI.c-myc) were pooled and purified using MinElute Reaction Cleanup Kit (Qiagen, Hilden, Germany).

Table 1: Pipetting instructions for a 50 µl standard PCR reaction

Component	Volume	Final Concentration
5x Phusion HF Buffer	10 µl	1x
10 mM dNTPs	1 µl	200 µM each
10 µM Primer A	0.25 µl	2.5 µM
10 µM Primer B	0.25 µl	2.5 µM
1 µg/µl Template plasmid DNA	0.1 µl	100 ng
Phusion Hot Start II DNA Polymerase (2 U/µl)	0.5 µl	0.02 U/µl
Purified water	add to 50 µl	-

Table 2: Cycling instructions for a gradient PCR program

Cycling Step	Temperature	Time	Cycles
Initial Denaturation	98 °C	30 min	1
Denaturation	98 °C	10 min	35
Annealing	50-70 °C	30 min	
Extension	72 °C	1 min	1
Final Extension	10 °C	∞	1

4.1.3 Restriction digestion and gel extraction

The final reporter construct was generated by digestion of the PCR product SR-BI.c-myc and ligation into the multiple cloning site (MCS) of the digested target vector backbone pRRLSIN.cPPT.SFFV.MCS.IRES.eGFP.WPre (LV.IRES.eGFP; kindly provided by Prof. Dr. Hannes Klump, Institute of Transfusion Medicine, University Hospital Essen, Germany). The target vector backbone was composed of a spleen focus-forming virus (SFFV) promoter, an internal ribosome entry site (IRES), and an eGFP reporter gene. Digestion reactions of both the PCR product and vector

backbone were set up in 100 µl volumes (see Table 3) and carried out for 30 min at 37 °C.

Table 3: Digestion instructions for a 100 µl reaction

Component	Volume	Final Concentration
DNA sample	-	10 µg
10x Fast Digest Green Buffer	10 µl	1x
1 U/µl Restriction *Mlu*I	5 µl	5 U
1 U/µl Restriction *Xba*I	5 µl	5 U
Purified water	add to 100 µl	

Digested DNA samples and a 1 kb DNA ladder (GeneRuler™, Thermo Fisher Scientific, Waltham, MA, USA) were separated on a 0.8 % (w/v) agarose gel at 100 V for 30 min. The desired fragments were excised and purified using the QIAquick Gel Extraction Kit (Qiagen, Hilden, Germany) according to the manufacturer's instructions.

4.1.4 Ligation

The target plasmid pRRLSIN.cPPT.SFFV.SR-BI.c-myc.IRES.eGFP.WPre (LV.SR-BI.IRES.eGFP) was made by ligation of insert DNA SR-BI.c-myc into the vector backbone LV.IRES.eGFP. Ligation was carried out in a 30 µl volume at room temperature for five minutes. Linearized vector and insert DNA were combined in a molar ration of 1:3. A control reaction was included to verify recirculation of the linear vector backbone LV.IRES.eGFP.

Table 4: Ligation of insert DNA and vector DNA

Component	Volume
Vector backbone DNA	0.5 µl
Insert DNA (SR-BI.c-myc)	0.5 µl
5x Rapid Ligation Buffer	6 µl
5 U/µl T4 DNA Ligase	1 µl
Nuclease-free water	add to 30 µl

Table 5: Recirculation of linear vector

Component	Volume
Vector backbone DNA	0.5 µl
5x Rapid Ligation Buffer	6 µl
5 U/µl T4 DNA Ligase	1 µl
Nuclease-free water	add to 30 µl

4.1.5 Bacterial transformation by the heat-shock method

Chemically competent *Escherichia coli* of the strain XL-10 Gold (Agilent Technologies, Santa Clara, CA, USA) were used for heat-shock transformation. An aliquot of 6 µl of the ligation mixture was mixed with 100 µl bacteria thawed on ice. The cells were then heat-shock treated for 90 sec at 42 °C and immediately chilled on ice for two minutes. A volume of 500 µl pre-warmed (37 °C) LB medium was added. The cells were spread onto LB agar plates containing ampicillin for selection, and incubated overnight at 37 °C.

4.1.6 Colony PCR and large-scale preparation of plasmid DNA

Colony PCR was used to screen for the presence or absence of insert DNA in the vector backbone. Growing bacterial colonies on the agar plates confirmed successful bacterial transformation. Single colonies were picked using sterile commercially

available toothpicks, scratched onto LB agar plates containing ampicillin and incubated overnight at 37 °C, and toothpicks were finally added directly to PCR reactions (see Tab. 6). The PCR reactions were performed using Taq DNA Polymerase Kit (Qiagen, Hilden, Germany) according to manufacturer's instructions.

Table 6: Pipetting instructions for a 50 µl colony PCR reaction

Component	Volume	Final Concentration
10x PCR buffer containing 15 mM $MgCl_2$	5 µl	1x
5x Q solution	10 µl	1x
1 % NP-40	5 µl	0.1 x
10 µM Primer A	2 µl	0.4 µM
10 µM Primer B	2 µl	0.4 µM
dNTP mix (10 mM of each)	1 µl	200 mM of each dNTP
5 U/µl Taq polymerase	1 µl	5 U/reaction
Template colony DNA	from toothpick	-
Purified water	add to 50 µl	-

Table 7: Cycling instructions for a 3-Step PCR program

Cycling Step	Temperature	Time	Cycles
Initial Denaturation	94 °C	1 min	1
Denaturation	94 °C	30 min	30
Annealing	50°C	30 min	
Extension	72 °C	1 min	1
Final Extension	10 °C	10 min	1

Amplified PCR products were separated on a 1 % (w/v) agarose gel alongside with a DNA size marker (1 kb GeneRuler™, Thermo Fisher Scientific, Waltham, MA, USA)

using 20 µl of a mixture containing 30 µl PCR product and 5 µl of 6x loading dye (Thermo Fisher Scientific, Waltham, MA, USA). DNA fragments were separated at 100 V for 90 min.

Single bacterial colonies with the desired ligation product were picked using sterile pipette tips, and 900 ml LB medium with ampicillin was inoculated overnight at 37 °C with continuous shaking at 170 rpm. The Plasmid Maxi Kit (Qiagen, Hilden, Germany) was used to isolate and purify plasmid DNA.

4.1.7 Diagnostic restriction digest

To verify the correct orientation of DNA insert, the recombinant plasmids were digested by restriction enzymes, which cut within the insert. The digestion reactions were set up in 30 µl volumes for 30 min at 37 °C (see Tab. 8). The digested reactions were run on a 1 % (w/v) agarose gel. About 2 µg of isolated and purified plasmid DNA were sequenced by LGC Genomics GmbH to confirm successful cloning.

Table 8: Digestion reactions for a 30 ml reaction

Component	Volume	Final Concentration
DNA sample	-	1 µg
10x Fast Digest Green Buffer	3 µl	1x
1 U/µl Restriction Enzyme *Pst*I FD	0.5 µl	0.5 U
1 U/µl Restriction Enzyme *Sca*I FD	0.5 µl	0.5 U
Purified water	add to 30 µl	

4.2 Production of lentiviral particles

4.2.1 Transfection of HEK293T cells

SIN lentiviral vectors derived from the human immunodeficiency virus type 1 (HIV-1) were produced in human embryonic kidney (HEK293T) cells (ATCC, Manassas, VA, USA). HEK293T packaging cells were transfected with the transfer vector encoding the transgene together with plasmids expressing the packaging proteins gag-pol and

Rev, and another expression plasmid encoding the envelope glycoprotein of the vesicular stomatitis virus (VSV-G). Transfection was performed by the calcium phosphate precipitation method.
Cells were seeded at a density of 2 x 10^6 cells per 10 cm tissue culture dish in 8 ml HEK293T medium (section 3.12) one day before transfection. On day of transfection, the cell culture medium was changed to transfection medium (section 3.12).

Each transfection mix was prepared as follows: one tube containing the lentiviral plasmids and purified water were prepared. Then 2.5 M calcium chloride was added. Another tube was filled with 2x HBS solution. The transfection mix was dropped slowly (1 drop/second) into the 2x HBS solution while blowing air into the 2x HBS solution using a pipet controller. After an incubation time of 20 min, crystallization occurred and was monitored by microscopy. Three transfection mixes where prepared as documented in Table 9.

Table 9: Preparation of transfection mixes

Component	Plasmid of interest	Fluorescence Control	Transfection Control
15 µg pGag-Pol	+	+	-
5 µg pRSV-Rev	+	+	-
2 µg pVSV-G	+	+	-
5 µg LV.eGFP	-	+	+
5 µg LV.SR-B1. eGFP	+	-	-
2.5 M $CaCl_2$	+	+	+
purified water	add to 500 µl	add to 500 µl	add to 500 µl

The transfection mixes in 2x HBS solution were added dropwise to HEK293T cells and the cells were incubated at 37 °C and 5 % CO_2. After six hours, the transfection medium was replaced by HEK293T medium supplemented with 20 mM HEPES. Cell

culture supernatants containing the lentiviral vector particles were harvested 24 hours and 48 hours post transfection, sterile filtered, concentrated and stored at 4 °C. An aliquot of concentrated supernatants of the fluorescence control and the vector of interest were stored at -80 °C. The remaining viral supernatants were centrifuged for 90 min at 27,000 x *g* at 4 °C. The centrifuged supernatants were discarded and the pellets containing virus suspended overnight at 4 °C in 400 µl cold HEK293T medium supplemented with 20 mM HEPES. The resuspended viral pellets were stored in 200 µl aliquots at -80 °C.

4.2.2 Titration of lentiviral vectors

Titration of supernatants containing lentiviral vector particles was performed using HT1080 fibroblasts. On day one of titration, the cells were plated in two 24-well plates with a density of 1 x 10^5 cells/well. The cells were allowed to attach for six hours at 37 °C and 5 % CO_2. A serial dilution with concentrated virus stock solution was performed as follows:

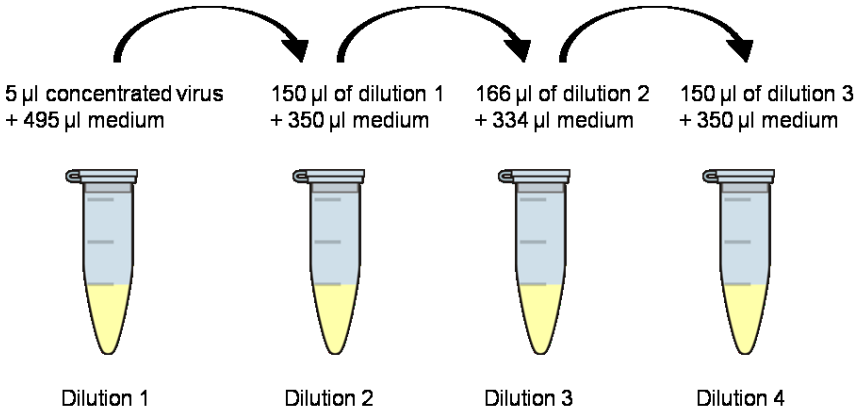

Figure 7: Titration scheme of lentiviral particles.

An aliquot of 200 µl of each viral dilution was added to 800 µl HT1080 medium (section 3.12). Immediately before adding 500 µl/well of each viral dilution, the culture medium on the cells was changed to 500 µl of HT1080 medium supplemented with 2x protamine sulfate (1:500; Sigma-Aldrich, St. Louis, MO, USA). Protamine sulfate was used to increase the efficiency of transduction. The 24-well plates were centrifuged for 90 min at 2,000 rpm at room temperature and the cells with the viral

dilutions were then allowed to incubate overnight at 37 °C, 5 % CO_2. On the second day, the cell culture medium was changed to fresh HT1080 medium. The viral titers were quantified on day three of titration. Quantification of vector titers was performed by flow cytometry (FACSAria™ III, Becton Dickinson, Franklin Lakes, NJ, USA).

The virus titer was calculated using the following equation:

$$\text{Titer}\left[\frac{\text{infectious units}}{\text{ml}}\right] = \frac{\text{\% GFP positive cells}}{100} \times \frac{\text{Seeded cell number x dilution factor}}{\text{Volume of supernatant [ml]}}$$

The multiplicity of infection (MOI) was then calculated to determine the volume of viral stock solution needed for transduction. Calculation of the MOI allows to estimate the average number of viral particles infecting a host cell.

4.3 Lentiviral transduction of host cells

CHO-K1 and CHO-hS1P1 cells were seeded in transduction medium in 24-well plates for suspension cells with a density of 3 x 10^5 cells/well. To transduce the cells with the MOI of two and five, calculated amounts of virus stock solution were added to the cells. The 24-well plates were sealed with Parafilm® M (Bemis, Neenah, WI, USA) and centrifuged for 90 min at 2,000 rpm at room temperature. The centrifuged cells were transferred to 24-well tissue culture plates for adherent cells and incubated overnight at 37 °C, 5 % CO_2. The culture medium was changed to normal cell culture medium one day post transduction. The cells were monitored daily with an inverted microscope in order verify GFP expression. The cells were sorted on the basis of their fluorescence by flow cytometry (FACSAria™ III, Becton Dickinson, Franklin Lakes, NJ, USA) three days post transduction. Positive cell populations were transferred to 6-well tissue culture plates and expanded. Flow cytometric analysis of transduced cells were performed routinely on a Gallios flow cytometer (Beckman Coulter, Krefeld, Germany), to verify consistent eGFP expression.

4.4 Isolation of human HDL

HDL was isolated from different frozen human plasma samples of healthy individuals by sequential density gradient ultracentrifugation (*d* = 1.069 – 1.21 g/ml) according to a protocol by Havel et al. from 1955 with modifications.
Ultracentrifugation was carried out in a 90Ti fixed angle rotor in the Optima™ LE-80K centrifuge by Beckman Coulter. The human serum was delivered in 8 ml to screw capped centrifuge tubes (Beckman Coulter, Brea, CA, USA) and 37.72 µl of a potassium bromide solution (*d* = 1.35 g/ml) was added to 1 ml of plasma. The tubes were filled with potassium bromide solution as a solvent with a density of 1.019 g/ml. After centrifugation at 60,000 rpm for 23 h at 4 °C, HDL was concentrated at the bottom of the centrifuge tubes with a density higher than 1.019 g/ml. The top phase contained all lipoproteins with densities less than solvent density and the clear phase beneath the top phase contained the solvent. The top and the clear phases were removed and the yellow phase at the bottom was mixed by pipetting up and down. Potassium bromide solution with a density of 1.019 g/ml was added to reach equal volumes in all centrifugation tubes. The tubes were then filled with potassium bromide solution with a density of 1.35 g/ml to obtain a density of 1.069 g/ml. After centrifugation at 60,000 rpm for 20 h at 4 °C, the top phase contained LDL, and HDL was concentrated in the lower phase. The top and clear phases were removed, the yellow lower phase was mixed by pipetting and a potassium bromide solution with a density of 1.069 g/ml was added to obtain an equal volume in each centrifugation tube. Solid potassium bromide was added (0.236 g/ml) and a solution of potassium bromide with a density of 1.21g/ml to fill the tubes. The samples were centrifuged at 46,000 rpm for 69 h at 4 °C and HDL, concentrated now in the top phase, was carefully transferred to 15-ml centrifugation tubes, and stored at 4 °C until further processing. Protein concentration of HDL was determined by the Pierce BCA Protein Assay Kit (Thermo Fisher Scientific, Waltham, MA; USA) (see section 4.8.1).

4.4.1 Desalting and buffer exchange of isolated HDL by dialysis

Excess potassium bromide salt was removed using ZelluTrans dialysis membranes (Roth, Karlsruhe, Germany). Before desalting HDL, the membranes were boiled in 2 % $NaHCO_3$/1 mM EDTA at 60 °C for three to four hours. Subsequently, the membranes were washed several times with pure water. Desalting was performed in cold PBS at

4 °C for six hours and PBS was changed twice before continuing desalting overnight. The protein concentration of HDL was measured after dialysis using the Pierce BCA Protein Assay Kit (Thermo Fisher scientific, Waltham, MA, USA).

4.5 Cell culture

4.5.1 General working standards

Buffers and solutions prepared were sterilized by filtration or autoclaving. Passaging and treatment of cells as well as preparation of buffers and solutions were carried out under sterile conditions using LaminAir® HB 2472 safety cabinet (Heraeus, Hanau, Germany). Plastic materials used were packed sterile and glassware was autoclaved prior to use. An incubator (Binder, Tuttlingen, Germany) was used to cultivate cells at 37 °C and 5 % CO_2 at 95 % humidity.

4.5.2 Passaging of cells

All cell lines used were adherent cells. When the cells reached 70-80 % confluency, they were detached using Trypsin-EDTA solution (0.025 %) and centrifuged at 500 x *g* for 5 min after adding FBS containing culture medium. The centrifuged supernatant was aspired, and cell pellets were suspended in 1 ml of culture medium. Cells were subcultured in new tissue culture flasks.
Seeding cells for experiments in 6-well, 24-well or 96-well plates required cell counting using a Neubauer hemocytometer (Paul Marienfeld, Lauda-Königshofen, Germany).

4.6 Cholesterol efflux assay

The rate of cholesterol efflux from cultured cells towards an acceptor can be quantified with the cholesterol efflux assay.

Transduced CHO cells were plated in 96-well tissue culture plates (Sarstedt, Nümbrecht, Germany) and allowed to adhere overnight. The cells were washed twice with sterile PBS and cultured overnight in culture medium supplemented with 1 % FBS. All CHO cells were loaded the next day with ^{3}H-cholesterol (1 µCi/ml; Perkin Elmer, Waltham, MA, USA) in culture medium supplemented with 1 % FBS and an inhibitor

of the acyl-CoA:cholesterol acyltransferase (ACAT inhibitor named Sandoz 58-035, 2 µg/ml; Sigma-Aldrich, St. Louis, MO, USA) for 22-24 h. The cells were then washed once with PBS and efflux medium supplemented with ACAT inhibitor (2 µg/ml) and human HDL (0.1 mg/ml) or apolipoprotein A-I (apoA-I; 0.01 mg/ml) was added for 5 h. Stimulation with S1P (1 µM) was performed 30 min prior to HDL or apoA-I incubation. The cell supernatant was harvested and centrifuged at 2000 rpm for 5 min at room temperature to pellet cellular debris. Radioactivity was measured in 100 µl supernatant by liquid scintillation counting (Perkin Elmer, Krefeld, Germany). The cells were extracted by adding 200 µl hexane:isopropanol (3:2, v:v) for 30 min at room temperature. The hexan/isopropanol fraction was transferred to microfuge tubes and hexan/isopropanol was added again for 15 min. The extracts were allowed to dry overnight and then dissolved in 200 µl isopropanol:Nonident P-40 (NP-40; 9:1, v:v) and radioactivity was determined by liquid scintillation counting. The background cholesterol efflux obtained in the absence of an acceptor was subtracted from the efflux obtained with cholesterol acceptors. The cholesterol efflux was expressed as the percentage of radioactivity (in counts per minute) released from the cells to the cell medium relative to the total amount of radioactivity within medium and cells. All efflux measurements were performed in triplicate for each sample.

4.7 Expression analyses in cell cultures

4.7.1 RNA isolation and first strand cDNA synthesis

Total RNA was extracted from cells with the innuPrep Mini Kit (Analytik Jena, Jena, Germany) according to manufacturer's instructions. The concentration of isolated RNA was measured using the BioPhotometer® (Eppendorf, Hamburg, Germany). First strand cDNA was synthesized from 100 nM total RNA. RNA was reverse transcribed using oligo(dT) primers and the RevertAid First Strand cDNA Kit (Thermo Fisher Scientific, Waltham, MA, USA) according to manufacturer's instructions.

4.7.2 Quantitative RT-PCR

To calculate relative gene expressions, the $2^{-\Delta\Delta Ct}$ method was used. The threshold cycle (Ct value) represents the cycle number at which the signal of the fluorescence dye reaches a certain threshold, and therefore inversely representing the amount of

amplified DNA generated in the PCR reaction. The relative expression of a target gene was calculated by normalizing the Ct value of the target to the Ct value of a reference gene. Therefore, the normalized Ct value (ΔCt) was calculated as the difference in threshold cycles between target gene and reference gene. Reference genes were represented by housekeeping genes, which were stably expressed in all cell lines (Schmittgen and Livak, 2008). Quantitative RT-PCR was carried out with the Thermal Cycler C1000^{TM} (Bio-Rad, Hercules, CA, USA) running the program shown in Table 11. Amplification of 1 µl template cDNA was performed in a total volume of 20 µl and detected by iQ SYBR Green Supermix (Bio-Rad, Hercules, CA, USA). The protocol for one reaction is shown in Table 10. The housekeeping gene GAPDH was used to relatively standardize the probes. Duplicate reactions were carried out in 96-well plates. Plates were sealed with transparent adhesive qPCR foil (Sarstedt, Nümbrecht, Germany) and shortly centrifuged at 2,000 rpm at 4 °C.

Table 10: Set up for a 20 µl RT-PCR reaction

Component	Volume per Reaction	Final Concentration
Aqua ad iniectabilia	8 µl	
iQ SYBR Green Supermix	10 µl	
Forward primer	0.5 µl	1.25 µM
Reverse primer	0.5 µl	1.25 µM
cDNA Template	1 µl	

Table 11: Cycling Instructions for a RT-PCR

Cycling Step	Temperature	Time	Cycles
Initial Denaturation	95 °C	3 min	1
Denaturation	95 °C	20 sec	
Annealing	55°C	20 sec	
Extension	72 °C	20 sec	
Final Extension	10 °C	10 min	30
Fluorescence detection			
Dissociation	95 °C		1

4.8 Biochemical techniques

4.8.1 Cell stimulation, protein isolation and quantification

To monitor the phosphorylation of ERK-1/2, cells were seeded in 6-well plates and serum-starved for 8 hours before exposition to S1P (1 µM) or HDL (0.1 mg/ml) for various times (2-10 min). S1P-stimulated cells were detached by scraping in 50 µl lysis buffer and harvested. The cells were incubated for 30 min on ice and centrifuged at 14,000 rpm for 15 min at 4 °C to pellet cellular debris. All other cells were detached and harvested by trypsinization and centrifuged at 500 x *g* for 5 min. Cell pellets were lyzed in 100 µl lysis buffer, incubated for 30 min on ice, sonicated for 10 sec (Ultrasonic homogenizer Labsonic®, B. Braun Biotech International, Melsungen, Germany), and centrifuged at 14,000 rpm for 15 min at 4 °C. All cell lysates were transferred into 1.5 ml reaction tubes and stored at -20 °C until further processing. The concentration of protein was determined using the Pierce BCA Protein Assay Kit (Thermo Fisher Scientific, Waltham, MA, USA). The bovine serum albumin (BSA) standard (0.5-2 µg/µl) and 1 µl sample were mixed with 200 µl BCA working reagent in a microtiter plate. The mixture was incubated for 30 min at 37 °C in the dark and the absorbance was measured at 562 nm on a Synergy HT multiplate reader (BioTek, Winooski, VT, USA).

4.8.2 SDS-PAGE

Cell extracts with 20 µg protein were separated by the Laemmli buffer system. The 4 % stacking gels and 12 % resolving gels were prepared (see section 3.14) in 1.5 mm gel cassettes. Protein samples were prepared with 4x sample buffer, heated at 95 °C for 5 min and loaded on the gels. Electrophoresis was performed in 1x running buffer in a Mini-PROTEAN® 3 cell system (Bio-Rad, Hercules, CA, USA) at 80-110 V.

4.8.3 Immunoblot

Proteins were transferred to a Immobilon-P PVDF membrane (Merck Millipore, Burlington, MA, USA) by tank blotting (Mini Trans-Blot®, Bio-Rad, Hercules, CA; USA) after SDS-PAGE. The polyacrylamide gel, filter paper and sponges were equilibrated in transfer buffer. The gel was placed on three to four layers of buffer-soaked filter paper. The PVDF membrane was soaked in methanol, placed on top of the gel and covered with buffer-soaked filter paper. This sandwich of gel, membrane and filter paper was placed between buffer-soaked sponges in the transfer cell. The blotting apparatus was filled with cooled transfer buffer and a cooling unit was added. Western blotting was performed at 100 V for 60 min on a magnetic stirrer.

4.8.4 Immunodetection

Following protein transfer, the membrane was blocked in 5 % nonfat dried milk (AppliChem, Darmstadt, Germany) in PBS for 60 min to block unoccupied binding sites. The membrane was incubated with primary antibody diluted in 0.5 % nonfat dried milk (1:1000) at 4 °C overnight, washed three times for 10 min with washing buffer, and incubated with a second antibody conjugated to horseradish peroxidase (HRP; anti-mouse-HRP 1:5000 or anti-rabbit-HRP 1:5000 in 0.5 % nonfat dried milk) for 60 min at room temperature. The membrane was washed again three times for 10 min and developed in the imager ChemiDoc™ XRS+ (Bio-Rad, Hercules, CA, USA) using our self-made ECL mixture.

4.9 Statistical analysis

Statistical analyses were performed using GraphPad Prism version 5.0 (GraphPad Software, La Jolla, CA, USA). Statistical significance was evaluated by unpaired Student's t-test or by one-way analysis of variance (ANOVA) followed by Tukey's post hoc test. In case of multiple comparison, statistical significance was evaluated by two-way ANOVA followed by Bonferroni's post hoc test wherever appropriate. Statistical test applied was indicated in each figure legend. Values were considered significant at $P < 0.05$. Results are given in mean ± SD or mean ± SEM of at least three independent experiments as indicated in the figure legends.

5 Results

The first part of this thesis aimed to evaluate a putative contribution of S1P receptors S1P1-3 to the cholesterol efflux to lipid-free apoA-I or mature HDL in CHO cell lines overexpressing these receptors with or without S1P stimulation.
The goal of the second part was to generate a lentiviral vector encoding a murine SR-BI (mSR-BI) protein tagged by a c-myc peptide. This vector was used to overexpress SR-BI in CHO cells co-expressing human S1P1 (hS1P1) in order to evaluate the effects of SR-BI and S1P1 co-expression on the cholesterol efflux to apoA-I and mature HDL.

5.1 Investigation of the impact of S1P receptor overexpression in the apoA-I and HDL-mediated cholesterol efflux

Previous studies with murine S1P2-deficient macrophages showed a decreased foam cell formation and an increased cholesterol efflux to HDL compared to S1P2-expressing macrophages (Wang et al., 2010). In the present study, the impact of S1P receptor overexpression on the cholesterol efflux was investigated. The efflux to lipid-free apoA-I and mature HDL was assessed in ^{3}H-cholesterol-loaded CHO cell lines expressing human S1P1, S1P2, or S1P3, and was compared to the cholesterol efflux in CHO-K1 control cells. The results obtained for the cholesterol efflux capacity of apoA-I are shown in Figure 8. The net cholesterol efflux was relatively low and similar between CHO-K1 and CHO-hS1P1, CHO-hS1P2, and CHO-hS1P3 cell lines, respectively. The mean cholesterol efflux to apoA-I in CHO-hS1P1 cells was below 1 % (Fig. 8A), in CHO-hS1P2 cells at 1.24 ± 0.7 % (Fig. 8B), in CHO-hS1P3 cells at 2.5 ± 0.8 % (Fig. 8C).

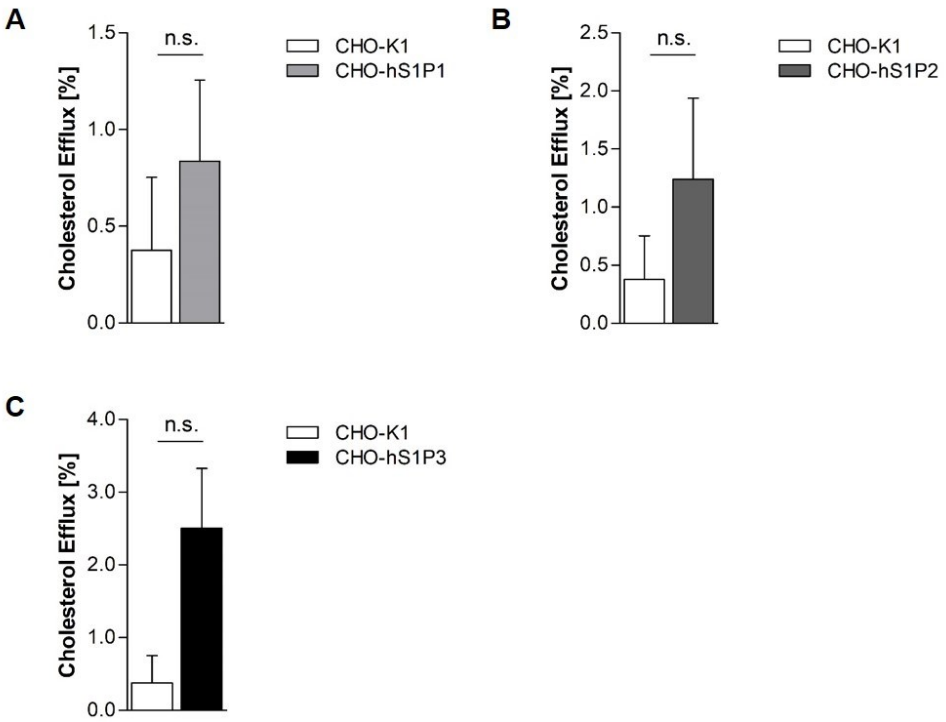

Figure 8: Net cholesterol efflux to apoA-I in CHO-hS1P1, CHO-hS1P2, and CHO-hS1P3 compared to CHO-K1 cells.
To achieve the net cholesterol efflux, background efflux was subtracted. Lipid-free apoA-I (0.01 mg/ml) was incubated for 5 h before harvesting the cell supernatants and cell extracts. (A) Cholesterol efflux in CHO-hS1P1 cells compared to CHO-K1 cells. (B) Cholesterol efflux in CHO-hS1P2 cells compared to CHO-K1 cells. (C) Cholesterol efflux in CHO-hS1P3 cells compared to CHO-K1 cells. Triplicate measurements were performed in each experiment. Results are presented as mean ± SEM from three independent experiments; n = 3; n.s., not significant.

Compared to apoA-I, the cholesterol efflux to HDL in CHO-K1, CHO-hS1P1, CHO-hS1P2, and CHO-hS1P3 cells was much higher (Fig. 9). Still, the net cholesterol efflux to HDL was not significantly different among the four CHO cell lines. HDL removed 28.54 ± 3.1 % cholesterol in CHO-K1 cells, 36.75 ± 3.2 % in CHO-hS1P1 cells, 31.75 ± 4.3 % in CHO-hS1P2 and 36.06 ± 4.7 % in CHO-hS1P3 cells. Thus, the overexpression of hS1P1-3 had no impact on the HDL-mediated cholesterol efflux.

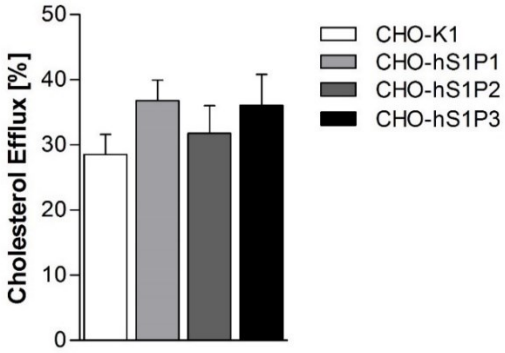

Figure 9: Cholesterol efflux to HDL in CHO-K1, CHO-hS1P1, CHO-hS1P2, CHO-hS1P3 cells.
To achieve the net cholesterol efflux, background efflux was subtracted. Human HDL (0.1 mg/ml protein) from healthy individuals was incubated for 5 h before harvesting the cell supernatants and cell extracts. Comparison of CHO-hS1P1, CHO-hS1P2, CHO-hS1P3 cells to CHO-K1 control cells. Triplicate measurements were performed in each experiment. Results are presented as mean ± SEM from independent experiments; n = 4-8.

5.2 Impact of S1P stimulation on the apoA-I and HDL-mediated cholesterol efflux in S1P receptor overexpressing CHO cell lines

CHO-K1 control cells and CHO cells overexpressing hS1P1-3 were stimulated with S1P to investigate a possible impact of S1P on the apoA-I and HDL-mediated cholesterol efflux.

Stimulation of CHO-K1 cells with exogenously supplied S1P resulted in no significant differences compared to non-stimulated cholesterol efflux to apoA-I (Fig. 10A). Interestingly, cholesterol efflux to apoA-I in CHO-hS1P1 cells was completely abolished (below background efflux) after S1P stimulation (Fig. 10B). In contrast, S1P stimulation in CHO-hS1P2 and CHO-hS1P3 cells did not alter the amount of cholesterol removed by lipid-free apoA-I (Fig. 10C+D).

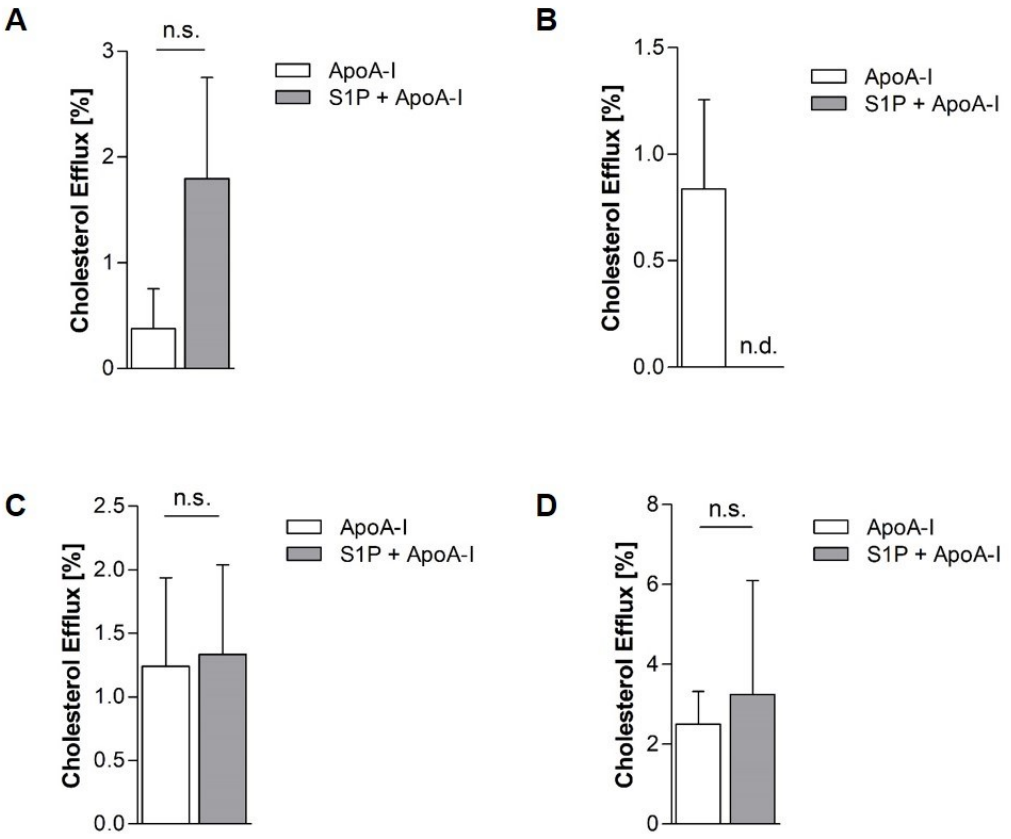

Figure 10: Cholesterol efflux to apoA-I in CHO-K1, CHO-hS1P1, CHO-hS1P2, CHO-hS1P3 cells without and with prior S1P stimulation.
S1P (1 µM) was incubated 30 min before apoA-I (0.01 mg/ml, 5 h) was added. To achieve the net cholesterol efflux to apoA-I, background efflux was subtracted. (A) Cholesterol efflux in CHO-K1 control cells (n = 4). (B) Cholesterol efflux in CHO-hS1P1 cells (n = 4). (C) Cholesterol efflux in CHO-hS1P2 cells (n = 8). (D) Cholesterol efflux in CHO-hS1P3 cells (n = 4). Results are presented as mean ± SEM from independent experiments. Triplicate measurements were performed in each experiment; n.s., not significant; n.d., not detected.

In a next step, the efflux to HDL under S1P stimulation was investigated in a similar manner. As the results in Figure 11 show, stimulation with S1P did not alter the cholesterol efflux capacity of HDL in any tested cell line.

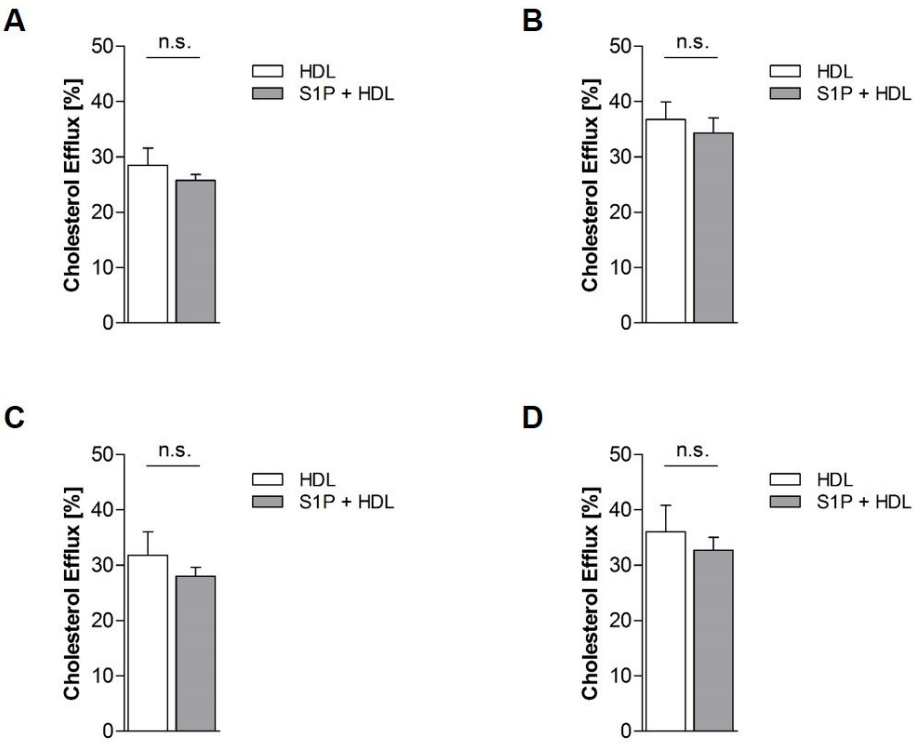

Figure 11: Removal of cholesterol from CHO-K1, CHO-hS1P1, CHO-hS1P2, and CHO-hS1P3 cells by HDL with and without prior S1P stimulation.
S1P (1 µM) was incubated 30 min before HDL (0.1 mg/ml protein, 5 h) was added. To achieve the net cholesterol efflux to HDL, background efflux was subtracted. (A) Cholesterol efflux in CHO-K1 control cells (A; n = 4), CHO-hS1P1 cells (B; n = 4), CHO-hS1P2 cells (C; n = 8) and CHO-hS1P3 cells (D; n = 4). Triplicate measurements were performed in each experiment. Results are presented as mean ± SEM from independent experiment; n.s., not significant.

5.3 Assessment of *Abca1*, *Abcg1*, and *Scarb1* mRNA expression levels

The ABC transporters ABCA1 and ABCG1 as well as the HDL-receptor SR-BI play pivotal roles in the efflux of cholesterol (Phillips, 2014). Thus, the effect of S1P receptor overexpression on the mRNA expression of ABCA1, ABCG1 and SR-BI was determined.

Quantitative PCR analysis revealed that *Abca1* was expressed at very low levels in CHO-K1 and CHO-hS1P1-3 cell lines (Fig. 12A). This result was consistent with the weak cholesterol efflux to lipid-free apoA-I, the major ABCA1-dependent cholesterol acceptor. Interestingly, overexpression of hS1P1 resulted in a significant decrease in the *Abca1* expression level compared to CHO-K1 control cells, whereas no differences were determined in CHO-hS1P2 and CHO-hS1P3 cells.

CHO cells did not express endogenous *Abcg1*. In a next step, the mRNA expression of *Scarb1* (SR-BI) was determined. The *Scarb1* level was increased in the three S1P receptor overexpressing CHO cell lines compared to the CHO-K1 control cell line (Fig. 12B). The *Scarb1* expression in CHO-hS1P1 was 2.5-fold higher, in CHO-hS1P2 cells 2.9-fold higher, and in CHO-hS1P3 cells 3.0-fold higher compared to CHO-K1 control cells. No significant differences were detected among the S1P1-3 overexpressing cell lines.

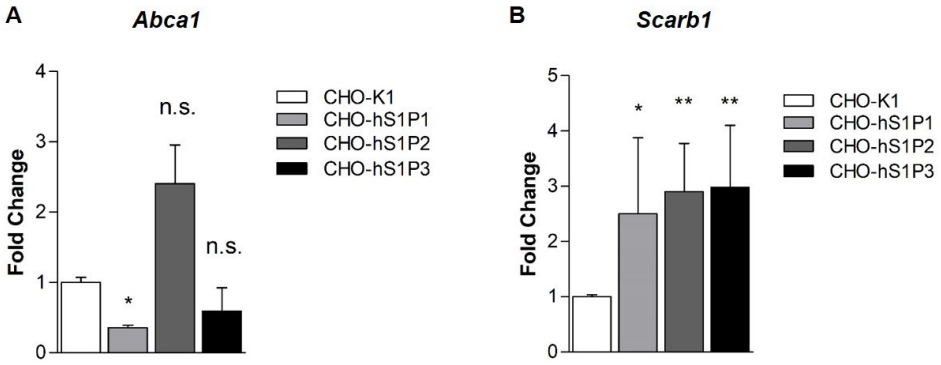

Figure 12: Quantitative PCR analyses of *Abca1* and *Scarb1* in CHO-hS1P1, CHO-hS1P2, CHO-hS1P3 cells compared to CHO-K1 control cells.
Gene expression analyses were performed from three to four independent experiments in duplicates. *Gapdh* was used as an endogenous control. (A) Fold change of *Abca1* expression. (B) Fold change of *Scarb1*. Duplicate measurements were performed in each experiment. Results are expressed in mean ± SD; **P* < 0.05; ***P* < 0.005; n.s., not significant.

In summary, overexpression of S1P receptors was not involved in the apoA-I and HDL-mediated cholesterol efflux without S1P stimulation. S1P stimulation abolished the cholesterol efflux to apoA-I in CHO-hS1P1 cells but not in CHO-hS1P2 and CHO-hS1P3 cells and had no effect on the cholesterol efflux to HDL. The mRNA expression of *Abca1* in CHO-hS1P1 but not CHO-hS1P2 and CHO-hS1P3 cells was significantly reduced compared to control cells. The *Scarb1* expression level was significantly higher in all three CHO cell lines expressing hS1P1-3 compared to control cells.

5.4 Cloning of the murine *Scarb1* gene into a lentiviral vector

To study the role of simultaneous S1P1 and SR-BI overexpression, a lentiviral vector system expressing the murine SR-BI was integrated into two CHO cell lines.
Lentiviral vectors have been used for years as tools for the delivery of genes *in vitro* into cells. With lentiviral vectors, cells can be stably transduced and the transgene becomes part of the host genome. This has the advantage that the foreign gene is replicated in duplicating cells. Therefore, the implementation of transgenic cell lines represents a well-established and useful strategy to evaluate the effects of various receptors *in vitro* in order to investigate cellular functions.

A standard PCR using a temperature gradient was performed to amplify the coding sequence of SR-BI.c-myc from a template plasmid. Successful amplification was confirmed by agarose gel electrophoresis (Fig. 13A). Digestions of the pooled amplification products and the empty lentiviral vector backbone LV.IRES.eGFP were done in order to prepare the ligation step (Fig. 13B). The correct gel bands from the DNA fragment (1560 bp) and empty vector (8000 bp) were cut, purified and used for ligation. As shown in Figure 13C, successful ligation was confirmed by agarose gel electrophoresis after double digestion of the cloned lentiviral plasmid LV.SR-BI.IRES.eGFP. This generated lentiviral vector as well as the provided empty vector LV.eGFP were used for further experiments.
Figure 14 shows the physical maps of the self-inactivating IRES-based bicistronic lentiviral vector LV.SR-BI.IRES.eGFP and the fluorescence control vector LV.eGFP. Both vectors were constructed with the eGFP sequence in order to track the transduced cells by eGFP expression. The internal ribosome entry site (IRES) in the bicistronic expression vector allows the translation of both the murine myc-tagged SR-BI gene (*Scarb1*) and eGFP coded by the same mRNA transcript. This assures that the SR-BI protein is present in all cells in which the eGFP can be detected. Both vectors contained the spleen focus-forming virus (SFFV) promoter to drive gene expressions.

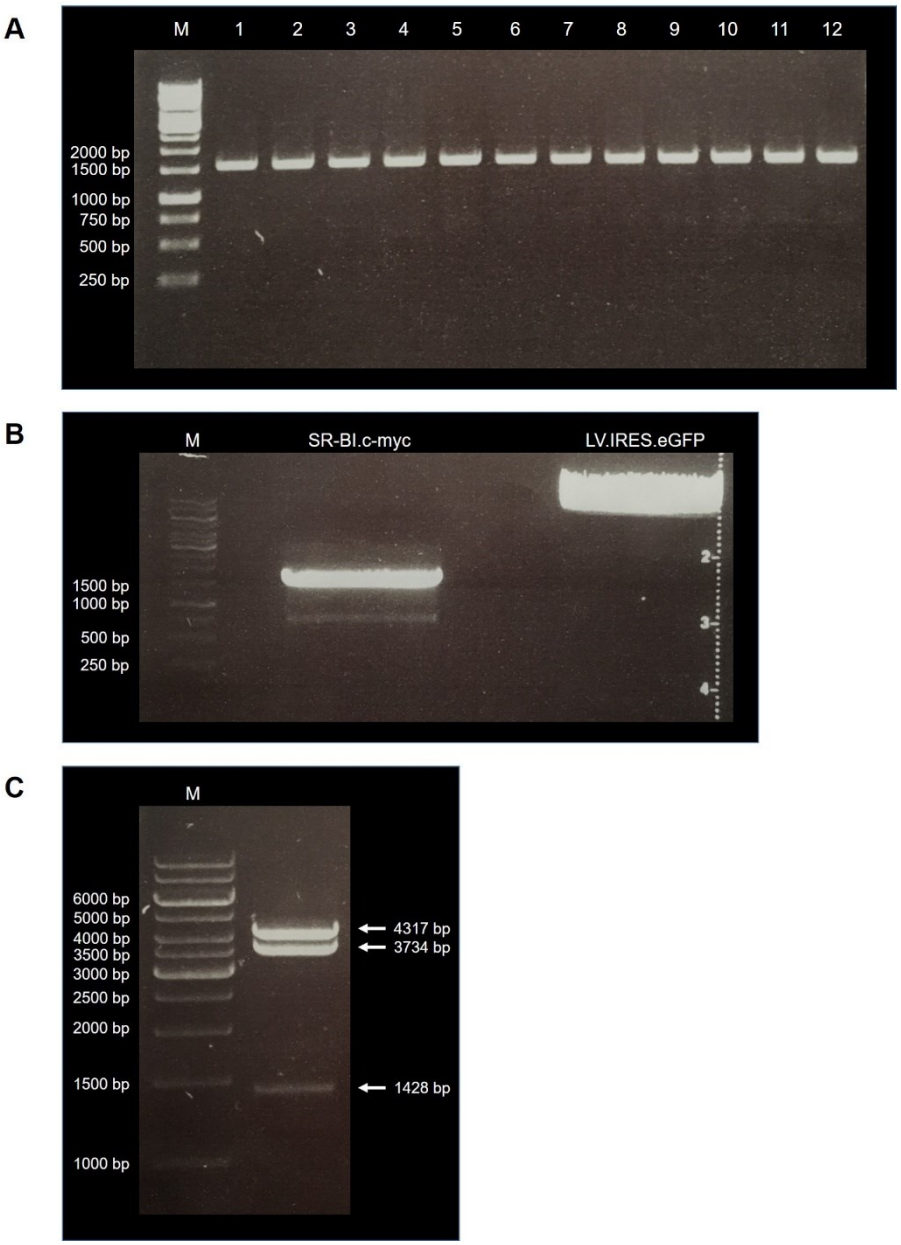

Figure 13: Cloning steps to generate final lentiviral vector LV.SR-BI.IRES.eGFP.
(A) PCR amplification of SR-BI.c-myc using a temperature gradient and detection of the expected band at 1560 bp; probing 12 samples at temperatures varying from 50 °C to 70 °C. (B) Digestion of the pooled amplified PCR products from (A) as well as the empty vector LV.IRES.eGFP with *Xba*I and *Mlu*I; resulting bands at 1560 bp and 8000 bp. (C) Digestion of the ligation product LV.SR-BI.IRES.eGFP from (B) with *Pst*I and *Sca*I. M, DNA marker.

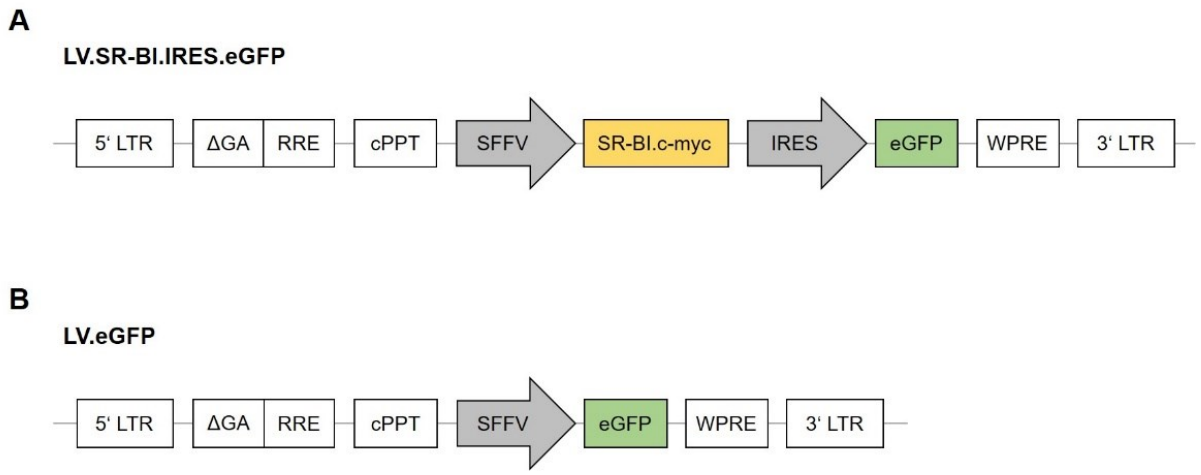

Figure 14: Schematic diagram of the lentiviral vectors.
Transcripts from SIN lentiviral vectors of the third generation. (A) Construct of a dual-promoter lentivirus (LV) with the SFFV promoter driving the *Scarb1* gene for SR-BI production, followed by IRES which drives the *eGFP* gene. (B) Expression of the cassette is driven by a single SFFV promoter. The cassettes in (A) and (B) are flanked by 5' and 3' long terminal repeats (LTRs), which are necessary for proviral integration into the host genome. ΔGA, deleted *gag* region; RRE, Rev-responsive element; cPPT, central polypurine tract upstream of the transgene improves the gene transfer performance; c-myc, *c-myc* gene. The post-transcriptional regulatory element of the woodchuck hepatitis virus (WPRE) downstream of the transgene enhances the expression of the reporter gene.

5.5 Transduction of CHO cells with lentiviral particles

Lentiviral particles of LV.SR-BI.IRES.eGFP (SR-BI vector) and LV.eGFP (MOCK vector) were produced in HEK293T cells. To determine successful transfection of HEK293T cells, eGFP expression was examined 24 hours post-infection using fluorescence microscopy (Fig. 15). Cells transfected with either the SR-BI-vector or the MOCK-vector showed high eGFP expression. Calculated viral titers resulted to be in range of 5.7×10^7 to 6.6×10^7 infectious units per milliliter (see section 4.2.2 for the calculations).

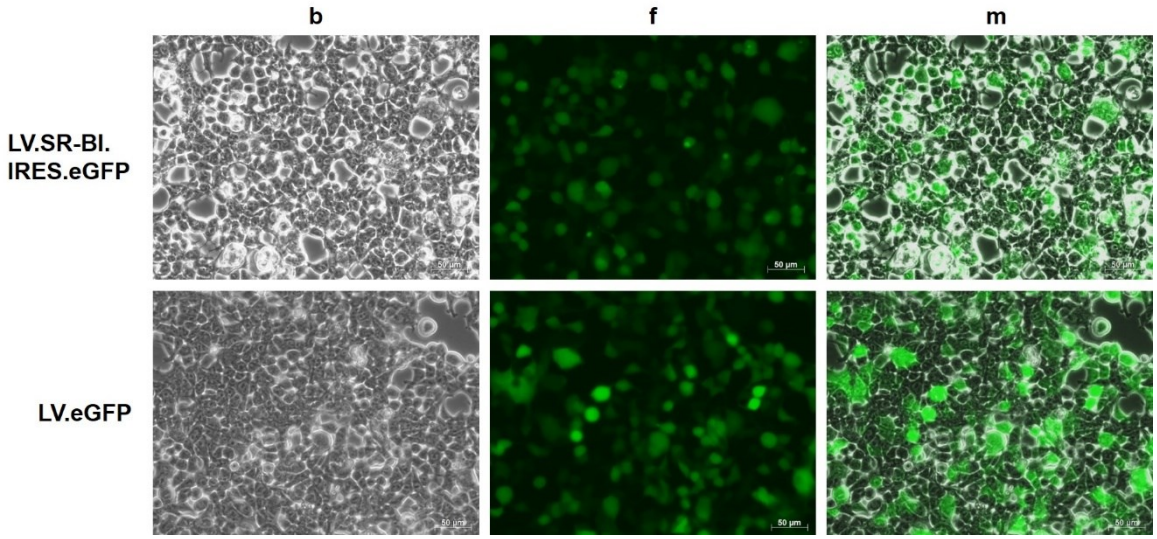

Figure 15: Monitoring transfection efficiency of HEK293T cells by fluorescence microscopy.
Visualization of eGFP expression 24 hours post transfection. Comparison of bright field, fluorescent field and merged images of LV.SR-BI.IRES.eGFP and LV.eGFP transfected HEK293T cells. Representative images to verify GFP fluorescence in cell lines. B, bright field; f, fluorescent field; m, merge. Scale bars, 50 µm.

CHO-K1 and CHO-hS1P1 cells were transduced with the bicistronic lentiviral SR-BI vector expressing murine SR-BI and eGFP. The monocistronic MOCK vector expressing eGFP alone was used as a transduction control. Transduction was performed with two different multiplicities of infection (MOI), MOI of two and MOI of five. The generated cells were CHO-MOCK, CHO-SRB1, CHO-hS1P1-MOCK, and CHO-hS1P1-SRB1. Efficiency of transduction was determined by monitoring eGFP expression using fluorescence microscopy 24 hours after transduction (Fig. 16-17). CHO-K1 cells transduced with the MOCK vector at both MOIs showed similar expressions observed by fluorescence microscopy (Fig. 16A). The eGFP expression in CHO-SRB1 cells (Fig. 16B), however, was less intense than the expression of the fluorescence protein in CHO-MOCK cells. Similar results were obtained for transduced CHO-hS1P1 cells. CHO-hS1P1-MOCK cells showed high eGFP expression at both MOIs (Fig. 17A), whereas the eGFP expression in CHO-hS1P1-SRB1 cells was less intense (Fig. 17B) compared to the MOCK-transduced control cells.
Transduced cells with the MOI of two were selected for further experiments in this study.

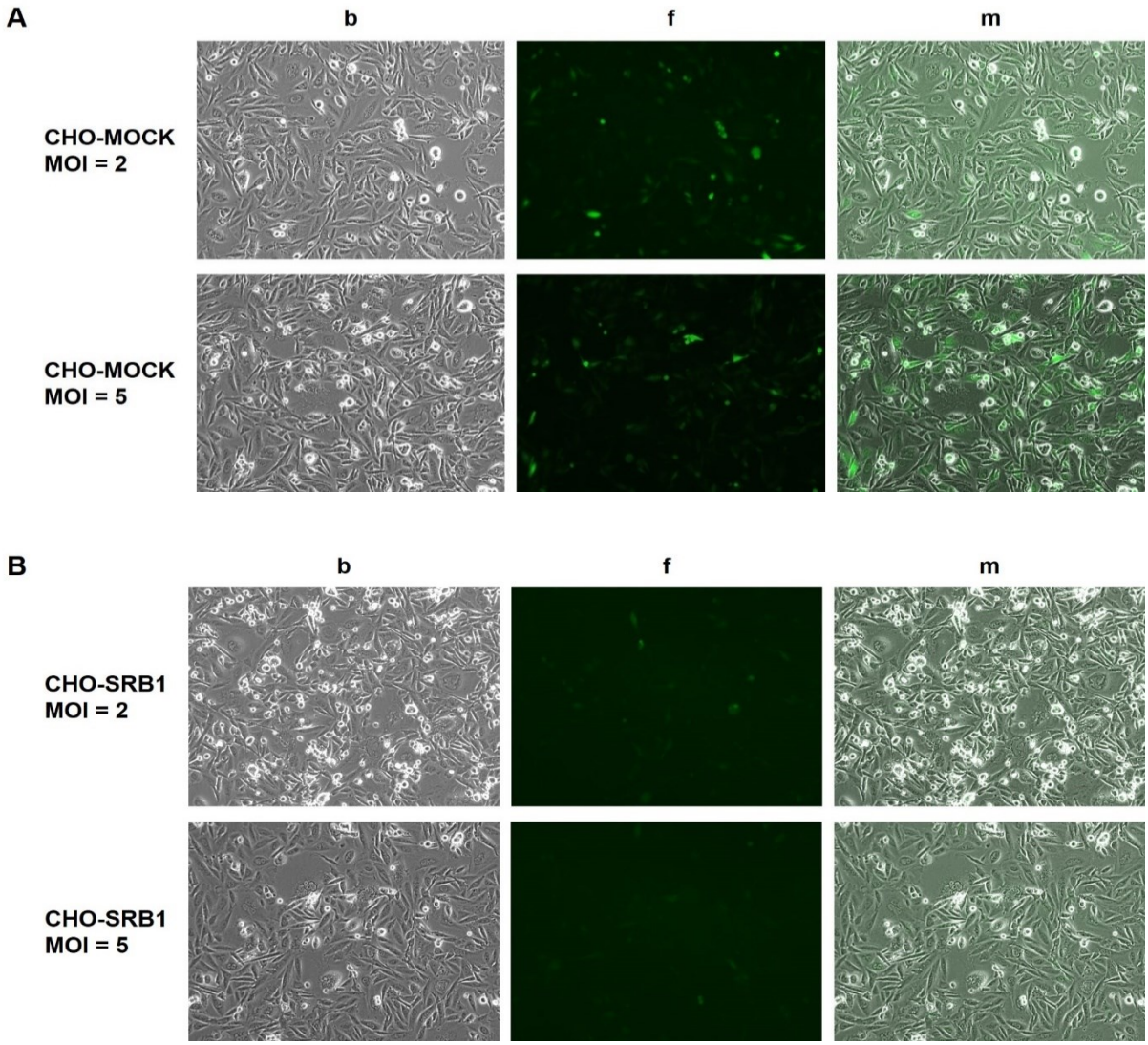

Figure 16: Visualization of eGFP expression in transduced CHO-MOCK and CHO-SRB1 cells by fluorescence microscopy 24 hours after transduction.
Comparison of bright field (b), fluorescent field (f) and merged images (m). (A) CHO-MOCK cells transduced with the MOCK vector (MOI at 2 and 5). (B) CHO-SRB1 cells transduced with the SR-BI vector (MOI of 2 and 5). Representative images to verify GFP fluorescence in transduced cells.

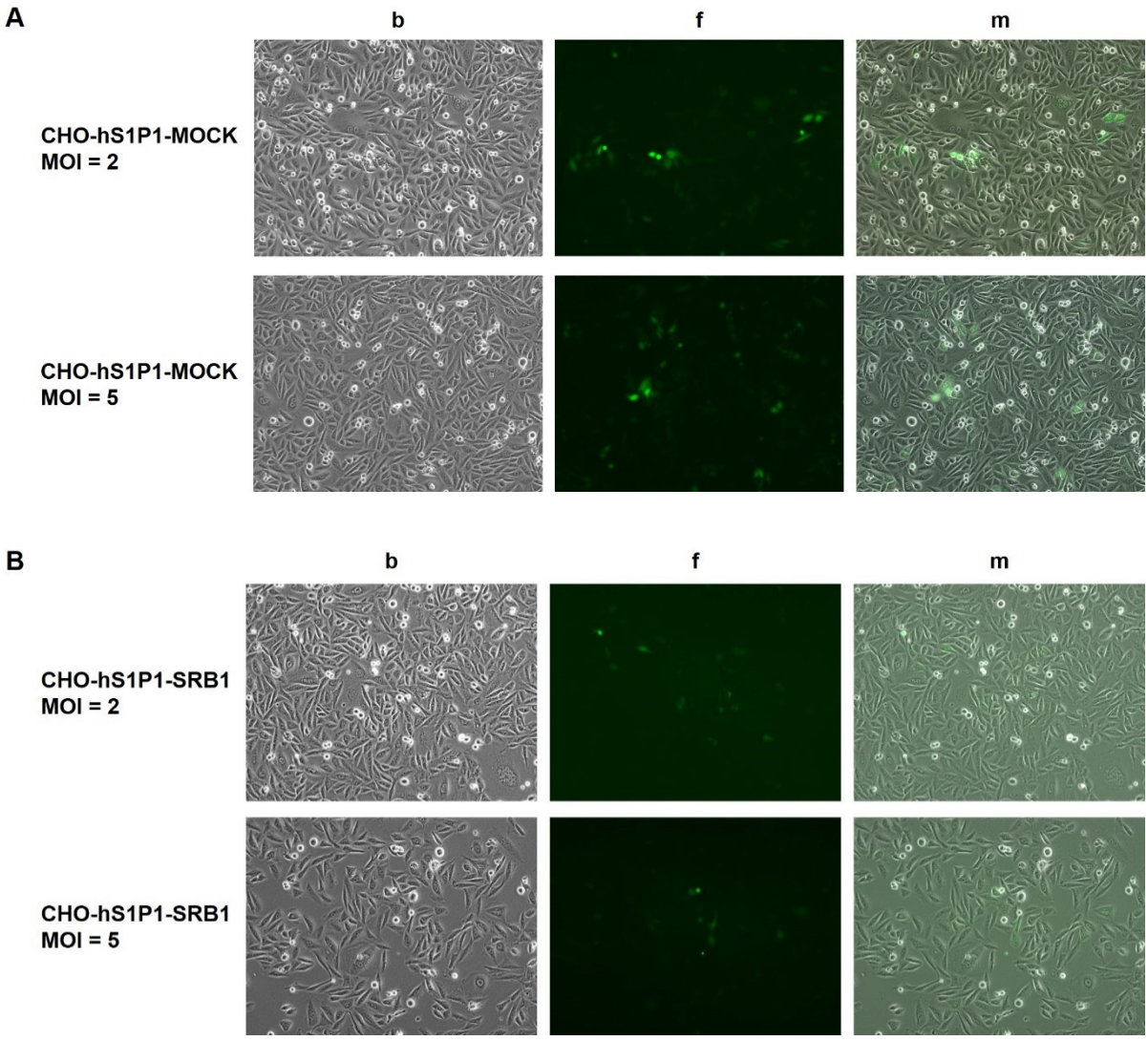

Figure 17: Monitoring eGFP expression in transduced CHO-hS1P1-MOCK and CHO-hS1P1-SRB1 cells by fluorescence microscopy 24 hours post transduction.
Comparison of bright field (b), fluorescent field (f) and merged images (m). (A) CHO-hS1P1-MOCK cells transduced with the MOCK vector (MOI at 2 and 5). (B) CHO-hS1P1-SRB1 cells transduced with the SR-BI vector (MOI of 2 and 5). Representative images to verify GFP fluorescence in transduced cells.

Flow cytometric analysis after cell sorting of eGFP-positive cells from transduced CHO-MOCK and CHO-SRB1 cells are presented in Figure 18. Flow cytometry confirmed similar eGFP expressions in cells at MOI of two and MOI of five. A population of more than 99 % were eGFP-positive in CHO-MOCK (Fig. 18A) and the population of CHO-SRB1 cells was 100 % eGFP-positive (Fig. 18B). However, the mean fluorescence intensity (MFI) of eGFP in CHO-MOCK cells was four times higher than the MFI in CHO-SRB1 cells (MFI: 46 vs. 10.4).

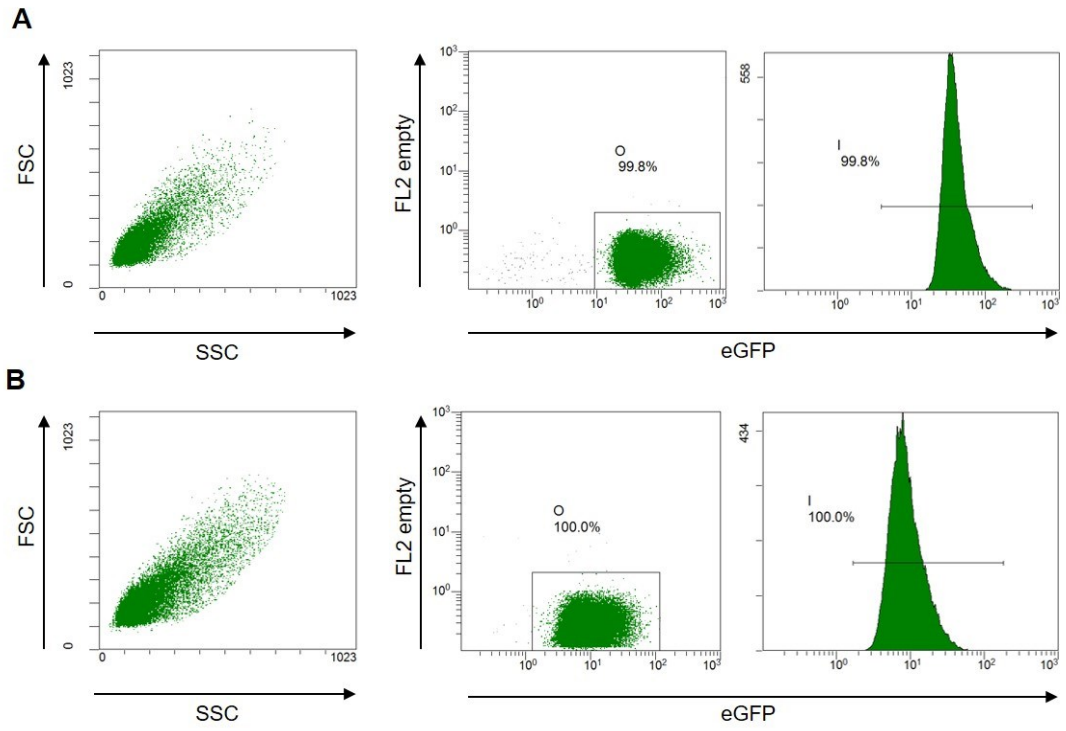

Figure 18: Analysis of GFP fluorescence in CHO-MOCK and CHO-SRB1 cells by flow cytometry.
(A) EGFP-positive population in CHO-MOCK cells, MOI = 2. (B) EGFP-positive population in CHO-SRB1 cells, MOI = 2. Gated populations represent eGFP-positive cells. Histograms represent the gated eGFP-positive populations. Untransduced CHO-K1 cells were used as a negative control in all measurements. Representative graphs to verify GFP fluorescence in cell lines.

Analyses of transduced CHO-hS1P1-MOCK and CHO-hS1P1-SRB1 cells are shown in Figure 19. MOCK-transduced CHO-hS1P1-MOCK cells expressed 99.8 % eGFP-positive cells and 99.9 % of CHO-hS1P1-SRB1 cells were eGFP-positive. However, the calculated MFI was almost 60 times higher in CHO-hS1P1-MOCK cells compared to the CHO-hS1P1-SRB1 population (MFI: 60.7 vs. 14.2).

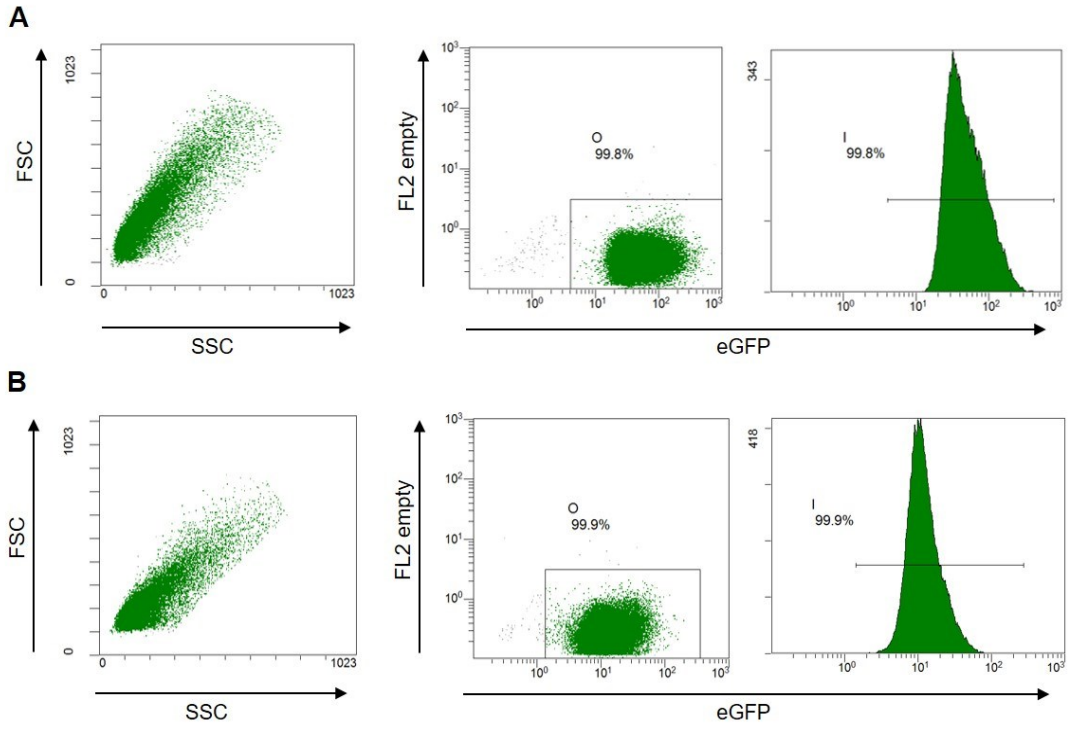

Figure 19: Analysis of eGFP fluorescence in CHO-hS1P1-MOCK and CHO-hS1P1-SRB1 cells by flow cytometry.
(A) EGFP-positive population in CHO-hS1P1-MOCK cells, MOI = 2. (B) Fluorescence of eGFP in CHO-hS1P1-SRB1 cells, MOI = 2. Gated populations represent the eGFP-positive cells. Histograms represent the gated eGFP-positive populations. Untransduced CHO-hS1P1 cells were used as a negative control in all measurements. Representative graphs to verify GFP fluorescence in cell lines.

In summary, the lentiviral vector LV.SR-BI.IRES.eGFP (SR-BI vector) expressing the murine SR-BI was successfully cloned. CHO-K1 and CHO-hS1P1 cells were transduced with this vector to overexpress SR-BI together with eGFP. CHO-MOCK and CHO-hS1P1-MOCK cells containing an empty vector expressing eGFP only were generated as control cell lines.

5.6 Impact of lentiviral transduction on SR-BI and S1P1 expression on mRNA and protein levels

5.6.1 Establishment of controls

First, the MOCK-transduced CHO cell lines were used for gene expression analysis to determine their ability to function as controls for further experiments. Untransduced CHO-K1 and CHO-hS1P1 cells were compared with CHO-MOCK and CHO-hS1P1-MOCK cells to ensure that there were no changes in the genes to be compared through the lentiviral transduction procedure. For this, *Abca1* and *Scarb1* expression levels in CHO-MOCK and CHO-hS1P1-MOCK cell lines were analyzed by quantitative RT-PCR and compared to expression levels in CHO-K1 and CHO-hS1P1 cells (Fig. 20). No significant alterations were determined in *Scarb1* or *Abca1* expressions in CHO-MOCK cells compared to the CHO-K1 control cell line and CHO-hS1P1-MOCK cells compared to CHO-hS1P1 control cells, respectively (Fig. 20A+B). In a next step, mRNA expression of *S1PR1* in transduced CHO-hS1P1-MOCK and CHO-hS1P1 control cells was determined by quantitative RT-PCR analysis and no significant differences were detected between the two cell lines (Fig. 20C).

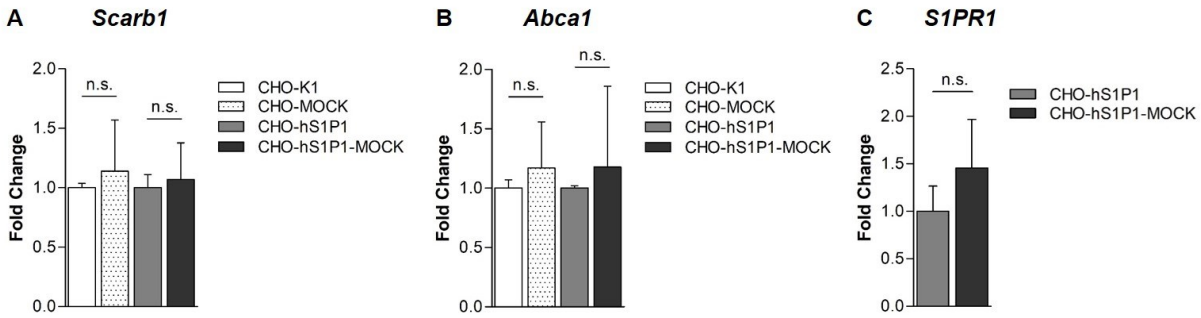

Figure 20: Analysis of *Scarb1, Abca1* and *S1PR1* mRNA expression in MOCK-transduced CHO cells compared to untransduced CHO control cells.
(A) *Scarb1* expression in CHO-MOCK and CHO-hS1P1-MOCK cells compared CHO-K1 and CHO-hS1P1, respectively (n = 4). (B) *Abca1* expression in CHO-MOCK and CHO-hS1P1-MOCK cells compared to their respective controls (n = 3/4). (C) Expression of *S1PR1* in CHO-hS1P1 cells (n = 4) compared to CHO-hS1P1-MOCK cells (n = 7). Independent experiments performed in duplicates. *Gapdh* was used as an endogenous control. Results are shown in mean ± SD; n.s., not significant.

Due to the results shown in Figure 20, CHO-MOCK and CHO-hS1P1-MOCK cells replaced the CHO-K1 and CHO-hS1P1 as control cell lines for further gene expression and functional studies involving transduction with *Scarb1*.

In a next step, the mRNA expression level of *Scarb1* was determined in transduced SR-BI-overexpressing CHO-SRB1 and CHO-hS1P1-SRB1 cells (Fig. 21A). As expected, transduction with *Scarb1* resulted in increased levels of *Scarb1* in both CHO-SRB1 and CHO-hS1P1-SRB1 cells compared to CHO-MOCK and CHO-hS1P1-MOCK cells by quantitative PCR analysis. In CHO-SRB1 cells, *Scarb1* was more than 50-fold higher expressed compared to CHO-MOCK control cells. The *Scarb1* expression in CHO-hS1P1-SRB1 cells was 40-fold higher than in CHO-hS1P1-MOCK cells but comparable to that in CHO-SRB1.

In addition to *Scarb1*, the mRNA expression levels of *eGFP* were also compared between CHO-SRB1 and CHO-hS1P1-SRB1 cells as the relative *eGFP* expression is a reflection of the copy number of the integrated mSR-BI gene. As expected from the *Scarb1* gene expression results, *eGFP* expression was also induced but without significant differences between the two SR-BI-overexpressing cell lines (Fig. 21B).

In addition to mRNA levels, SR-BI protein expression was also determined by Western blotting for the myc-tag. Western blot analysis showed no myc-tagged SR-BI expression in MOCK-transduced cells. Myc-tagged SR-BI protein was highly expressed in both SR-BI-overexpressing cells, CHO-SRB1 and CHO-hS1P1-SRB1. The quantified protein level of myc-tagged SR-BI, however, was higher in CHO-hS1P1-SRB1 cells compared to CHO-SRB1 cells (Fig. 21C). Subsequently a polyclonal anti SR-BI/SR-BII antibody chosen specifically to recognize the extracellular domain was used to determine the cell surface expression of SR-BI (Fig. 21D). SR-BI-transduced CHO cells showed increased surface expression as compared to CHO cells expressing only native SR-BI (CHO-MOCK and CHO-hS1P1-MOCK). Again, confirming the Western blotting results, comparison of the two cell lines CHO-SRB1 and CHO-hS1P1-SRB1 indicated that the CHO-hS1P1-SRB1 cells had a higher surface expression of SR-BI.

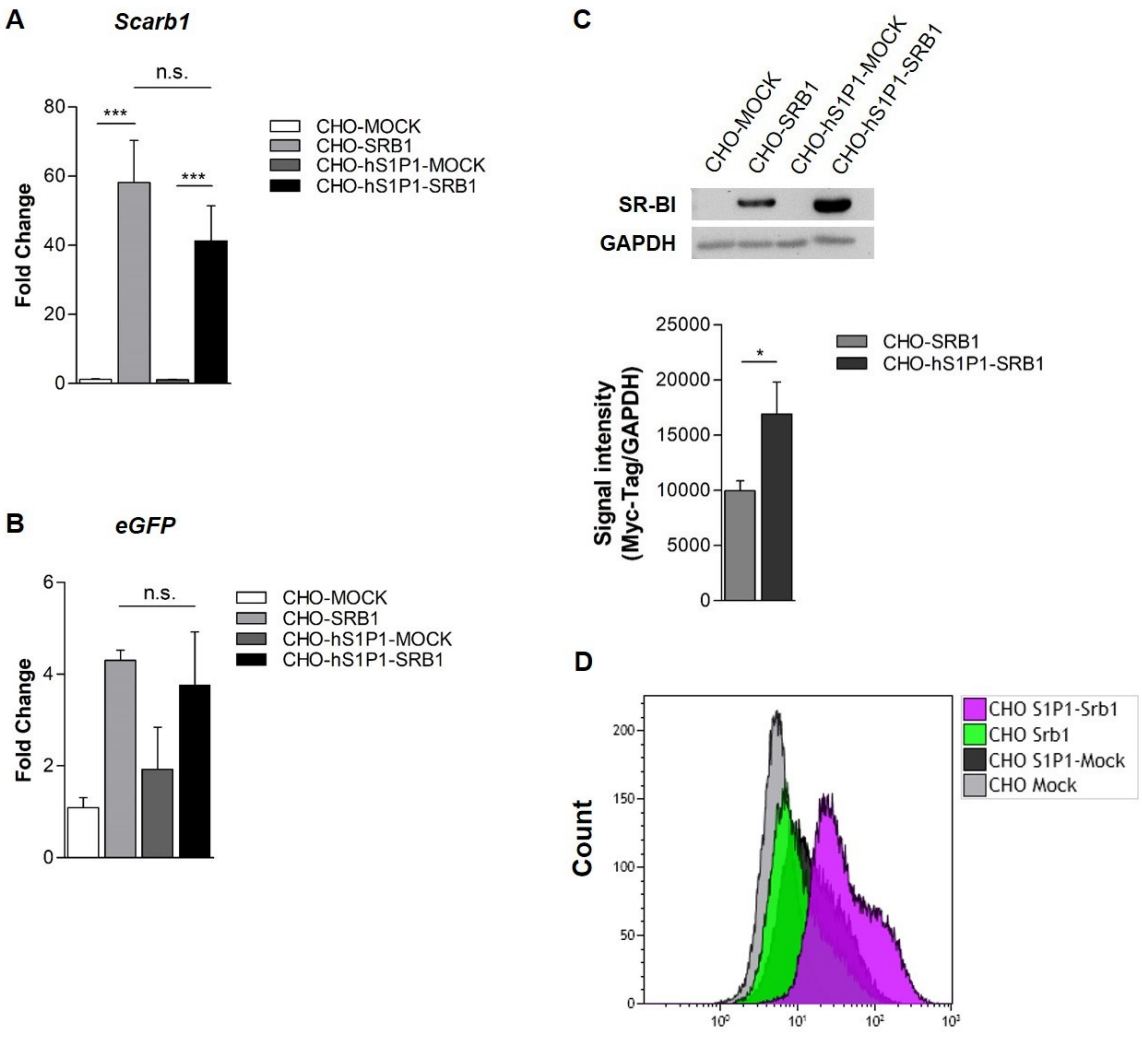

Figure 21: SR-BI expression on mRNA and protein level in SR-BI- and MOCK-transduced CHO cells.

Gene expression analyses were performed from three to four independent experiments in duplicates. *Gapdh* was used as an endogenous control. (A) Expression of *Scarb1* (n = 4). (B) Expression of *eGFP* (n = 3). (C) Western blot analysis of myc-tagged SR-BI from SR-BI- and MOCK-transduced CHO cell lysates. Blot shown represents an example from six independent experiments with similar results. Bands were quantified and normalized against GAPDH. (D) Flow cytometric analysis of SR-BI surface expression. Results are shown in mean ± SEM; **P* < 0.05, ****P* < 0.0001; n.s., not significant.

In a next step, a potential impact of SR-BI overexpression on S1P1 mRNA and protein level was investigated in CHO-hS1P1-SRB1 cells compared to CHO-hS1P1-MOCK cells (Fig. 22). Interestingly, *S1PR1* mRNA was downregulated in cells co-expressing SR-BI compared to CHO-hS1P1-MOCK control cells (Fig. 22A). Western blot analysis, however, showed higher protein levels of S1P1 in CHO-hS1P1-SRB1 cells compared to CHO-hS1P1-MOCK control cells (Fig. 22B).

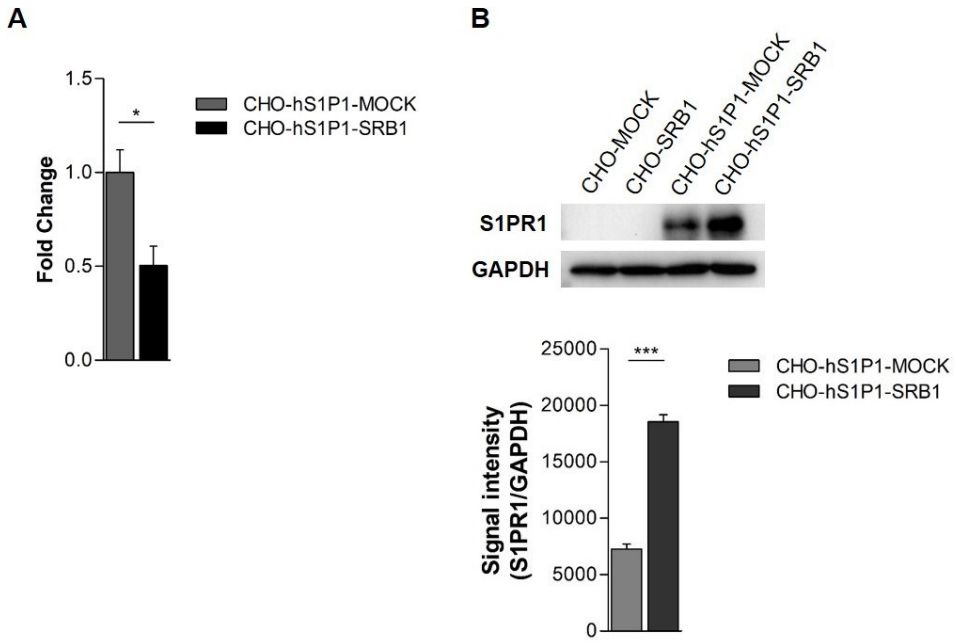

Figure 22: Expression analysis of S1PR1 on mRNA and protein level.
(A) Expression of *S1PR1* in CHO-hS1P1-MOCK and CHO-hS1P1-SRB1 cells. Quantitative RT-PCR was performed from four independent experiments in duplicates. *Gapdh* was used as an endogenous control. (B) Western blot analysis of S1P1 from CHO-hS1P1-MOCK and CHO-hS1P1-SRB1 cell lysates. Blot shown represents an example from five independent experiments with similar results. Bands were quantified and normalized against GAPDH. Results are shown in mean ± SEM; $*P < 0.05$, $***P < 0.0001$.

In summary, the murine SR-BI was successfully overexpressed in all cell lines. Interestingly, expression of SR-BI was higher in the presence of S1P1 and expression of S1P1 was higher in the presence of SR-BI. This suggests that overexpression of each one protein positively affected the expression of the other.

5.7 Effect of S1P1 on the SR-BI-mediated cholesterol efflux to HDL

5.7.1 Assessment of CHO-MOCK and CHO-hS1P1-MOCK as controls in the cholesterol efflux

CHO-MOCK and CHO-hS1P1-MOCK cell lines were compared to CHO-K1 and CHO-hS1P1 cells in their cholesterol efflux capability to HDL. CHO-MOCK cells showed no significant differences in cholesterol efflux to HDL compared to CHO-K1 control cells (Fig 23A). Similar results were obtained for CHO-hS1P1-MOCK cells and corresponding CHO-hS1P1 control cells. Movement of free cholesterol from

CHO-hS1P1-MOCK cells to HDL was equal to efflux of cholesterol from CHO-hS1P1 to HDL (Fig. 23B). Therefore, CHO-MOCK and CHO-hS1P1-MOCK transduced cells were used as controls in following cholesterol efflux assays as none of the interventions had an effect compared to the respective non-transduced cell line.

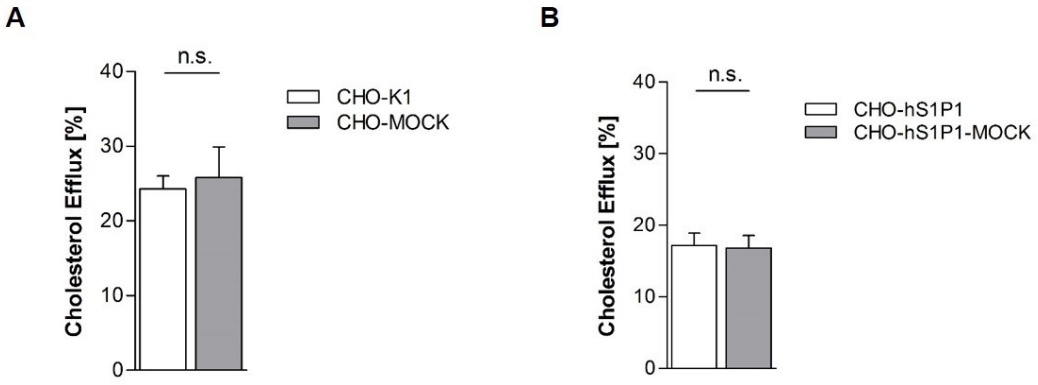

Figure 23: Corrected cholesterol efflux from CHO control and MOCK-transduced CHO cell lines to the cholesterol acceptor HDL.
(A) Comparison of cholesterol efflux to HDL (0.1 mg protein/ml) from CHO-K1 control cells and CHO-MOCK transduced cells (n = 4). (B) Cholesterol efflux from CHO-hS1P1 control cells and CHO-hS1P1-MOCK transduced cells to HDL (0.1 mg protein/ml; n = 4). HDL from different preparations was used. Results are shown in mean ± SEM; n.s., not significant.

5.7.2 Cholesterol efflux to HDL in SR-BI-transduced cells without and with S1P1

The hypothesis, whether the cholesterol efflux to HDL is not only dependent on the SR-BI receptor but altered by S1P1, was tested in transduced CHO-MOCK, CHO-SRB1, CHO-hS1P1-MOCK, and CHO-hS1P1-SRB1 cells. The cells were loaded with ^{3}H-cholesterol and subsequently incubated with HDL. The results obtained for the net cholesterol efflux capacity to HDL are shown in Figure 24A. CHO-MOCK cells showed a mean cholesterol efflux of 25.8 ± 4.1 %. The SR-BI overexpression in CHO-SRB1 cells significantly increased the cholesterol efflux to HDL (45.4 ± 4.7 %). No significant differences in the cholesterol efflux were determined between the control cell lines CHO-hS1P1-MOCK and CHO-MOCK. Interestingly, CHO-hS1P1-SRB1 cells co-expressing S1P1 and SR-BI reduced the cholesterol efflux to HDL to the efflux level of CHO-MOCK cells (21.9 % ± 2.5 vs 25.8 % ± 4.1) abolishing the effect of SR-BI overexpression.

In a next step, the effect of additional S1P stimulation was assessed. Cells were loaded with ^{3}H-cholesterol overnight and stimulated with S1P (1 µM) 30 min before adding HDL. The results obtained are shown in Figure 24B. Stimulation with exogenously supplied S1P did not affect the cholesterol efflux in any of these cell lines.

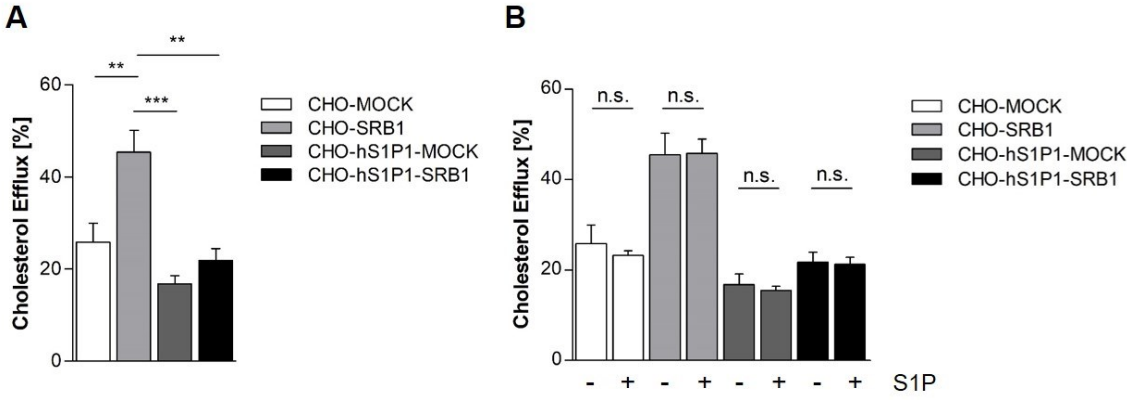

Figure 24: Cholesterol efflux to HDL in transduced CHO-MOCK, CHO-SRB1, CHO-hS1P1-MOCK, CHO-hS1P1-SRB1 cells.
(A) Cholesterol efflux to HDL (0.1 mg protein/ml, 5 h incubation); n = 7. (B) Cholesterol efflux with and without S1P stimulation (1 µM, 30 min) before incubation of HDL; n = 4. Results are expressed as mean ± SEM from independent experiments performed in triplicates; $^{**}P < 0.005$, $^{***}P < 0.0005$, n.s., not significant.

In summary, SR-BI overexpression increased the cholesterol efflux to HDL in CHO-SRB1 cells. However, this was not the case in CHO-hS1P1-SRB1 cells despite their higher total and cell surface SR-BI protein levels.

5.8 S1P1-mediated activation of ERK-1/2 MAP kinase phosphorylation in transduced CHO-hS1P1-SRB1 cells

S1P receptors activated by S1P and HDL-associated S1P induce several downstream signaling pathways, including activation of MAPK kinases. Therefore, the involvement of SR-BI in the extracellular signal-related kinases 1/2 (ERK-1/2) phosphorylation in CHO-hS1P1-MOCK and CHO-hS1P1-SRB1 cells was explored upon S1P and HDL stimulation.

Stimulation with S1P (1 µM) was performed in a time-dependent manner and resulted in an increase in the phosphorylation of ERK-1/2 in both cell lines. The phosphorylation

of ERK-1/2 in CHO-hS1P1-MOCK cells was detectable from two minutes after S1P stimulation, peaked at five minutes and decreased at 10 minutes. Activation of pERK-1/2 in CHO-hS1P1-SRB1 cells also increased in a time-dependent manner. It appeared that pERK-1/2 was more effective in CHO-hS1P1-SRB1 than in CHO-hS1P1-MOCK cells, but significance was not reached after quantification (Fig. 25A). Activation of pERK-1/2 by HDL was also assessed in CHO-hS1P1-MOCK and CHO-hS1P1-SRB1 cells. Stimulation with HDL (0.1 mg/ml protein) resulted in an increase in pERK-1/2 phosphorylation in a time-dependent manner in both cell lines but no differences between the two cell lines were detected (Fig. 25B).

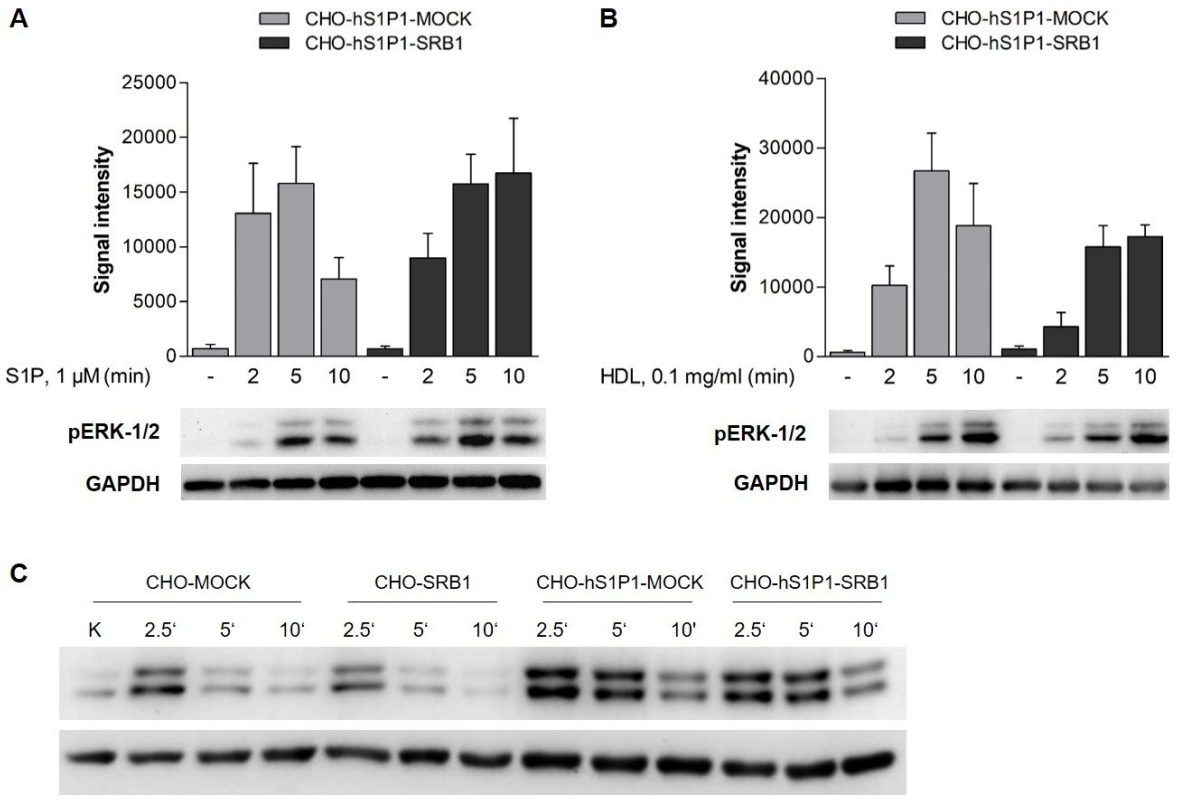

Figure 25: Activation of pERK-1/2 by S1P and HDL in CHO-hS1P1-MOCK and CHO-hS1P1-SRB1 cells.

(A) Time course of pERK-1/2 activation by S1P. Cells were stimulated with S1P (1 µM) for the indicated times (min). (B) Time course of pERK-1/2 activation by HDL. Cells were stimulated with HDL (0.1 mg protein/ml) for the indicated time points (min). (A+B) Cell lysates were analyzed by Western blotting, quantified and normalized against GAPDH. Blots shown (bottom) are representative examples from seven independent experiments with similar results. (C) Phospho-ERK-1/2 signaling by HDL (0.1 mg protein/ml) in CHO-MOCK, CHO-SRB1, CHO-hS1P1-MOCK and CHO-hS1P1-SRB1 cells (n = 1). Data in the graphs are expressed as mean ± SEM.

Phospho-ERK-1/2 activation by HDL was then compared in CHO-MOCK, CHO-SRB1, CHO-hS1P1-MOCK and CHO-hS1P1-SRB1 cells (Fig. 25C). The four cell lines were stimulated with HDL (0.1 mg/ml protein) in a time-dependent manner. Cells expressing hS1P1 (CHO-hS1P1-MOCK and CHO-hS1P1-SRB1) showed higher pERK-1/2 signaling than cells without hS1P1 expression (CHO-MOCK and CHO-SRB1), confirming that HDL-S1P activated pERKs through S1P1. However, cells overexpressing S1P1 exhibited the same pERK-1/2 signaling profile no matter whether SR-BI was co-expressed or not.

In summary, overexpression of SR-BI had no effect on S1P-mediated or HDL-S1P-mediated pERK-1/2 signaling in CHO cells despite the increase in S1P1 protein levels after SR-BI overexpression.

6 Discussion

HDL is well known to play an essential role in the RCT, in which it removes excess free cholesterol from cells and transports it to the liver where it is excreted into the bile (Glass et al., 1983; Saddar et al., 2010). High concentrations of HDL-cholesterol are inversely related to the risk of atherosclerotic cardiovascular diseases (Assmann et al., 2004; Gordon and Rifkind, 1989). Several studies have identified S1P as a constituent of HDL which mediates many functions involved in the cardiovascular system by signaling through one of the S1P receptors S1P1-3 (Kimura et al., 2003; Sato and Okajima, 2010; Sattler et al., 2015, 2010; Theilmeier et al., 2006). Various studies have examined the role of S1PRs or SR-BI in HDL-mediated signaling or in the biological functions exerted by HDL. However, the potential joint involvement of both receptors in HDL-mediated biological effects has only been investigated in a limited number of studies (Kimura et al., 2006, 2010; Lee et al., 2017).
The results in the present study indicate that S1P1 has an effect on the efflux of cholesterol from CHO cells to lipid-free apoA-I and mature HDL. The results also suggest a relationship between S1P1 and SR-BI on HDL-mediated cholesterol efflux.

6.1 Influence of S1P receptors on the cholesterol efflux to apoA-I and HDL

To gain further insight into the involvement of S1P receptor activity in the removal of cholesterol, CHO cells overexpressing S1P1-3 were used to investigate the transport of cholesterol from cells to lipid-free apoA-I and mature HDL. Several biological responses, including cell proliferation and migration (Kimura et al., 2000; Lee et al., 2001), vasorelaxation (Nofer et al., 2004), endothelial barrier function (Garcia et al., 2001), vascular maturation (Liu et al., 2000), and immunological effects (Gräler et al., 2005) are mediated by S1PRs. The role of S1PRs in the transport of free cholesterol to apoA-I and HDL has not been examined yet.

ApoA-I is the major protein component in HDL, which interacts with binding sites on the cell surface to enable movement of free cholesterol from peripheral cells to HDL (Spady, 1999). The data of this study clearly show that the ability of lipid-free apoA-I to induce efflux of free cholesterol from CHO cells was unaltered in the presence of high levels of S1P1, 2 and 3. The main cellular cholesterol transporter to apoA-I is

ABCA1, whereas ABCG1 and SR-BI mediate the transport of free cholesterol to lipidated HDL particles (Larrede et al., 2009). Interestingly, *Abca1* gene expression was significantly decreased in CHO-hS1P1 cells although the cholesterol efflux was unaffected, suggesting that even such low ABCA1 levels are sufficient for cholesterol efflux. However, additional stimulation of S1P1 by S1P almost completely abolished cholesterol efflux to apoA-I in CHO-hS1P1 cells, suggesting that there is a functional relationship between S1P1 and ABCA1 at the transcriptional as well as functional level. One possibility is that this occurs through the well-known negative impact of S1P1/Gi signaling on adenylyl cyclase (Means et al., 2008) as cAMP is a potent stimulator of ABCA1 transcription and function (Hokland et al., 1993; Lawn et al., 1999; Oram et al., 2000; Smith et al., 1996). To follow up on this, experiments where ABCA1 transcription and function are stimulated, e.g. by LXR agonists and cAMP generating agents, respectively, will have to be conducted in the presence and absence of S1P. Further circumstantial support comes from the findings in this study showing that S1P2 and S1P3 – the S1P receptors with a smaller or no effect on cAMP – had no effect on ABCA1 expression or cholesterol efflux under basal or S1P-stimulated conditions. Finally, our laboratory just published a study where LXR-stimulated cholesterol efflux in macrophages is dependent on endogenous S1P production through sphingosine kinases (Vaidya et al., 2019).

In respect to HDL, the results in the present study reveal that there were no significant differences in cholesterol efflux between control and CHO cells overexpressing S1P1-3 or among the different S1P receptor overexpressing cell lines. The efflux of free cholesterol to HDL was also independent of stimulation with S1P (or stimulation with S1P-loaded HDL, data not shown) in CHO cells overexpressing S1PRs. This is in agreement with Matuso et al. who reported that reconstituted HDL (rHDL) containing S1P showed a similar effect on the cholesterol efflux in macrophages compared to rHDL without S1P (Matsuo et al., 2007). However, *Scarb1* expression was two to three-fold higher in all S1PR-overexpressing CHO cells, still suggesting a subtle relationship. Such a relationship may have not been visible at the level of cholesterol efflux with the HDL concentrations used and considering that SR-BI is not the only way of cholesterol efflux to HDL. Indeed, the efflux to HDL is extremely efficient and of much higher capacity compared to that to apoA-I. Thus, the impact of S1P on ABCA1-mediated

cholesterol efflux to apoA-I, which was described above, might have been detected because of its much lower efficiency.
These observations led to the design of further experiments using lentiviral reporter constructs overexpressing SR-BI in the presence or absence of high S1P1 expression and the search for functional interrelations.

6.2 Development of a bicistronic lentiviral vector co-expressing SR-BI along with eGFP

A lentiviral vector encoding the murine SR-BI and the eGFP gene was developed in order to co-express both SR-BI and eGFP in CHO cells from a single mRNA. Both SR-BI-overexpressing cell lines used in this study, CHO-SRB1 and CHO-hS1P1-SRB1, showed efficient expression of SR-BI as well as eGFP. However, compared to their respective MOCK-transduced control cell lines, the eGFP expression in SR-BI-overexpressing cells was extremely low. An explanation for these differences might be the use of two different lentiviral backbones in SR-BI-transduced and MOCK-transduced cell lines. A monocistronic vector was used for the MOCK-transduced cells, driving eGFP expression from one cistron. A bicistronic vector was used for the simultaneous expression of SR-BI and eGFP. Consequently, the monocistronic MOCK-vector may not be an appropriate negative control for the bicistronic SR-BI vector. Bi- and multicistronic vectors containing an IRES element have been widely used as tools for the expression of multiple transgenes in mammalian cell culture or transgenic animals (Attal et al., 1999). Eukaryotic mRNA usually requires the 5’ cap structure, which is added to the 5’-end of the pre-mRNA during transcription and participates in the recruitment of the ribosome to the mRNA for the initiation of the translation. In contrast, IRES elements permit the initiation of translation of additional genes independent of the cap structure (Licursi et al., 2011). In this study, the translation of the SR-BI gene upstream of the IRES sequence was initiated by the cap-dependent mechanism, whereas the translation of the fluorescent marker eGFP downstream of the IRES sequence was initiated by a cap-independent mechanism. With the use of an IRES element, the eGFP expression was expected to reflect the amount of target protein produced in a cell. However, the expression levels of a transgene downstream of the IRES sequence can be lower compared to the expression of the upstream transgene (Mizuguchi et al., 2000; Zhou et al., 1998) and

may vary among different cell lines. Indeed, flow cytometric analysis revealed that the IRES-dependent expression of eGFP gene was lower compared to the eGFP-expression in the monocistronic MOCK vectors. In contrast, the results reveal that mRNA and protein of SR-BI were highly expressed, suggesting that this gene upstream of IRES was not negatively affected by IRES-dependent translation.

6.3 Interactions of S1P1 and SR-BI in cholesterol efflux, protein levels and pERK-1/2 signaling

The SR-BI receptor is known to be enriched in caveolae, structures in the plasma membrane known to be involved in the transport of cholesterol (Babitt et al., 1997). Previous studies localized SR-BI mainly on the plasma membrane (Lee et al., 2017; Peng et al., 2004), whereas others showed that SR-BI was mainly distributed in the cytoplasm, e.g. in 3T3-L1 adipocytes. Stimulation with HDL, insulin or angiotensin II caused SR-BI to be translocated to the cell surface (Tondu et al., 2005). In this study, flow cytometric analysis was used to determine the surface expression of native SR-BI and overexpressed murine SR-BI receptor conjugated to GFP as only this part of the SR-BI pool is expected to be involved in cholesterol efflux. As hoped for, not only total but also cell surface expression of SR-BI was increased after lentiviral SR-BI transduction.

Interestingly, S1PRs have also been identified to localize in caveolae in different cell types (Igarashi and Michel, 2000; Means et al., 2008). So far, the majority of studies have determined only on the involvement of S1PRs or that of SR-BI in HDL and HDL-S1P-mediated functions. Recently, however, it has been shown that SR-BI and S1P1 move into close proximity and form complexes when stimulated with HDL (Lee et al., 2017). Only few studies actually focused on HDL-S1P-mediated effects dependent on both receptors simultaneously (Al-Jarallah et al., 2014; Kimura et al., 2006; Lee et al., 2017). Many studies have suggested that S1PRs and SR-BI might interact to mediate certain HDL-mediated biological functions, such as NO-dependent vasodilation where HDL acts in part through S1P3 (Nofer et al., 2004) and for which SR-BI is indispensable (Mineo et al., 2003; Yuhanna et al., 2001). Other studies have confirmed functional interactions between S1PRs and SR-BI in HDL-induced inhibition of adhesion molecule expression in endothelial cells (Kimura et al., 2006), in HDL-

induced calcium flux (Lee et al., 2017) and macrophage migration (Al-Jarallah et al., 2014).

The impact of S1PRs on SR-BI-mediated cholesterol efflux has not been investigated until now. To address this, cells overexpressing S1P1, SR-BI or both were loaded with ^{3}H-cholesterol and cholesterol efflux to HDL was measured with and without S1P-stimulation. As expected, overexpression of SR-BI resulted in an elevated efflux of free cholesterol to HDL in agreement with previous studies (Ji et al., 1997; Jian et al., 1998; de la Llera-Moya et al., 1999). Overexpression of S1P1 alone had no effect on efflux but it completely abolished the induction by SR-BI overexpression. This was not due to negative effects on SR-BI expression at the protein or mRNA levels (SR-BI protein was even induced), suggesting a functional interaction. This reflects the functional interplay investigated for S1P1 and ABCA1. In the case of HDL, the suppressive effect of S1P1 on cAMP production through inhibition of the adenylyl cyclase may be involved, as cAMP also stimulates SR-BI (Shen et al., 2016). This is an exciting possibility that remains to be addressed in future studies.

In fact, that SR-BI gene expression was not downregulated with S1P1 overexpression also supports a functional rather than transcriptional or mRNA stability-based mechanism of downregulation of cholesterol efflux when SR-BI and S1P1 are co-expressed. Published studies indicate that the expression and function of SR-BI can be regulated by post-transcriptional mechanisms. Proteins containing PDZ domains (so named from postsynaptic density 95/discs-large/zonula occludens-1) can reduce SR-BI expression by binding to its C terminus. Two of these PDZ domain-containing proteins, NHERF1 and NHERF2 (Na^{+}/H^{+} exchanger regulatory factors), downregulate the protein expression of SR-BI in steroidogenic tissues by degradation and altering cholesterol trafficking without changing SR-BI mRNA levels (Fenske et al., 2008; Hu et al., 2013; Kocher et al., 2003; Leiva et al., 2011). NHERF2-induced degradation of SR-BI underlies the ubiquitin-proteasome pathway. Interestingly, NHERF2 is also known to be involved in recycling mechanisms of GPCRs (Hanyaloglu and Zastrow, 2008). Previous studies have speculated that stimulation with HDL-S1P promotes increased S1P1 recycling to the cell surface through a mechanism involving cholesterol transfer from HDL to the endosomal membrane (Wilkerson and Argraves, 2014). Binding of S1P1 to PDZ domain-containing proteins may be involved in the receptor recycling process (Hanyaloglu and Zastrow, 2008; Wilkerson and Argraves, 2014). S1P1 does not contain a PDZ binding site but the receptor binds to thyroid

receptor interacting protein 6 (TRIP6), a PDZ domain-binding protein which in turn complexes with the PDZ domain of NHERF2 (Hanyaloglu and Zastrow, 2008; Shuyu et al., 2009; Wilkerson and Argraves, 2014). Thus, NHERF2 expression may not only reduce S1P1 turnover but also reduce S1P1 degradation usually taking place through ubiquitination and proteasomal degradation. This may occur by influencing protein stability, S1P1 phosphorylation at sites required for initiation of the ubiquitination process, or by affecting the activity of the S1P1 specific ubiquitin E3 ligase (Oo et al., 2011). Ubiquitination is a well-recognized regulatory mechanism in GPCR signaling (Alonso and Friedman, 2013). Indeed, the S1P1 agonist FTY720 (Fingolimod) has been shown to induce phosphorylation of the receptor's carboxyterminal domain at several sites promoting receptor internalization, polyubiquitinylation by the NEDD4 family member E3 ubiquitin ligase WWP2 (also known as atrophin-1-interacting protein 2) and proteasomal degradation (Oo et al., 2011). Thus, further investigations regarding the mechanism involved in the S1P1 recycling process in context of SR-BI are still warranted.

Another surprising finding was the upregulation of S1P1 protein expression in cells overexpressing SR-BI. It is known that S1P-induced signaling upon binding to S1P1 activates the phosphorylation of ERK-1/2 and induces internalization of the receptor (Estrada et al., 2009; Lee et al., 1996, 1998). Recently published data showed faster internalization of S1P1 upon S1P stimulation (10 min) compared to the stimulation with HDL-S1P (15 min; Lee et al., 2017). Ligand binding to SR-BI such as that of HDL is known to stimulate ERK-1/2 phosphorylation in some studies (Grewal et al., 2003; Mineo et al., 2003; Osada et al., 2006; Sachinidis et al., 1999). Thus, activation of ERK phosphorylation was chosen in this study as a functional readout for S1P, HDL and HDL-S1P signaling through S1P1 and SR-BI. Additional overexpression of SR-BI did not result in a more prolonged or stronger pERK-1/2 activation by HDL in S1P1 overexpressing cells (CHO-hS1P1-SRB1 compared to CHO-hS1P1-MOCK), which could have been assumed if binding of HDL was mediated by SR-BI prior or simultaneously with S1P1 activation. This suggests either that HDL did not need SR-BI for S1P1 engagement or that the amounts of endogenous SR-BI were sufficient to do so. The results could be confirmed by additional experimentation performed in SR-BI knockout cells. In addition, the increase in total S1P1 protein in SR-BI overexpressing cells did not result in better S1P-stimulated ERK signaling and needs to be further

investigated as it suggests that there may be an inhibitory effect of SR-BI on S1P1 signaling similar to the inhibitory effect of S1P1 on SR-BI-mediated cholesterol efflux. In conclusion, this study is the first to identify a functional interaction between S1P1 and SR-BI, where S1P1 was able to downregulate SR-BI function with clear inhibitory consequences for cholesterol efflux. The exact mechanisms remain to be investigated in much more detail in the future.

7 Conclusion and outlook: future investigations of the physical and functional interaction between S1P1 and SR-BI

The results obtained in this study identified for the first time a functional interaction of S1P1 and SR-BI receptors on SR-BI-mediated cholesterol efflux. To further investigate this interaction, inhibition and knockout studies will have to complement and confirm the overexpression studies presented here. In case of SR-BI, binding of HDL to SR-BI can be successfully inhibited by the use of an antibody against the extracellular domain of SR-BI as shown in HDL-mediated activation of Ras (Grewal et al., 2003). Co-localization and physical interactions also need to be investigated: e.g. interactions between S1P1 and SR-BI during cholesterol efflux could be characterized in living cells using fluorescently tagged versions and will be of importance to understand the functional aspect in detail. Several techniques have been developed to do this (Rao et al., 2014). For physical interactions, co-immunoprecipitation may be the most straightforward method to study protein-protein associations. Previously, a putative direct S1P1-/SR-BI-interaction has been shown only in protein-fragment complementation assays and confocal microscopy (Kimura et al., 2006; Lee et al., 2017). To further understand the physiological role of such interactions in cholesterol efflux it would be necessary to study the process in intact cells and to do this in macrophages as the classical cell type involved in cholesterol efflux. Cholesterol efflux could also be evaluated in macrophages overexpressing or lacking either S1P1 or SR-BI and using specific S1PR agonists and antagonists as well as a SR-BI neutralizing antibody or specific SR-BI inhibitors such as BLT-1 (blocker of lipid transport 1) (Raldúa and Babin, 2007; Yu et al., 2011). *In vivo*, cholesterol disposal with the feces as the only reliable parameter of net RCT in the presence of such interventions will define the significance for physiological and pathophysiological cholesterol homeostasis. Any insights into mechanisms allowing a more efficient RCT will be of benefit for potential cholesterol-lowering therapies in humans.

8 Summary

High-density lipoprotein (HDL) is well known to play an essential role in the reverse cholesterol transport, in which it removes excess free cholesterol from cells and transports it to the liver where it is excreted into the bile. The reverse cholesterol transport is considered as an important anti-atherogenic function of HDL, as it prevents macrophage foam cell formation. The HDL-receptor SR-BI is known as an important mediator in this transport mechanism. Various functions of HDL can be attributed to HDL-associated sphingosine-1-phosphate (S1P). S1P is a bioactive sphingolipid, which mediates many functions involved in the cardiovascular system by signaling through one of the five G protein-coupled S1P receptors (S1P1-5). The majority of studies have examined the role of S1P receptors or that of SR-BI in HDL and HDL-S1P-mediated functions. However, the potential joint involvement of both receptors in HDL-mediated biological effects has only been investigated in a limited number of studies. As an important step toward understanding a possible relationship between S1P receptors and the SR-BI-mediated removal of cholesterol from cells to acceptors, cell lines overexpressing the SR-BI receptor and/or S1P receptors were generated to study the interaction between both in the removal of cholesterol. This study is the first to identify a functional interaction of S1P1 and SR-BI receptors. S1P1 was able to downregulate SR-BI function with clear inhibitory consequences for cholesterol efflux.

9 Zusammenfassung

Das High-Density Lipoprotein (HDL) spielt eine entscheidende Rolle im reversen Cholesterintransport. HDL transportiert freies Cholesterin aus dem extrahepatischen Gewebe zurück zur Leber. Den HDL-Partikeln wird eine anti-atherogene Wirkung zugeschrieben, da sie durch die Aufnahme von Cholesterin der Bildung von Schaumzellen entgegenwirken. Der HDL-Rezeptor SR-BI spielt bei diesem reversen Cholesterintransport ebenfalls eine entscheidende Rolle. Außerdem werden verschiedenste HDL-Funktionen dem biologisch aktiven Sphingolipid Sphingosin-1-Phosphat (S1P) zugeordnet, das gebunden an HDL vorliegt. Dieses Sphingolipid findet zunehmend Beachtung beispielsweise in der Herz-Kreislauf-Physiologie. An HDL gebundenes S1P entfaltet seine Signalwirkung auf an Arteriosklerose beteiligten Zellen über fünf G-Protein gekoppelte S1P Rezeptoren (S1P1-5). Die Mehrheit der bisherigen Studien zeigten entweder die Wirkung der S1P-Rezeptoren oder die des HDL Rezeptors SR-BI in HDL-vermittelten Effekten. Eine mögliche Interaktion beider Rezeptoren bei HDL-vermittelten Funktionen wurde jedoch bisher nur wenig untersucht. Um ein mögliches Zusammenspiel von S1P Rezeptoren im SR-BI-vermittelten reversen Cholesterintransport zu untersuchen und zu identifizieren, wurden in dieser Arbeit Zelllinien generiert, die den SR-BI Rezeptor und/oder S1P Rezeptoren überexprimieren. Die vorliegende Arbeit zeigt zum ersten Mal eine funktionelle Interaktion von S1P1 und SR-BI. S1P1 konnte die Funktion von SR-BI herunterregulieren und hatte damit einen inhibierenden Einfluss auf den Cholesterin-Efflux.

10 References

Ader, I., Malavaud, B. and Cuvillier, O. (2009), “When the Sphingosine Kinase 1/Sphingosine 1-Phosphate Pathway Meets Hypoxia Signaling: New Targets for Cancer Therapy”, *Cancer Research*, Vol. 69 No. 9, pp. 3723–3726.

Al-Jarallah, A., Chen, X., González, L. and Trigatti, B.L. (2014), “High Density Lipoprotein Stimulated Migration of Macrophages Depends on the Scavenger Receptor Class B, Type I, PDZK1 and Akt1 and Is Blocked by Sphingosine 1 Phosphate Receptor Antagonists”, edited by Kocher, O.*PLoS ONE*, Public Library of Science, Vol. 9 No. 9, p. e106487.

Alonso, V. and Friedman, P.A. (2013), “Minireview: Ubiquitination-regulated G Protein-Coupled Receptor Signaling and Trafficking”, *Molecular Endocrinology*, Oxford University Press, Vol. 27 No. 4, pp. 558–572.

Anliker, B. and Chun, J. (2004), “Cell surface receptors in lysophospholipid signaling”, *Seminars in Cell & Developmental Biology*, Academic Press, Vol. 15 No. 5, pp. 457–465.

Ansell, B.J., Navab, M., Watson, K.E., Fonarow, G.C. and Fogelman, A.M. (2004), “Anti-Inflammatory Properties of HDL”, *Reviews in Endocrine and Metabolic Disorders*, Kluwer Academic Publishers, Vol. 5 No. 4, pp. 351–358.

Aoki, S., Yatomi, Y., Ohta, M., Osada, M., Kazama, F., Satoh, K., Nakahara, K., et al. (2005), “Sphingosine 1-Phosphate–Related Metabolism in the Blood Vessel”, *The Journal of Biochemistry*, Vol. 138 No. 1, pp. 47–55.

Arai, T., Wang, N., Bezouevski, M., Welch, C. and Tall, A.R. (1999), “Decreased atherosclerosis in heterozygous low density lipoprotein receptor-deficient mice expressing the scavenger receptor BI transgene.”, *The Journal of Biological Chemistry*, American Society for Biochemistry and Molecular Biology, Vol. 274 No. 4, pp. 2366–71.

Argraves, K.M. and Argraves, W.S. (2007), “HDL serves as a S1P signaling platform mediating a multitude of cardiovascular effects.”, *Journal of Lipid Research*, American Society for Biochemistry and Molecular Biology, Vol. 48 No. 11, pp. 2325–33.

Assmann, G., Gotto, A.M., Herrmann, J., Keul, P., Schäfers, M., Herrgott, I., Mersmann, J., et al. (2004), “HDL cholesterol and protective factors in atherosclerosis.”, *Circulation*, American Heart Association, Inc., Vol. 109 No. 23 Suppl 1, pp. III8-14.

ATCC. (2014), “HT-1080 [HT1080] ATCC ® CCL-121™ Homo sapiens connective tis”, available at: https://www.lgcstandards-atcc.org/Products/All/CCL-121.aspx?geo_country=de#generalinformation (accessed 17 April 2018).

ATCC. (2017), “CHO-K1 (ATCC ® CCL-61™) Cricetulus griseus ovary”, available at: https://www.lgcstandards-atcc.org/products/all/CCL-61.aspx?geo_country=de (accessed 17 April 2018).

ATCC. (2018), “293T ATCC® CRL-3216™”, available at: https://www.lgcstandards-atcc.org/Products/All/CRL-3216.aspx?geo_country=de#characteristics (accessed 17 April 2018).

Attal, J., Théron, M.-C. and Houdebine, L.M. (1999), “The optimal use of IRES (internal ribosome entry site) in expression vectors”, *Genetic Analysis: Biomolecular Engineering*, Elsevier, Vol. 15 No. 3–5, pp. 161–165.

Aviram, M., Rosenblat, M., Bisgaier, C.L., Newton, R.S., Primo-Parmo, S.L. and La Du, B.N. (1998), “Paraoxonase inhibits high-density lipoprotein oxidation and preserves its functions. A possible peroxidative role for paraoxonase.”, *Journal of Clinical Investigation*, Vol. 101 No. 8, pp. 1581–1590.

Babiak, J. and Rudel, L.L. (1987), “Lipoproteins and atherosclerosis.”, *Bailliere’s Clinical Endocrinology and Metabolism*, Vol. 1 No. 3, pp. 515–50.

Babitt, J., Trigatti, B., Rigotti, A., Smart, E.J., Anderson, R.G., Xu, S. and Krieger, M. (1997), “Murine SR-BI, a high density lipoprotein receptor that mediates selective lipid uptake, is N-glycosylated and fatty acylated and colocalizes with plasma membrane caveolae.”, *The Journal of Biological Chemistry*, American Society for Biochemistry and Molecular Biology, Vol. 272 No. 20, pp. 13242–9.

Brinkmann, V. (2007), “Sphingosine 1-phosphate receptors in health and disease: Mechanistic insights from gene deletion studies and reverse pharmacology”, *Pharmacology & Therapeutics*, Pergamon, Vol. 115 No. 1, pp. 84–105.

Brown, M.S. and Goldstein, J.L. (1986), “A receptor-mediated pathway for cholesterol homeostasis.”, *Science (New York, N.Y.)*, Vol. 232 No. 4746, pp. 34–47.

Cavelier, C., Lorenzi, I., Rohrer, L. and von Eckardstein, A. (2006), “Lipid efflux by the ATP-binding cassette transporters ABCA1 and ABCG1”, *Biochimica et Biophysica Acta (BBA) - Molecular and Cell Biology of Lipids*, Vol. 1761 No. 7, pp. 655–666.

Christoffersen, C., Nielsen, L.B., Axler, O., Andersson, A., Johnsen, A.H. and Dahlbäck, B. (2006), “Isolation and characterization of human apolipoprotein M-containing lipoproteins.”, *Journal of Lipid Research*, American Society for Biochemistry and Molecular Biology, Vol. 47 No. 8, pp. 1833–43.

Christoffersen, C., Obinata, H., Kumaraswamy, S.B., Galvani, S., Ahnström, J., Sevvana, M., Egerer-Sieber, C., et al. (2011), “Endothelium-protective sphingosine-1-phosphate provided by HDL-associated apolipoprotein M.”, *Proceedings of the National Academy of Sciences of the United States of America*, Vol. 108 No. 23, pp. 9613–8.

Coant, N., Sakamoto, W., Mao, C. and Hannun, Y.A. (2017), “Ceramidases, roles in sphingolipid metabolism and in health and disease”, *Advances in Biological Regulation*, Pergamon, Vol. 63, pp. 122–131.

Cohen, D.E. (2008), “Balancing cholesterol synthesis and absorption in the gastrointestinal tract.”, *Journal of Clinical Lipidology*, NIH Public Access, Vol. 2 No. 2, pp. S1-3.

Conklin, B.R. and Bourne, H.R. (1993), “Structural elements of Gα subunits that interact with Gβγ, receptors and effectors”, *Cell*, Vol. 73, pp. 631–641.

Covey, S.D., Krieger, M., Wang, W., Penman, M. and Trigatti, B.L. (2003), “Scavenger receptor class B type I-mediated protection against atherosclerosis in LDL receptor-negative mice involves its expression in bone marrow-derived cells.”, *Arteriosclerosis, Thrombosis, and Vascular Biology*, American Heart Association, Inc., Vol. 23 No. 9, pp. 1589–94.

Crockett, E.L. (1998), “Cholesterol Function in Plasma Membranes from Ectotherms: Membrane-Specific Roles in Adaptation to Temperature”, *American Zoologist*, Oxford University Press, Vol. 38 No. 2, pp. 291–304.

Cuvillier, O., Pirianov, G., Kleuser, B., Vanek, P.G., Coso, O.A., Gutkind, J.S. and Spiegel, S. (1996), “Suppression of ceramide-mediated programmed cell death by sphingosine-1-phosphate”, *Nature*, Vol. 381 No. 6585, pp. 800–803.

von Eckardstein, A., Nofer, J.R. and Assmann, G. (2001), “High density lipoproteins and arteriosclerosis. Role of cholesterol efflux and reverse cholesterol transport.”, *Arteriosclerosis, Thrombosis, and Vascular Biology*, American Heart Association, Inc., Vol. 21 No. 1, pp. 13–27.

Ellulu, M.S., Patimah, I., Khaza’ai, H., Rahmat, A., Abed, Y. and Ali, F. (2016), “Atherosclerotic cardiovascular disease: a review of initiators and protective factors”, *Inflammopharmacology*, Springer International Publishing, Vol. 24 No. 1, pp. 1–10.

Estrada, R., Wang, L., Jala, V.R., Lee, J.-F., Lin, C.-Y., Gray, R.D., Haribabu, B., et al. (2009), “Ligand-induced nuclear translocation of S1P 1 receptors mediates Cyr61 and CTGF transcription in endothelial cells”, *Histochem Cell Biol*, Vol. 131, pp. 239–249.

Evangelisti, C., Evangelisti, C., Buontempo, F., Lonetti, A., Orsini, E., Chiarini, F., Barata, J.T., et al. (2016), “Therapeutic potential of targeting sphingosine kinases and sphingosine 1-phosphate in hematological malignancies”, *Leukemia*, Nature Publishing Group, Vol. 30 No. 11, pp. 2142–2151.

Fairweather, D. (2014), “Sex differences in inflammation during atherosclerosis.”, *Clinical Medicine Insights. Cardiology*, SAGE Publications, Vol. 8 No. Suppl 3, pp. 49–59.

Feingold, K.R. and Grunfeld, C. (2000), *Introduction to Lipids and Lipoproteins*, *Endotext*, MDText.com, Inc., available at: http://www.ncbi.nlm.nih.gov/pubmed/26247089 (accessed 25 February 2018).

Fenske, S.A., Yesilaltay, A., Pal, R., Daniels, K., Rigotti, A., Krieger, M. and Kocher, O. (2008), “Overexpression of the PDZ1 domain of PDZK1 blocks the activity of hepatic scavenger receptor, class B, type I by altering its abundance and cellular localization.”, *The Journal of Biological Chemistry*, American Society for Biochemistry and Molecular Biology, Vol. 283 No. 32, pp. 22097–104.

Fielding, C.J. and Fielding, P.E. (1995), “Molecular physiology of reverse cholesterol transport.”, *Journal of Lipid Research*, Vol. 36 No. 2, pp. 211–28.

Frostegård, J. (2013), “Immunity, atherosclerosis and cardiovascular disease.”, *BMC Medicine*, BioMed Central, Vol. 11, p. 117.

Fukuhara, S., Simmons, S., Kawamura, S., Inoue, A., Orba, Y., Tokudome, T., Sunden, Y., et al. (2012), “The sphingosine-1-phosphate transporter Spns2 expressed on endothelial cells regulates lymphocyte trafficking in mice”, *Journal of Clinical Investigation*, Vol. 122 No. 4, pp. 1416–1426.

Garcia, J.G.N., Liu, F., Verin, A.D., Birukova, A., Dechert, M.A., Gerthoffer, W.T., Bamberg, J.R., et al. (2001), “Sphingosine 1-phosphate promotes endothelial cell barrier integrity by Edg-dependent cytoskeletal rearrangement”, *Journal of Clinical Investigation*, Vol. 108 No. 5, pp. 689–701.

Gault, C.R., Obeid, L.M. and Hannun, Y.A. (2010), “An overview of sphingolipid metabolism: from synthesis to breakdown.”, *Advances in Experimental Medicine and Biology*, NIH Public Access, Vol. 688, pp. 1–23.

Glass, C., Pittman, R.C., Weinstein, D.B. and Steinberg, D. (1983), “Dissociation of tissue uptake of cholesterol ester from that of apoprotein A-I of rat plasma high density lipoprotein: selective delivery of cholesterol ester to liver, adrenal, and gonad.”, *Proceedings of the National Academy of Sciences of the United States of America*, National Academy of Sciences, Vol. 80 No. 17, pp. 5435–9.

Glomset, J.A. (1968), “The plasma lecithins:cholesterol acyltransferase reaction.”, *Journal of Lipid Research*, Vol. 9 No. 2, pp. 155–67.

Goldstein, J.L. and Brown, M.S. (1984), “Progress in understanding the LDL receptor and HMG-CoA reductase, two membrane proteins that regulate the plasma cholesterol.”, *Journal of Lipid Research*, Vol. 25 No. 13, pp. 1450–61.

Gordon, D. and Rifkind, B. (1989), “High-density lipoprotein--the clinical implications of recent studies.”, *The New England Journal of Medicine*, Vol. 321 No. 19, pp. 1311–16.

Graf, G.A., Connell, P.M., van der Westhuyzen, D.R. and Smart, E.J. (1999), “The class B, type I scavenger receptor promotes the selective uptake of high density lipoprotein cholesterol ethers into caveolae.”, *The Journal of Biological Chemistry*, American Society for Biochemistry and Molecular Biology, Vol. 274 No. 17, pp. 12043–8.

Gräler, M.H., Bernhardt, G. and Lipp, M. (1998), “EDG6, a Novel G-Protein-Coupled Receptor Related to Receptors for Bioactive Lysophospholipids, Is Specifically Expressed in Lymphoid Tissue”, *Genomics*, Vol. 53 No. 2, pp. 164–169.

Gräler, M.H., Huang, M.-C., Watson, S. and Goetzl, E.J. (2005), “Immunological effects of transgenic constitutive expression of the type 1 sphingosine 1-phosphate receptor by mouse lymphocytes.”, *Journal of Immunology (Baltimore, Md. : 1950)*, Vol. 174 No. 4, pp. 1997–2003.

Gratton, J.-P., Bernatchez, P. and Sessa, W.C. (2004), “Caveolae and caveolins in the cardiovascular system.”, *Circulation Research*, American Heart Association, Inc., Vol. 94 No. 11, pp. 1408–17.

Grewal, T., de Diego, I., Kirchhoff, M.F., Tebar, F., Heeren, J., Rinninger, F. and Enrich, C. (2003), “High density lipoprotein-induced signaling of the MAPK pathway involves scavenger receptor type BI-mediated activation of Ras.”, *The Journal of Biological Chemistry*, American Society for Biochemistry and Molecular Biology, Vol. 278 No. 19, pp. 16478–81.

Hammad, S.M., Al Gadban, M.M., Semler, A.J. and Klein, R.L. (2012), “Sphingosine 1-phosphate distribution in human plasma: associations with lipid profiles.”, *Journal of Lipids*, Hindawi Limited, Vol. 2012, p. 180705.

Hannun, Y.A. and Bell, R.M. (1989), “Functions of sphingolipids and sphingolipid breakdown products in cellular regulation.”, *Science (New York, N.Y.)*, American Association for the Advancement of Science, Vol. 243 No. 4890, pp. 500–7.

Hannun, Y.A. and Obeid, L.M. (2008), “Principles of bioactive lipid signalling: lessons from sphingolipids”, *Nature Reviews Molecular Cell Biology*, Nature Publishing Group, Vol. 9 No. 2, pp. 139–150.

Hannun, Y.A. and Obeid, L.M. (2017), “Sphingolipids and their metabolism in physiology and disease”, *Nature Reviews Molecular Cell Biology*, Nature Publishing Group, Vol. 19 No. 3, pp. 175–191.

Hanyaloglu, A.C. and Zastrow, M. von. (2008), “Regulation of GPCRs by Endocytic Membrane Trafficking and Its Potential Implications”, *Annual Review of Pharmacology and Toxicology*, Vol. 48 No. 1, pp. 537–568.

Hartman, J. and Frishman, W.H. (2014), “Inflammation and Atherosclerosis: a review of the role of interleukin-6 in the development of atherosclerosis and the potential for targeted drug therapy.”, *Cardiology in Review*, Vol. 22 No. 3, pp. 147–151.

Havel, R.J., Eder, H.A. and Bragdon1, J.H. (1955), “The distribution and chemical composition of ultracentrifugally separated lipoproteins in human serum.”, *The Journal of Clinical Investigation*, American Society for Clinical Investigation, Vol. 34 No. 9, pp. 1345–1353.

Hayden, M.R., Brooks-Wilson, A., Marcil, M., Clee, S.M., Zhang, L.-H., Roomp, K., van Dam, M., et al. (1999), “Mutations in ABC1 in Tangier disease and familial high-density lipoprotein deficiency.”, *Nature Genetics*, Vol. 22 No. 4, pp. 336–345.

Hegele, R.A. (2009), “Plasma lipoproteins: genetic influences and clinical implications”, *Nature Reviews Genetics*, Nature Publishing Group, Vol. 10 No. 2, pp. 109–121.

Hla, T. and Maciag, T. (1990), “An abundant transcript induced in differentiating human endothelial cells encodes a polypeptide with structural similarities to G-protein-coupled receptors.”, *The Journal of Biological Chemistry*, Vol. 265 No. 16, pp. 9308–13.

Hokland, B.M., Slotte, J.P., Bierman, E.L. and Oram, J.F. (1993), “Cyclic AMP stimulates efflux of intracellular sterol from cholesterol-loaded cells.”, *The Journal of Biological Chemistry*, Vol. 268 No. 34, pp. 25343–9.

Hu, Z., Hu, J., Zhang, Z., Shen, W.J., Yun, C.C., Berlot, C.H., Kraemer, F.B., et al. (2013), "Regulation of expression and function of scavenger receptor class B, type i (SR-BI) by Na+/H+exchanger regulatory factors (NHERFs)", *Journal of Biological Chemistry*, Vol. 288 No. 16, pp. 11416–11435.

Huszar, D., Varban, M.L., Rinninger, F., Feeley, R., Arai, T., Fairchild-Huntress, V., Donovan, M.J., et al. (2000), "Increased LDL cholesterol and atherosclerosis in LDL receptor-deficient mice with attenuated expression of scavenger receptor B1.", *Arteriosclerosis, Thrombosis, and Vascular Biology*, Vol. 20 No. 4, pp. 1068–73.

Igarashi, J. and Michel, T. (2000), "Agonist-modulated targeting of the EDG-1 receptor to plasmalemmal caveolae. eNOS activation by sphingosine 1-phosphate and the role of caveolin-1 in sphingolipid signal transduction.", *The Journal of Biological Chemistry*, American Society for Biochemistry and Molecular Biology, Vol. 275 No. 41, pp. 32363–70.

Ikonen, E. (2006), "Mechanisms for Cellular Cholesterol Transport: Defects and Human Disease", *Physiological Reviews*, Vol. 86 No. 4, pp. 1237–1261.

Ishii, I., Fukushima, N., Ye, X. and Chun, J. (2004), "Lysophospholipid Receptors: Signaling and Biology", *Annual Review of Biochemistry*, Vol. 73 No. 1, pp. 321–354.

Ji, Y., Jian, B., Wang, N., Sun, Y., Moya, M.L., Phillips, M.C., Rothblat, G.H., et al. (1997), "Scavenger receptor BI promotes high density lipoprotein-mediated cellular cholesterol efflux.", *The Journal of Biological Chemistry*, American Society for Biochemistry and Molecular Biology, Vol. 272 No. 34, pp. 20982–5.

Ji, Y., Wang, N., Ramakrishnan, R., Sehayek, E., Huszar, D., Breslow, J.L. and Tall, A.R. (1999), "Hepatic scavenger receptor BI promotes rapid clearance of high density lipoprotein free cholesterol and its transport into bile.", *The Journal of Biological Chemistry*, Vol. 274 No. 47, pp. 33398–402.

Jian, B., de la Llera-Moya, M., Ji, Y., Wang, N., Phillips, M.C., Swaney, J.B., Tall, A.R., et al. (1998), "Scavenger receptor class B type I as a mediator of cellular cholesterol efflux to lipoproteins and phospholipid acceptors.", *The Journal of Biological Chemistry*, American Society for Biochemistry and Molecular Biology, Vol. 273 No. 10, pp. 5599–606.

Jolly, P.S., Bektas, M., Olivera, A., Gonzalez-Espinosa, C., Proia, R.L., Rivera, J., Milstien, S., et al. (2004), "Transactivation of Sphingosine-1–Phosphate Receptors by FcεRI Triggering Is Required for Normal Mast Cell Degranulation and Chemotaxis", *The Journal of Experimental Medicine*, Vol. 199 No. 7, pp. 959–970.

Jolly, P.S., Bektas, M., Watterson, K.R., Sankala, H., Payne, S.G., Milstien, S. and Spiegel, S. (2005), "Expression of SphK1 impairs degranulation and motility of RBL-2H3 mast cells by desensitizing S1P receptors", *Blood*, Vol. 105 No. 12, pp. 4736–4742.

Karuna, R., Park, R., Othman, A., Holleboom, A.G., Motazacker, M.M., Sutter, I., Kuivenhoven, J.A., et al. (2011), "Plasma levels of sphingosine-1-phosphate and apolipoprotein M in patients with monogenic disorders of HDL metabolism", *Atherosclerosis*, Vol. 219 No. 2, pp. 855–863.

Kawahara, A., Nishi, T., Hisano, Y., Fukui, H., Yamaguchi, A. and Mochizuki, N. (2009), "The Sphingolipid Transporter Spns2 Functions in Migration of Zebrafish Myocardial Precursors", *Science*, Vol. 323 No. 5913, pp. 524–527.

Kimura, T., Sato, K., Malchinkhuu, E., Tomura, H., Tamama, K., Kuwabara, A., Murakami, M., et al. (2003), "High-Density Lipoprotein Stimulates Endothelial Cell Migration and Survival Through Sphingosine 1-Phosphate and Its Receptors", *Arteriosclerosis, Thrombosis, and Vascular Biology*, Vol. 23 No. 7, pp. 1283–1288.

Kimura, T., Tomura, H., Mogi, C., Kuwabara, A., Damirin, A., Ishizuka, T., Sekiguchi, A., et al. (2006), “Role of scavenger receptor class B type I and sphingosine 1-phosphate receptors in high density lipoprotein-induced inhibition of adhesion molecule expression in endothelial cells.”, *The Journal of Biological Chemistry*, American Society for Biochemistry and Molecular Biology, Vol. 281 No. 49, pp. 37457–67.

Kimura, T., Tomura, H., Sato, K., Ito, M., Matsuoka, I., Im, D.-S., Kuwabara, A., et al. (2010), “Mechanism and role of high density lipoprotein-induced activation of AMP-activated protein kinase in endothelial cells.”, *The Journal of Biological Chemistry*, American Society for Biochemistry and Molecular Biology, Vol. 285 No. 7, pp. 4387–97.

Kimura, T., Watanabe, T., Sato, K., Kon, J., Tomura, H., Tamama, K., Kuwabara, A., et al. (2000), “Sphingosine 1-phosphate stimulates proliferation and migration of human endothelial cells possibly through the lipid receptors, Edg-1 and Edg-3.”, *The Biochemical Journal*, Portland Press Ltd, Vol. 348 Pt 1 No. Pt 1, pp. 71–6.

Kobayashi, N., Kobayashi, N., Yamaguchi, A. and Nishi, T. (2009), “Characterization of the ATP-dependent Sphingosine 1-Phosphate Transporter in Rat Erythrocytes”, *Journal of Biological Chemistry*, Vol. 284 No. 32, pp. 21192–21200.

Kocher, O., Yesilaltay, A., Cirovic, C., Pal, R., Rigotti, A. and Krieger, M. (2003), “Targeted disruption of the PDZK1 gene in mice causes tissue-specific depletion of the high density lipoprotein receptor scavenger receptor class B type I and altered lipoprotein metabolism.”, *The Journal of Biological Chemistry*, American Society for Biochemistry and Molecular Biology, Vol. 278 No. 52, pp. 52820–5.

Kono, M., Mi, Y., Liu, Y., Sasaki, T., Allende, M.L., Wu, Y.-P., Yamashita, T., et al. (2004), “The Sphingosine-1-phosphate Receptors S1P1 , S1P2 , and S1P3 Function Coordinately during Embryonic Angiogenesis”, *Journal of Biological Chemistry*, Vol. 279 No. 28, pp. 29367–29373.

Kontush, A. and Chapman, M.J. (2006), “Functionally defective high-density lipoprotein: a new therapeutic target at the crossroads of dyslipidemia, inflammation, and atherosclerosis.”, *Pharmacological Reviews*, American Society for Pharmacology and Experimental Therapeutics, Vol. 58 No. 3, pp. 342–74.

Kontush, A., Lindahl, M., Lhomme, M., Calabresi, L., Chapman, M.J. and Davidson, W.S. (2015), “Structure of HDL: Particle Subclasses and Molecular Components”, in von Eckardstein, A. and Kardassis, D. (Eds.), *High Density Lipoproteins, From Biological Understanding to Clinical Exploitation*, Springer, pp. 3–51.

Kontush, A., Therond, P., Zerrad, A., Couturier, M., Negre-Salvayre, A., de Souza, J.A., Chantepie, S., et al. (2007), “Preferential Sphingosine-1-Phosphate Enrichment and Sphingomyelin Depletion Are Key Features of Small Dense HDL3 Particles: Relevance to Antiapoptotic and Antioxidative Activities”, *Arteriosclerosis, Thrombosis, and Vascular Biology*, Vol. 27 No. 8, pp. 1843–1849.

Kozarsky, K.F., Donahee, M.H., Glick, J.M., Krieger, M. and Rader, D.J. (2000), “Gene transfer and hepatic overexpression of the HDL receptor SR-BI reduces atherosclerosis in the cholesterol-fed LDL receptor-deficient mouse.”, *Arteriosclerosis, Thrombosis, and Vascular Biology*, Vol. 20 No. 3, pp. 721–7.

Kozarsky, K.F., Donahee, M.H., Rigotti, A., Iqbal, S.N., Edelman, E.R. and Krieger, M. (1997), “Overexpression of the HDL receptor SR-BI alters plasma HDL and bile cholesterol levels”, *Nature*, Vol. 387 No. 6631, pp. 414–417.

Krieger, M. (2001), “Scavenger receptor class B type I is a multiligand HDL receptor that influences diverse physiologic systems.”, *The Journal of Clinical Investigation*, American Society for Clinical Investigation, Vol. 108 No. 6, pp. 793–7.

Książek, M., Chacińska, M., Chabowski, A. and Baranowski, M. (2015), “Sources, metabolism, and regulation of circulating sphingosine-1-phosphate.”, *Journal of Lipid Research*, American Society for Biochemistry and Molecular Biology, Vol. 56 No. 7, pp. 1271–81.

de la Llera-Moya, M., Rothblat, G.H., Connelly, M.A., Kellner-Weibel, G., Sakr, S.W., Phillips, M.C. and Williams, D.L. (1999), “Scavenger receptor BI (SR-BI) mediates free cholesterol flux independently of HDL tethering to the cell surface.”, *Journal of Lipid Research*, American Society for Biochemistry and Molecular Biology, Vol. 40 No. 3, pp. 575–80.

Larrede, S., Quinn, C.M., Jessup, W., Frisdal, E., Olivier, M., Hsieh, V., Kim, M.-J., et al. (2009), “Stimulation of Cholesterol Efflux by LXR Agonists in Cholesterol-Loaded Human Macrophages Is ABCA1-Dependent but ABCG1-Independent”, *Arteriosclerosis, Thrombosis, and Vascular Biology*, Vol. 29 No. 11, pp. 1930–1936.

Lawn, R.M., Wade, D.P., Garvin, M.R., Wang, X., Schwartz, K., Porter, J.G., Seilhamer, J.J., et al. (1999), “The Tangier disease gene product ABC1 controls the cellular apolipoprotein-mediated lipid removal pathway.”, *The Journal of Clinical Investigation*, American Society for Clinical Investigation, Vol. 104 No. 8, pp. R25-31.

Lee, M.-H., Appleton, K.M., El-Shewy, H.M., Sorci-Thomas, M.G., Thomas, M.J., Lopes-Virella, M.F., Luttrell, L.M., et al. (2017), “S1P in HDL promotes interaction between SR-BI and S1PR1 and activates S1PR1-mediated biological functions: calcium flux and S1PR1 internalization.”, *Journal of Lipid Research*, American Society for Biochemistry and Molecular Biology, Vol. 58 No. 2, pp. 325–338.

Lee, M.J., Van Brocklyn, J.R., Thangada, S., Liu, C.H., Hand, A.R., Menzeleev, R., Spiegel, S., et al. (1998), “Sphingosine-1-phosphate as a ligand for the G protein-coupled receptor EDG-1.”, *Science (New York, N.Y.)*, American Association for the Advancement of Science, Vol. 279 No. 5356, pp. 1552–5.

Lee, M.J., Evans, M. and Hla, T. (1996), “The inducible G protein-coupled receptor edg-1 signals via the G(i)/mitogen-activated protein kinase pathway.”, *The Journal of Biological Chemistry*, American Society for Biochemistry and Molecular Biology, Vol. 271 No. 19, pp. 11272–9.

Lee, M.J., Thangada, S., Paik, J.H., Sapkota, G.P., Ancellin, N., Chae, S.S., Wu, M., et al. (2001), “Akt-mediated phosphorylation of the G protein-coupled receptor EDG-1 is required for endothelial cell chemotaxis.”, *Molecular Cell*, Vol. 8 No. 3, pp. 693–704.

Leiva, A., Verdejo, H., Benítez, M.L., Martínez, A., Busso, D. and Rigotti, A. (2011), “Mechanisms regulating hepatic SR-BI expression and their impact on HDL metabolism”, *Atherosclerosis*, Vol. 217 No. 2, pp. 299–307.

Levkau, B. (2015), “HDL-S1P: cardiovascular functions, disease-associated alterations, and therapeutic applications.”, *Frontiers in Pharmacology*, Frontiers Media SA, Vol. 6, p. 243.

Libby, P. (2002), “Inflammation in atherosclerosis”, *Nature*, Vol. 420 No. 6917, pp. 868–874.

Licursi, M., Christian, S., Pongnopparat, T. and Hirasawa, K. (2011), “In vitro and in vivo comparison of viral and cellular internal ribosome entry sites for bicistronic vector expression”, *Gene Therapy*, Vol. 1811, pp. 631–636.

Liu, Y., Wada, R., Yamashita, T., Mi, Y., Deng, C.-X., Hobson, J.P., Rosenfeldt, H.M., et al. (2000), “Edg-1, the G protein–coupled receptor for sphingosine-1-phosphate, is essential for vascular maturation”, *Journal of Clinical Investigation*, Vol. 106 No. 8, pp. 951–961.

Lund-Katz, S., Liu, L., Thuahnai, S.T. and Phillips, M.C. (2003), “High density lipoprotein structure.”, *Frontiers in Bioscience : A Journal and Virtual Library*, Vol. 8, pp. d1044-54.

Lusis, A.J. (2000), “Atherosclerosis”, *Nature 2000 407:6801*, Nature Publishing Group.

Mabtech. (2019), “Apolipoproteins”, available at: https://www.mabtech.com.

Matsuo, Y., Miura, S., Kawamura, A., Uehara, Y., Rye, K.-A. and Saku, K. (2007), “Newly developed reconstituted high-density lipoprotein containing sphingosine-1-phosphate induces endothelial tube formation.”, *Atherosclerosis*, Elsevier, Vol. 194 No. 1, pp. 159–68.

Means, C.K., Miyamoto, S., Chun, J. and Brown, J.H. (2008), “S1P1 receptor localization confers selectivity for Gi-mediated cAMP and contractile responses.”, *The Journal of Biological Chemistry*, American Society for Biochemistry and Molecular Biology, Vol. 283 No. 18, pp. 11954–63.

Mineo, C., Yuhanna, I.S., Quon, M.J. and Shaul, P.W. (2003), “High Density Lipoprotein-induced Endothelial Nitric-oxide Synthase Activation Is Mediated by Akt and MAP Kinases”, *Journal of Biological Chemistry*, Vol. 278 No. 11, pp. 9142–9149.

Mitra, P., Oskeritzian, C.A., Payne, S.G., Beaven, M.A., Milstien, S. and Spiegel, S. (2006), “Role of ABCC1 in export of sphingosine-1-phosphate from mast cells”, *Proceedings of the National Academy of Sciences*, Vol. 103 No. 44, pp. 16394–16399.

Miura, S. -i., Fujino, M., Matsuo, Y., Kawamura, A., Tanigawa, H., Nishikawa, H. and Saku, K. (2003), “High Density Lipoprotein-Induced Angiogenesis Requires the Activation of Ras/MAP Kinase in Human Coronary Artery Endothelial Cells”, *Arteriosclerosis, Thrombosis, and Vascular Biology*, Vol. 23 No. 5, pp. 802–808.

Mizuguchi, H., Xu, Z., Ishii-Watabe, A., Uchida, E. and Hayakawa, T. (2000), “IRES-Dependent Second Gene Expression Is Significantly Lower Than Cap-Dependent First Gene Expression in a Bicistronic Vector”, *Molecular Therapy*, Vol. 1 No. 4, pp. 376–382.

Murata, N., Sato, K., Kon, J., Tomura, H., Yanagita, M., Kuwabara, A., Ui, M., et al. (2000), “Interaction of sphingosine 1-phosphate with plasma components, including lipoproteins, regulates the lipid receptor-mediated actions”, *Biochem. J*, Vol. 352, pp. 809–815.

Neer, E.J. (1995), “Heterotrimeric G Proteins: Organizers of Transmembrane Signals Review Signal Transduction by G Protein Subunits”, *Cell*, Vol. 80, pp. 249–257.

Nofer, J.-R., Levkau, B., Wolinska, I., Junker, R., Fobker, M., von Eckardstein, A., Seedorf, U., et al. (2001), “Suppression of Endothelial Cell Apoptosis by High Density Lipoproteins (HDL) and HDL-associated Lysosphingolipids”, *Journal of Biological Chemistry*, Vol. 276 No. 37, pp. 34480–34485.

Nofer, J.R., Van Der Giet, M., Tölle, M., Wolinska, I., Von Wnuck Lipinski, K., Baba, H. a., Tietge, U.J., et al. (2004), “HDL induces NO-dependent vasorelaxation via the lysophospholipid receptor S1P3”, *Journal of Clinical Investigation*, Vol. 113 No. 4, pp. 569–581.

Ohashi, R., Mu, H., Wang, X., Yao, Q. and Chen, C. (2005), “Reverse cholesterol transport and cholesterol efflux in atherosclerosis”, *QJM: An International Journal of Medicine*, Oxford University Press, Vol. 98 No. 12, pp. 845–856.

Olivera, A. and Spiegel, S. (1993), “Sphingosine-1-phosphate as second messenger in cell proliferation induced by PDGF and FCS mitogens”, *Nature*, Nature Publishing Group, Vol. 365 No. 6446, pp. 557–560.

Oo, M.L., Chang, S.-H., Thangada, S., Wu, M.-T., Rezaul, K., Blaho, V., Hwang, S.-I., et al. (2011), “Engagement of S1P1-degradative mechanisms leads to vascular leak in mice”, *Journal of Clinical Investigation*, Vol. 121 No. 6, pp. 2290–2300.

Oram, J.F. (2003), “HDL apolipoproteins and ABCA1: partners in the removal of excess cellular cholesterol.”, *Arteriosclerosis, Thrombosis, and Vascular Biology*, American Heart Association, Inc., Vol. 23 No. 5, pp. 720–7.

Oram, J.F., Lawn, R.M., Garvin, M.R. and Wade, D.P. (2000), “ABCA1 Is the cAMP-inducible Apolipoprotein Receptor That Mediates Cholesterol Secretion from Macrophages”, *Journal of Biological Chemistry*, Vol. 275 No. 44, pp. 34508–34511.

Osada, Y., Shiratsuchi, A. and Nakanishi, Y. (2006), “Involvement of mitogen-activated protein kinases in class B scavenger receptor type I-induced phagocytosis of apoptotic cells”, *Experimental Cell Research*, Academic Press, Vol. 312 No. 10, pp. 1820–1830.

Osborne, N., Brand-Arzamendi, K., Ober, E.A., Jin, S.-W., Verkade, H., Holtzman, N.G., Yelon, D., et al. (2008), “The Spinster Homolog, Two of Hearts, Is Required for Sphingosine 1-Phosphate Signaling in Zebrafish”, *Current Biology*, Vol. 18 No. 23, pp. 1882–1888.

Pappu, R., Schwab, S.R., Cornelissen, I., Pereira, J.P., Regard, J.B., Xu, Y., Camerer, E., et al. (2007), “Promotion of Lymphocyte Egress into Blood and Lymph by Distinct Sources of Sphingosine-1-Phosphate”, *Science*, Vol. 316 No. 5822, pp. 295–298.

Peng, Y., Akmentin, W., Connelly, M.A., Lund-Katz, S., Phillips, M.C. and Williams, D.L. (2004), “Scavenger receptor BI (SR-BI) clustered on microvillar extensions suggests that this plasma membrane domain is a way station for cholesterol trafficking between cells and high-density lipoprotein.”, *Molecular Biology of the Cell*, American Society for Cell Biology, Vol. 15 No. 1, pp. 384–96.

Pham, T.H.M., Baluk, P., Xu, Y., Grigorova, I., Bankovich, A.J., Pappu, R., Coughlin, S.R., et al. (2010), “Lymphatic endothelial cell sphingosine kinase activity is required for lymphocyte egress and lymphatic patterning.”, *The Journal of Experimental Medicine*, Rockefeller University Press, Vol. 207 No. 1, pp. 17–27.

Phillips, M.C. (2014), “Molecular mechanisms of cellular cholesterol efflux.”, *The Journal of Biological Chemistry*, American Society for Biochemistry and Molecular Biology, Vol. 289 No. 35, pp. 24020–9.

Pierce, K.L., Premont, R.T. and Lefkowitz, R.J. (2002), “Seven-transmembrane receptors”, *Nature Reviews Molecular Cell Biology*, Nature Publishing Group, Vol. 3 No. 9, pp. 639–650.

Rafieian-Kopaei, M., Setorki, M., Doudi, M., Baradaran, A. and Nasri, H. (2014), “Atherosclerosis: process, indicators, risk factors and new hopes.”, *International Journal of Preventive Medicine*, Wolters Kluwer -- Medknow Publications, Vol. 5 No. 8, pp. 927–46.

Raldúa, D. and Babin, P. (2007), “BLT-1, a specific inhibitor of the HDL receptor SR-BI, induces a copper-dependent phenotype during zebrafish development”, *Toxicology Letters*, Vol. 175 No. 1–3, pp. 1–7.

Rao, V.S., Srinivas, K., Sujini, G.N. and Kumar, G.N.S. (2014), “Protein-protein interaction detection: methods and analysis.”, *International Journal of Proteomics*, Hindawi, Vol. 2014, p. 147648.

Remaley, A.T., Norata, G.D. and Catapano, A.L. (2014), “Novel concepts in HDL pharmacology”, *Cardiovascular Research*, Oxford University Press, Vol. 103 No. 3, pp. 423–428.

Rodrigueza, W. V, Thuahnai, S.T., Temel, R.E., Lund-Katz, S., Phillips, M.C. and Williams, D.L. (1999), “Mechanism of scavenger receptor class B type I-mediated selective uptake of cholesteryl esters from high density lipoprotein to adrenal cells.”, *The Journal of Biological Chemistry*, American Society for Biochemistry and Molecular Biology, Vol. 274 No. 29, pp. 20344–50.

Rosenson, R.S., Brewer, H.B., Davidson, W.S., Fayad, Z.A., Fuster, V., Goldstein, J., Hellerstein, M., et al. (2012), “Cholesterol Efflux and Atheroprotection”, *Circulation*, Vol. 125 No. 15, pp. 1905–1919.

Ross, R. (1999), “Atherosclerosis — An Inflammatory Disease”, edited by Epstein, F.H.*New England Journal of Medicine*, Massachusetts Medical Society , Vol. 340 No. 2, pp. 115–126.

Russell, D.W. and Setchell, K.D. (1992), “Bile acid biosynthesis.”, *Biochemistry*, Vol. 31 No. 20, pp. 4737–49.

Rust, S., Rosier, M., Funke, H., Real, J., Amoura, Z., Piette, J.-C., Deleuze, J.-F., et al. (1999), “Tangier disease is caused by mutations in the gene encoding ATP-binding cassette transporter 1.”, *Nature Genetics*, Vol. 22 No. 4, pp. 352–355.

Saba, J.D. and Hla, T. (2004), “Point-counterpoint of sphingosine 1-phosphate metabolism.”, *Circulation Research*, Vol. 94 No. 6, pp. 724–34.

Sachinidis, A., Kettenhofen, R., Seewald, S., Gouni-Berthold, I., Schmitz, U., Seul, C., Ko, Y., et al. (1999), “Evidence that lipoproteins are carriers of bioactive factors.”, *Arteriosclerosis, Thrombosis, and Vascular Biology*, American Heart Association, Inc., Vol. 19 No. 10, pp. 2412–21.

Saddar, S., Mineo, C. and Shaul, P.W. (2010), “Signaling by the high-affinity HDL receptor scavenger receptor B type I.”, *Arteriosclerosis, Thrombosis, and Vascular Biology*, American Heart Association, Inc., Vol. 30 No. 2, pp. 144–50.

Sanchez, T. and Hla, T. (2004), “Structural and Functional Characteristics of S1P Receptors”, *Journal of Cellular Biochemistry J. Cell. Biochem*, Vol. 92 No. 92, pp. 913–922.

Santamarina-Fojo, S., Remaley, A.T., Neufeld, E.B. and Brewer, H.B. (2001), “Regulation and intracellular trafficking of the ABCA1 transporter.”, *Journal of Lipid Research*, American Society for Biochemistry and Molecular Biology, Vol. 42 No. 9, pp. 1339–45.

Sato, K., Malchinkhuu, E., Horiuchi, Y., Mogi, C., Tomura, H., Tosaka, M., Yoshimoto, Y., et al. (2007), “Critical role of ABCA1 transporter in sphingosine 1-phosphate release from astrocytes”, *Journal of Neurochemistry*, Vol. 0 No. 0, p. 071106212736004–???

Sato, K. and Okajima, F. (2010), “Role of sphingosine 1-phosphate in anti-atherogenic actions of high-density lipoprotein.”, *World Journal of Biological Chemistry*, Baishideng Publishing Group Inc, Vol. 1 No. 11, pp. 327–37.

Sattler, K., Gräler, M., Keul, P., Weske, S., Reimann, C.-M., Jindrová, H., Kleinbongard, P., et al. (2015), “Defects of High-Density Lipoproteins in Coronary Artery Disease Caused by Low Sphingosine-1-Phosphate Content: Correction by Sphingosine-1-Phosphate—Loading”, *Journal of the American College of Cardiology*, Elsevier, Vol. 66 No. 13, pp. 1470–1485.

Sattler, K. and Levkau, B. (2009), “Sphingosine-1-phosphate as a mediator of high-density lipoprotein effects in cardiovascular protection”, *Cardiovascular Research*, Vol. 82, pp. 201–211.

Sattler, K.J.E., Elbasan, S., Keul, P., Elter-Schulz, M., Bode, C., Gräler, M.H., Bröcker-Preuss, M., et al. (2010), “Sphingosine 1-phosphate levels in plasma and HDL are altered in coronary artery disease”, *Basic Research in Cardiology*, Vol. 105 No. 6, pp. 821–832.

Schmittgen, T.D. and Livak, K.J. (2008), “Analyzing real-time PCR data by the comparative CT method”, *Nature Protocols*, Nature Publishing Group, Vol. 3 No. 6, pp. 1101–1108.

Schmitz, G., Bodzioch, M., Orsó, E., Klucken, J., Langmann, T., Böttcher, A., Diederich, W., et al. (1999), “The gene encoding ATP-binding cassette transporter 1 is mutated in Tangier disease.”, *Nature Genetics*, Vol. 22 No. 4, pp. 347–351.

Shen, W.-J., Azhar, S. and Kraemer, F.B. (2016), “ACTH Regulation of Adrenal SR-B1.”, *Frontiers in Endocrinology*, Frontiers Media SA, Vol. 7, p. 42.

Shen, W.-J., Hu, J., Hu, Z., Kraemer, F.B. and Azhar, S. (2014), “Scavenger Receptor class B type I (SR-BI): A versatile receptor with multiple functions and actions”, *Metabolism*, W.B. Saunders, Vol. 63 No. 7, pp. 875–886.

Shuyu, E., Yun-Ju, L., Ryoko, T., Chen-Shan, C., Yuko, F., Junming, Y., Jei-Hwa, Y., et al. (2009), “Lysophosphatidic acid 2 receptor-mediated supramolecular complex formation regulates its antiapoptotic effect.”, *The Journal of Biological Chemistry*, American Society for Biochemistry and Molecular Biology, Vol. 284 No. 21, pp. 14558–71.

Simons, K. and Ikonen, E. (2000), “How cells handle cholesterol.”, *Science (New York, N.Y.)*, Vol. 290 No. 5497, pp. 1721–6.

Skoura, A., Michaud, J., Im, D.-S., Thangada, S., Xiong, Y., Smith, J.D. and Hla, T. (2011), “Sphingosine-1-Phosphate Receptor-2 Function in Myeloid Cells Regulates Vascular Inflammation and Atherosclerosis”, *Arteriosclerosis, Thrombosis, and Vascular Biology*, Vol. 31 No. 1, pp. 81–85.

Smith, J.D., Miyata, M., Ginsberg, M., Grigaux, C., Shmookler, E. and Plump, A.S. (1996), “Cyclic AMP induces apolipoprotein E binding activity and promotes cholesterol efflux from a macrophage cell line to apolipoprotein acceptors.”, *The Journal of Biological Chemistry*, American Society for Biochemistry and Molecular Biology, Vol. 271 No. 48, pp. 30647–55.

Spady, D.K. (1999), “Reverse cholesterol transport and atherosclerosis regression.”, *Circulation*, Vol. 100 No. 6, pp. 576–8.

Spiegel, S. and Milstien, S. (2003), “Sphingosine-1-phosphate: an enigmatic signalling lipid”, *Nature Reviews Molecular Cell Biology*, Nature Publishing Group, Vol. 4 No. 5, pp. 397–407.

Strub, G.M., Maceyka, M., Hait, N.C., Milstien, S. and Spiegel, S. (2010), “Extracellular and intracellular actions of sphingosine-1-phosphate.”, *Advances in Experimental Medicine and Biology*, NIH Public Access, Vol. 688, pp. 141–55.

Takabe, K., Kim, R.H., Allegood, J.C., Mitra, P., Ramachandran, S., Nagahashi, M., Harikumar, K.B., et al. (2010), “Estradiol Induces Export of Sphingosine 1-Phosphate from Breast Cancer Cells via ABCC1 and ABCG2”, *Journal of Biological Chemistry*, Vol. 285 No. 14, pp. 10477–10486.

Takabe, K., Paugh, S.W., Milstien, S. and Spiegel, S. (2008), “‘Inside-out’ signaling of sphingosine-1-phosphate: therapeutic targets.”, *Pharmacological Reviews*, NIH Public Access, Vol. 60 No. 2, pp. 181–95.

Tani, M., Sano, T., Ito, M. and Igarashi, Y. (2005), “Mechanisms of sphingosine and sphingosine 1-phosphate generation in human platelets.”, *Journal of Lipid Research*, American Society for Biochemistry and Molecular Biology, Vol. 46 No. 11, pp. 2458–67.

Theilmeier, G., Schmidt, C., Herrmann, J., Keul, P., Schäfers, M., Herrgott, I., Mersmann, J., et al. (2006), “High-Density Lipoproteins and Their Constituent, Sphingosine-1-Phosphate, Directly Protect the Heart Against Ischemia/Reperfusion Injury In Vivo via the S1P3 Lysophospholipid Receptor”, *Circulation*, Vol. 114 No. 13, pp. 1403–1409.

Thudichum, J.L.W. (1884), *A Treatise on the Chemical Constitution of the Brain*, London: Bailliere, Tindall, and Cox.

Tondu, A.-L., Robichon, C., Yvan-Charvet, L., Donne, N., Le Liepvre, X., Hajduch, E., Ferré, P., et al. (2005), “Insulin and angiotensin II induce the translocation of scavenger receptor class B, type I from intracellular sites to the plasma membrane of adipocytes.”, *The Journal of Biological Chemistry*, American Society for Biochemistry and Molecular Biology, Vol. 280 No. 39, pp. 33536–40.

Trigatti, B., Rayburn, H., Viñals, M., Braun, A., Miettinen, H., Penman, M., Hertz, M., et al. (1999), “Influence of the high density lipoprotein receptor SR-BI on reproductive and cardiovascular pathophysiology.”, *Proceedings of the National Academy of Sciences of the United States of America*, National Academy of Sciences, Vol. 96 No. 16, pp. 9322–7.

Tuteja, N. (2009), “Signaling through G protein coupled receptors.”, *Plant Signaling & Behavior*, Taylor & Francis, Vol. 4 No. 10, pp. 942–7.

Ueda, Y., Gong, E., Royer, L., Cooper, P.N., Francone, O.L. and Rubin, E.M. (2000), “Relationship between Expression Levels and Atherogenesis in Scavenger Receptor Class B, Type I Transgenics”, *Journal of Biological Chemistry*, Vol. 275 No. 27, pp. 20368–20373.

Ueda, Y., Royer, L., Gong, E., Zhang, J., Cooper, P.N., Francone, O. and Rubin, E.M. (1999), “Lower plasma levels and accelerated clearance of high density lipoprotein (HDL) and non-HDL cholesterol in scavenger receptor class B type I transgenic mice.”, *The Journal of Biological Chemistry*, Vol. 274 No. 11, pp. 7165–71.

Vaidya, M., Jentsch, J.A., Peters, S., Keul, P., Weske, S., Gräler, M.H., Mladenov, E., et al. (2019), “Regulation of ABCA1-mediated cholesterol efflux by sphingosine-1-phosphate signalling in macrophages”, *Journal of Lipid Research*, p. jlr.M088443.

Valacchi, G., Sticozzi, C., Lim, Y. and Pecorelli, A. (2011), “Scavenger receptor class B type I: a multifunctional receptor”, *Annals of the New York Academy of Sciences*, Vol. 1229 No. 1, pp. E1–E7.

Venkataraman, K., Lee, Y.-M., Michaud, J., Thangada, S., Ai, Y., Bonkovsky, H.L., Parikh, N.S., et al. (2008), “Vascular Endothelium As a Contributor of Plasma Sphingosine 1-Phosphate”, *Circulation Research*, Vol. 102 No. 6, pp. 669–676.

Wang, F., Okamoto, Y., Inoki, I., Yoshioka, K., Du, W., Qi, X., Takuwa, N., et al. (2010), “Sphingosine-1-phosphate receptor-2 deficiency leads to inhibition of macrophage proinflammatory activities and atherosclerosis in apoE-deficient mice”, *Journal of Clinical Investigation*, Vol. 120 No. 11, pp. 3979–3995.

Wang, N., Arai, T., Ji, Y., Rinninger, F. and Tall, A.R. (1998), “Liver-specific overexpression of scavenger receptor BI decreases levels of very low density lipoprotein ApoB, low density lipoprotein ApoB, and high density lipoprotein in transgenic mice.”, *The Journal of Biological Chemistry*, Vol. 273 No. 49, pp. 32920–6.

Wilkerson, B.A. and Argraves, K.M. (2014), “The role of sphingosine-1-phosphate in endothelial barrier function.”, *Biochimica et Biophysica Acta*, NIH Public Access, Vol. 1841 No. 10, pp. 1403–1412.

Xiong, Y., Lee, H.J., Mariko, B., Lu, Y.-C., Dannenberg, A.J., Haka, A.S., Maxfield, F.R., et al. (2013), “Sphingosine Kinases Are Not Required for Inflammatory Responses in Macrophages”, *Journal of Biological Chemistry*, Vol. 288 No. 45, pp. 32563–32573.

Yancey, P.G., Bortnick, A.E., Kellner-Weibel, G., de la Llera-Moya, M., Phillips, M.C. and Rothblat, G.H. (2003), “Importance of different pathways of cellular cholesterol efflux.”, *Arteriosclerosis, Thrombosis, and Vascular Biology*, American Heart Association, Inc., Vol. 23 No. 5, pp. 712–9.

Yatomi, Y., Igarashi, Y., Yang, L., Hisano, N., Qi, R., Asazuma, N., Satoh, K., et al. (1997), “Sphingosine 1-phosphate, a bioactive sphingolipid abundantly stored in platelets, is a normal constituent of human plasma and serum.”, *Journal of Biochemistry*, Vol. 121 No. 5, pp. 969–73.

Yu, M., Romer, K.A., Nieland, T.J.F., Xu, S., Saenz-Vash, V., Penman, M., Yesilaltay, A., et al. (2011), “Exoplasmic cysteine Cys384 of the HDL receptor SR-BI is critical for its sensitivity to a small-molecule inhibitor and normal lipid transport activity.”, *Proceedings of the National Academy of Sciences of the United States of America*, National Academy of Sciences, Vol. 108 No. 30, pp. 12243–8.

Yuhanna, I.S., Zhu, Y., Cox, B.E., Hahner, L.D., Osborne-Lawrence, S., Lu, P., Marcel, Y.L., et al. (2001), “High-density lipoprotein binding to scavenger receptor-BI activates endothelial nitric oxide synthase.”, *Nature Medicine*, Vol. 7, pp. 853–857.

Zhang, B., Tomura, H., Kuwabara, A., Kimura, T., Miura, S., Noda, K., Okajima, F., et al. (2005), “Correlation of high density lipoprotein (HDL)-associated sphingosine 1-phosphate with serum levels of HDL-cholesterol and apolipoproteins”, *Atherosclerosis*, Vol. 178 No. 1, pp. 199–205.

Zhou, K. and Blom, T. (2015), “Trafficking and Functions of Bioactive Sphingolipids: Lessons from Cells and Model Membranes.”, *Lipid Insights*, SAGE Publications, Vol. 8 No. Suppl 1, pp. 11–20.

Zhou, Y., Aran, J., Gottesman, M.M. and Pastan, I. (1998), “Co-Expression of Human Adenosine Deaminase and Multidrug Resistance Using a Bicistronic Retroviral Vector”, *Human Gene Therapy*, Mary Ann Liebert, Inc. 2 Madison Avenue Larchmont, NY 10538 USA , Vol. 9 No. 3, pp. 287–293.

11 Appendix

Plasmid map of pHRSIN.SFFV.eGFP.WPre

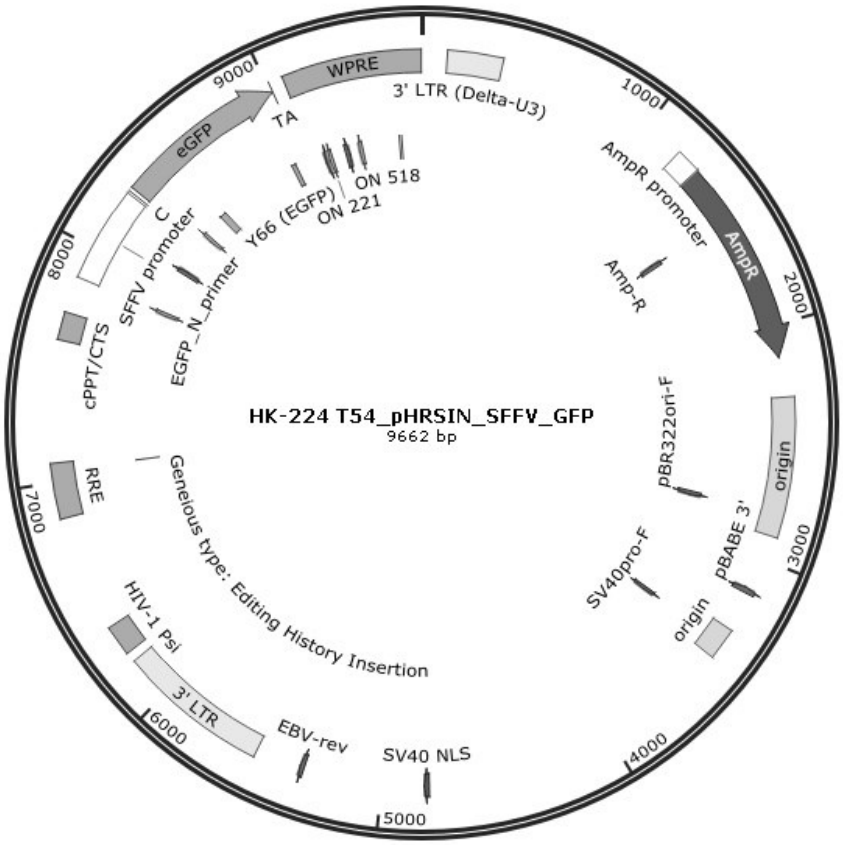

Plasmid map of pRRLSIN.cPPT.SFFV.SRB1.IRES.eGFP.WPre

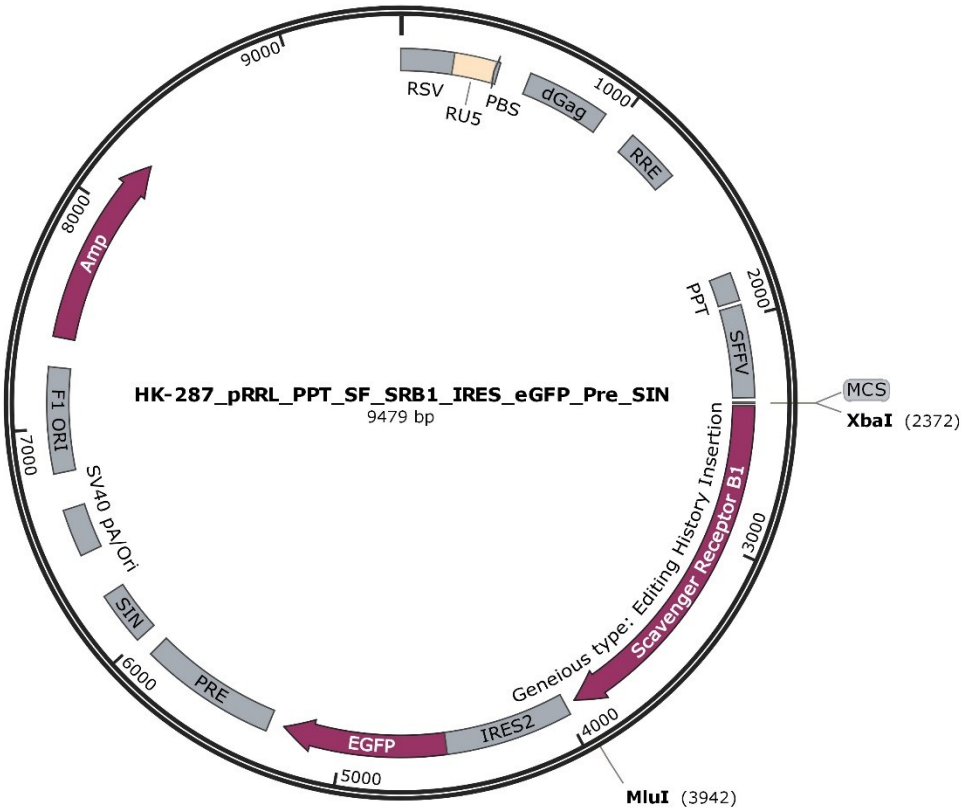

Acknowledgements

Eidesstattliche Erklärungen

Erklärung:

Hiermit erkläre ich, gem. § 7 Abs. (2) d) + f) der Promotionsordnung der Fakultät für Biologie zur Erlangung des Dr. rer. nat., dass ich die vorliegende Dissertation selbstständig verfasst und mich keiner anderen als der angegebenen Hilfsmittel bedient, bei der Abfassung der Dissertation nur die angegebenen Hilfsmittel benutzt und alle wörtlich oder inhaltlich übernommenen Stellen als solche gekennzeichnet habe.

Essen, den _____ _____

Unterschrift der Doktorandin

Erklärung:

Hiermit erkläre ich, gem. § 7 Abs. (2) e) + g) der Promotionsordnung der Fakultät für Biologie zur Erlangung des Dr. rer. nat., dass ich keine anderen Promotionen bzw. Promotionsversuche in der Vergangenheit durchgeführt habe und dass diese Arbeit von keiner anderen Fakultät/Fachbereich abgelehnt worden ist.

Essen, den _____ _____

Unterschrift der Doktorandin

Erklärung:

Hiermit erkläre ich, gem. § 6 Abs. (2) g) der Promotionsordnung der Fakultät für Biologie zur Erlangung des Dr. rer. nat., dass ich das Arbeitsgebiet, dem das Thema „*The Impact of S1P Receptors on the High-Density Lipoprotein-mediated Cholesterol Efflux in Chinese Hamster Ovary Cells“* zuzuordnen ist, in Forschung und Lehre vertrete und den Antrag von Kristina Manthe befürworte und die Betreuung auch im Falle eines Weggangs, wenn nicht wichtige Gründe dem entgegenstehen, weiterführen werde.

Prof. Dr. med. Bodo Levkau

Name des Mitglieds der Universität Duisburg-Essen in Druckbuchstaben

Essen, den _____ _____

Name des Mitglieds der Universität Duisburg-Essen

Curriculum Vitae

Der Lebenslauf ist in der Online-Version aus Gründen des Datenschutzes nicht enthalten.